

**MASTER'S THESIS  
BIOMEDICINE  
MAY 2021**

**Change in content of extracellular vesicles from human skeletal muscle cells after electrical pulse stimulation with focus on microRNA.**

**Student**

**Name:** Desima S. O. Eid  
**Course code:** MABIOD5900\_1  
Faculty of Health Sciences  
Oslo Metropolitan University

**The supervisors**

Professor Vigdis Aas  
Department of Life Sciences and Health  
Oslo Metropolitan University,

Reidun Øvstebø, PhD  
The Blood Cell Research Group,  
Department of Medical Biochemistry  
Oslo University Hospital,

Kari Bente Foss Haug, PhD  
The Blood Cell Research Group  
Department of Medical Biochemistry  
Oslo University Hospital

**OSLOMET**

 **Oslo  
University Hospital**



# 1 Preface

As the saying goes, “knowledge is power”. Taking on a master study and this thesis was the most daring thing that I have ever done besides moving to Norway some 13 years ago. I have learnt that nothing is impossible. I have learnt to be patient, since things don’t always go as planned. I have learnt to take nothing for granted and are grateful for anything and everything that has come my way.

My special and a huge thank you to professor Vigdis Aas, Reidun Øvstebø and Kari Bente Foss Haug, the three most knowledgeable and dedicated supervisors. A group of women who never gave up even when things looked gray and dark. Who collaborated and worked hard together as a team contributing a lot with their knowledge and skills. I am very grateful to Vigdis, ever smiling, always positive minded and sharing her unlimited knowledge. Always being available whenever needed, especially when I was really down and was crying my eyes out. Huge gratitude to Reidun and Kari Bente for being the engineering group, always coming up with new creative suggestions and trying out time and time again until a better solution is acquired. Who guided and contributed a lot in terms of time dedication, knowledge and a place to work from among others.

The last three years have been among the toughest, but everything was worth it, especially after being routed for by my family members. These are people who have cheered me on all the way. They are the people who kept me going on and encouraged me never to give up.

Oslo, May 2021

Desima Shitandi Otundo Eid

## 2 Table of Contents

<b>1</b>	<b><i>Preface</i></b> .....	<b><i>i</i></b>
<b>2</b>	<b><i>Table of Contents</i></b> .....	<b><i>ii</i></b>
<b>3</b>	<b><i>Abstract</i></b> .....	<b><i>v</i></b>
<b>3.1</b>	<b>Background and Aim</b> .....	<b>v</b>
<b>3.2</b>	<b>Methods</b> .....	<b>v</b>
<b>3.3</b>	<b>Results</b> .....	<b>v</b>
<b>3.4</b>	<b>Conclusion</b> .....	<b>vi</b>
<b>4</b>	<b><i>Sammendrag</i></b> .....	<b><i>vi</i></b>
<b>4.1</b>	<b>Bakgrunn og formål</b> .....	<b>vi</b>
<b>4.2</b>	<b>Metoder</b> .....	<b>vii</b>
<b>4.3</b>	<b>Resultater</b> .....	<b>vii</b>
<b>4.4</b>	<b>Konklusjon</b> .....	<b>viii</b>
<b>5</b>	<b><i>Abbreviation</i></b> .....	<b><i>ix</i></b>
<b>6</b>	<b><i>Introduction</i></b> .....	<b><i>1</i></b>
<b>6.1</b>	<b>Overweight, obesity and type 2 diabetes mellitus</b> .....	<b>1</b>
<b>6.2</b>	<b>Obesity and type 2 diabetes mellitus</b> .....	<b>2</b>
<b>6.3</b>	<b>Skeletal muscles</b> .....	<b>3</b>
6.3.1	Skeletal muscle cells in cell culture .....	4
6.3.2	Skeletal muscle as a secretory organ .....	6
6.3.3	Physical exercise.....	7
<b>6.4</b>	<b>Interleukin-6 (IL-6)</b> .....	<b>9</b>
<b>6.5</b>	<b>Extracellular vesicles</b> .....	<b>10</b>
6.5.1	Categorization of extracellular vesicles .....	11
6.5.2	Biogenesis and composition of extracellular vesicles .....	12
6.5.3	Extracellular vesicles' interaction with recipient cells and uptake.....	17
6.5.4	Extracellular vesicles in type 2 diabetes mellitus and obesity.....	19
6.5.5	Extracellular vesicles and training.....	20
6.5.6	Isolation and characterization of extracellular vesicles .....	21
<b>6.6</b>	<b>MicroRNA</b> .....	<b>22</b>
<b>7</b>	<b><i>Aim of the study</i></b> .....	<b><i>25</i></b>
<b>8</b>	<b><i>Methods and material</i></b> .....	<b><i>26</i></b>
<b>8.1</b>	<b>Materials and ethics</b> .....	<b>26</b>
<b>8.2</b>	<b>Study design</b> .....	<b>26</b>
<b>9</b>	<b><i>Cell cultures</i></b> .....	<b><i>27</i></b>
9.1.1	Pre-coating of the well plates with extracellular matrix (ECM) gel.....	28
9.1.2	The cell seeding .....	28
9.1.3	Cell proliferation and differentiation .....	28
<b>9.2</b>	<b>Electrical pulse stimulation (EPS)</b> .....	<b>29</b>
9.2.1	Harvesting of the conditioned medium.....	31

9.2.2	Skeletal muscle cell collection.....	31
<b>9.3</b>	<b>Protein quantitation .....</b>	<b>31</b>
9.3.1	Protein measurement using Bradford’s method.....	31
9.3.2	Interleukin-6 (IL-6) analysis.....	32
<b>10</b>	<b><i>Isolation of muscle derived extracellular vesicles.....</i></b>	<b>34</b>
10.1.1	Isolation of microvesicles .....	34
10.1.2	Isolation of exosomes .....	35
<b>11</b>	<b><i>Characterization of extracellular vesicles (EVs).....</i></b>	<b>36</b>
11.1	Transmission electron microscopy (TEM).....	37
11.2	Sizing and enumeration of extracellular vesicles by nanoparticle tracking analysis (NTA) 37	
11.3	Quantification of proteins in extracellular vesicles on NanoDrop One spectrophotometer.....	39
11.4	Western blotting.....	39
<b>12</b>	<b><i>Quantification of microRNA.....</i></b>	<b>40</b>
12.1	Total RNA extraction from exosomes .....	41
12.2	Quantification of total RNA from exosomes.....	42
12.2.1	NanoDrop One .....	42
12.3	Agilent 2100 Bioanalyzer .....	43
12.4	Qubit microRNA assay .....	45
12.5	Real-time reverse transcription quantitative polymerase chain reaction..... (RT-qPCR).....	45
12.6	Complimentary DNA (cDNA) template generation.....	47
12.7	Pilot real-time polymerase chain reaction (RT-qPCR) .....	49
12.8	Pilot Affymetrix microarray .....	50
12.8.1	Pilot Affymetrix trial.....	50
12.8.2	Poly (A) tailing .....	51
12.8.3	FlashTag biotin HSR ligation .....	51
12.8.4	Hybridization .....	52
12.9	Ingenuity pathways analysis (IPA) .....	52
12.10	Data and statistical analyses.....	52
<b>13</b>	<b><i>Results.....</i></b>	<b>54</b>
13.1	Concentration of IL-6 in cell medium .....	54
13.1	Protein quantification .....	54
13.2	Characterization of extracellular vesicles.....	55
13.2.1	Transmission electron microscopy (TEM) .....	55
13.2.2	Size and concentration of extracellular vesicles .....	56
13.3	Quantification of miRNA.....	60
13.3.1	Real-time RT-qPCR of miR from exosome derived RNA .....	60
13.3.2	Quantification of isolated RNA .....	60
13.3.3	Affymetrix microarray .....	64
<b>14</b>	<b><i>Discussion.....</i></b>	<b>71</b>
14.1	Effects of training on skeletal muscle cells.....	73

<b>14.2</b>	<b>Characterization of extracellular vesicles .....</b>	<b>75</b>
<b>14.3</b>	<b>Quantification of miRNA.....</b>	<b>77</b>
14.3.1	Total RNA extraction from exosomes .....	78
14.3.2	Agilent 2100 Bioanalyzer .....	78
14.3.3	Challenges and strategies for finding ways to solutions .....	79
<b>15</b>	<b><i>Evaluation of methods.....</i></b>	<b>81</b>
<b>15.1</b>	<b>Cell Cultures .....</b>	<b>81</b>
<b>15.2</b>	<b>Isolation of muscle derived extracellular vesicles.....</b>	<b>82</b>
<b>15.3</b>	<b>Characterization of extracellular vesicles .....</b>	<b>83</b>
<b>16</b>	<b><i>Conclusion remarks .....</i></b>	<b>85</b>
<b>17</b>	<b><i>Reference List.....</i></b>	<b>86</b>
<b>18</b>	<b><i>Appendixes.....</i></b>	<b>95</b>

## 3 Abstract

### 3.1 Background and Aim

Extracellular vesicles (EVs) are nanoparticles with a double membrane postulated to be released by cells of all types and can be detected in all body fluids. They are classified in three groups exosomes, microvesicles (MV) and apoptotic bodies and encompasses lipids, proteins, and nucleic acids (RNA and DNA). In a previous master thesis, studies were done on electrically stimulated skeletal muscle cell derived EVs. In that study, it was illustrated that, skeletal muscles release EVs. These EVs were found to contain proteins on which electrical pulse stimulation (EPS) had significant effects. In addition, a pilot experiment found that the EVs encompassed microRNAs, whose functions were not fully understood. EVs have been suggested to be mediators of cell-to-cell communication and regular physical activity has been proven to prevent T2DM and improve blood sugar levels. It was of interest to find out whether electrical pulse stimulation could have any effects on microRNA encompassed in EVs derived from extremely obese patients with type 2 diabetes mellitus (T2DM), since it had had significant effects on proteins.

### 3.2 Methods

Primary human skeletal muscle cells isolated from abdominal muscle biopsies were cultured and allowed to differentiate into myotubes. Half of the cells were stimulated using a low-frequency EPS for 24 hours. The media were collected and used for interleukin-6 (IL-6) concentration measurement. After incubation of the cells in serum free media for 24 hours, the media was harvested, and used for EVs (exosomes and microvesicles) isolation, and the EVs were characterized using transmission electron microscopy (TEM), nanoparticle tracking analysis (NTA and western blotting. Exosome content of microRNA was accessed by quantitative reverse transcription polymerase chain reaction (RT-qPCR) and Affymetrix microarray technology.

### 3.3 Results

The interleukin-6 concentrations in the cell media tended to be increased by 37 % after EPS, although not significant ( $p=0.11$ ). TEM pictures showed a spherical morphology and a cup shaped structure of EVs, typical characteristics. The mean size of unstimulated exosomes was 139 nm and 141 nm after EPS. Microvesicles were significantly larger, unstimulated 158 nm and stimulated 164 nm. In the identification of EVs surface biomarkers, the presence of

CD63 and Hsc70/Hsp70 was shown, whereas CD9 was not present. RT-qPCR illustrated that skeletal muscle cell derived EVs were enriched with microRNA, the three myo-miRs, miR-1-3p, miR-133a and miR-206 were detected.

Affymetrix microarray analysis performed on three donors were loaded in Ingenuity Pathway analysis software (IPA). A total of 271 transcripts were detected and out of the total, 219 were miR. Analysis of Affymetrix microarray data in IPA showed significant effects of EPS on 12 miRs. This was based on filtering the miRs by  $p < 0.05$ ,  $> 1.5$ -fold change and “signal value” above 5. Pathway analysis showed their involvement in diseases and biological functions, and these included neurological diseases, psychological disorders, post-translational modification, connective tissue development and function, cardiovascular system development and function. A prediction of top upstream regulators and their interaction network suggested AGO2 (argonaute RISC catalytic component 2), MET (MET Proto-Oncogene, Receptor Tyrosine Kinase), TGS1 (Trimethylguanosine synthase 1), XPO1 (Exportin 1) and TP53 (Tumor protein p53) among others. Database search for targets of the miRs identified several possible targets of the regulated miRs.

### 3.4 Conclusion

Electrical pulse stimulation had a noticeable effect on miR content in exosomes, with a significant difference in 12 specific miRs between unstimulated and stimulated (EPS) myotubes. Characterization of EVs illustrated that EPS had no effect on EVs concentrations and sizes. The changes caused in EVs' miR content by EPS might play an important role in numerous biological functions of mediating beneficial effects of exercise.

## 4 Sammendrag

### 4.1 Bakgrunn og formål

Extracellulære vesikler (EV) er nanopartikler med en dobbel membran som kan påvises i alle kroppsvæsker. De er klassifisert i tre grupper, eksosomer, mikrovesikler og apoptotiske legemer, og inneholder lipider, proteiner og nukleinsyrer (RNA og DNA). I en tidligere masteroppgave ble det gjort studier på EVer avledet fra elektrisk stimulerte skjelettmuskelceller. I studien ble det vist at skjelettmuskelceller frigjør EV. Disse EVene ble funnet å inneholde proteiner som elektrisk pulsstimulering (EPS) hadde signifikante effekter på. I tillegg, viste en pilotstudie at EVene inneholdt mikroRNA, men hvor deres



funksjoner ikke ble fullstendig undersøkt. EV har blitt foreslått å være formidlere av intercellulær kommunikasjon, og regelmessig fysisk aktivitet har vist å kunne forhindre T2DM og forbedre blodsukkernivå. Det var av interesse å finne ut om elektrisk pulsstimulering kunne ha noen innvirkning på mikroRNA i EV isolert fra sykkelig overvektige pasienter med T2DM siden det tidligere hadde hatt signifikante effekter på proteiner.

## 4.2 Metoder

Primære humane skjelettmuskelceller isolert fra magemuskelbiopsier ble dyrket og differensierte til myotuber. Etter differensiering ble halvparten av cellene stimulerte (EPS) ved en lav frekvens i 24 timer. Medier ble samlet og brukt til interleukin-6 (IL-6) konsentrasjonsmåling. Etter inkubering av cellene i serumfritt medium i 24 timer, ble mediene høstet for EV-isolering (eksosomer og mikrovesikler), og EV-ene ble karakterisert ved hjelp av transmisjon elektron mikroskopi (TEM), nanopartikkel tracking analyse (NTA), western blott, kvantitative revers transkripsjon polymerasekjedereaksjon (RT-qPCR) og Affymetrix mikroarray. MikroRNA-innholdet i eksosomer ble analyserte ved kvantitativ revers transkripsjon polymerasekjedereaksjon (RT-qPCR) of Affymetrix microarray teknologi.

## 4.3 Resultater

Interleukin-6-konsentrasjon, i cellediene viste tendens til økning med 37 % etter EPS, men det var ikke signifikant forskjeller ( $p=0,11$ ). TEM-bilder viste en sfærisk morfologi og en koppformet struktur som er typiske EV-karakteristikker. Gjennomsnittlig størrelse på ustimulerte eksosomer var 139 nm og 141 nm etter EPS. Mikrovesikler var betydelig større, ustimulerte 158 nm og stimulerte 164 nm. Ved identifisering av overflatebiomarkører i EVer ble tilstedeværelsen av CD63 og Hsc70/Hsp70 vist, mens CD9 ikke var til stede. RT-qPCR illustrerte at EVer avledet fra skjelettmuskelceller inneholdt mikroRNA. De tre myo-miRene, miR-1-3p, miR-133a og miR-206 ble detektert.

I Affymetrix mikroarray analyse utført på EVer fra tre givere ble lastet inn i Ingenuity Pathway analysis (IPA). Totalt 271 transkripter var detektert, og av totalen var det 219 som var miRer. Analyse av Affymetrix mikroarray-data i IPA viste signifikante effekter av EPS på 12 miRer. Dette var basert på filtrering av miRer ved  $p<0,05$ ,  $>1,5$  fold-change og «signalverdi» over 5. Pathway-analyse foreslo deres deltagelse i sykdommer og biologiske

funksjoner inkluderte nevrologiske sykdommer, psykologiske lidelser, posttranslasjonell modifisering, bindevevsutvikling og-funksjon, kardiovaskulær systemutvikling og funksjon. IPA prediksjon av topp oppstrøms regulatorer og deres interaksjonsnettverk pekte på blant annet AGO2 (argonaute RISC catalytic component 2), MET (MET Proto-Oncogene, Receptor Tyrosine Kinase), TGS1 (Trimethylguanosine synthase 1), XPO1 (Exportin 1) and TP53 (Tumor protein p53). Databasesøk identifiserte flere mulige mål for de regulerte miRene.

#### 4.4 Konklusjon

Elektrisk pulsstimulering hadde en signifikant effekt på miRer-innholdet i eksosomer, hvor det var en signifikant forskjell i 12 spesifikke miRer mellom ustimulerte og stimulerte (EPS) myotuber. Karakterisering av EVene viste at EPS ikke hadde noe effekt på EVs konsentrasjoner og størrelser. Endringene i EVs miR innhold forårsaket av EPS kan spille en viktig rolle i en rekke biologiske funksjoner som muligens gir gunstige effekter av trening.

## 5 Abbreviation

AGO2	Argonaute RISC catalytic component 2
ALIX	ALG-2- interaction protein X
AMP	Adenosine monophosphate
AMPK	AMP-activated protein kinase
ARF6	ADP-ribosylation factor 6
AT	Adipose tissue
ATM	Adipose tissue macrophage
ATP	Adenosine triphosphate
BDNF	Brain-derived neurotrophic factor
BMI	Body mass index
BSA	Bovine serum albumin
Ca <sup>2+</sup>	Calcium ions
°C	Celsius
CD	Cluster of differentiation
CDC	Centers for disease control and prevention
cDNA	Complementary deoxyribonucleic acid
CPR	C-reactive protein
CO <sub>2</sub>	Carbon dioxide
Ct	Cycle threshold
DMEM	Dulbecco's modified Eagle medium
DNA	Deoxyribonucleic acid
ECM	Extracellular matrix
EGFR	Epidermal growth factor
ELISA	Enzyme-Linked Immunosorbent Assay
eIF4	Signaling, regulation of eukaryotic translation initiation factor 4E
eNOS	Endothelial nitric oxide
EPS	Electrical pulse stimulation
ERK	Extracellular signal-regulated kinase
ESCRT	Endosomal sorting complex required for transport
EVs	Extracellular vesicles
EIF2	Eukaryotic initiation factor 2
FasL	Fas ligand

FFA	Free fatty acids
FCS	Foetal calf serum
g	Gravitation force
GLUT1	Glucose transporter type 1
GLUT4	Glucose transporter type 4
HbA1c	Hemoglobin A 1c
HDL	High density lipoprotein
Hz	Hertz
Hsa	Homo sapiens
Hsc70/Hsp70	Heat shock protein 70
IL	Interleukin
ILK	Signaling, integrin-linked kinase
ILVs	Intraluminal vesicles
IPA	Ingenuity pathway analysis
ISEV	International society for extracellular vesicles
kDs	Kilo dalton
Kg	Kilograms
kg/m <sup>2</sup>	Kilogram per meter squared
LAF	Laminar flow cabinet
LDL	Low density lipoprotein
M	Molar
M1	Cell seeding medium 1
M2	Cell proliferation medium 2
M3	Cell differentiation medium 3
M <sup>2</sup>	Meters squared
MEF2	Myocyte enhancer factor
mg	Milligrams
min	Minute
miR	MicroRNA
miRNA	MicroRNA
mL	Milliliters
ms	Milliseconds
mRNA	Messenger RNA
MLC	Myosin light chain

MLCK	Myosin light chain kinase
MV	Microvesicles
MVBs	Multivesicular bodies
myomiR	Muscle specific microRNA
NaOH	Sodium hydroxide
ng	Nanogram
NGT	Normal glucose tolerance
NFκB	Nuclear factor kappa-light-chain enhancer of activated B cells
NIPH	Norwegian institute of public health
Nm	Nano meter
NTA	Nanoparticle tracking analysis
p70S6K	70-kDa ribosomal protein S6 kinase
p value	Probability values
PBS	Phosphate buffered saline
PC	Phosphatidylcholine
PCR	Polymerase chain reaction
Pg	Picogram
PLD	Phospholipase D
Pri-miRNA	Primary miRNA
PTEN	Phosphatase and tensin homolog
REK	Regional Committees for Medical and Health Research Ethics
RhoA	Signaling, and ras homolog family, member A
RIN	Ribosomal integrity number
RISC	RNA-induced silencing complex
RNA	Ribonucleic acid
RNAse	Ribonuclease
rpm	Rotations per minute
RT	Room temperature
RT- qPCR	Real-time quantitative polymerase chain reaction
SARS-CoV-2	Severe acute respiratory syndrome coronavirus 2
SD	Standard deviation
SR	Sarcoplasmic reticulum
SEM	Standard error of mean
T2DM	Type 2 diabetes mellitus

TE	Tris-EDTA
TEM	Transmission electron microscopy
TGF	Transforming growth factor
TGF-beta	Transforming growth factor-beta
TGS1	Trimethylguanosine synthase 1
TSG101	Tumor susceptibility gen 101
TMB	3,3',5,5'-tetramethylbenzidine
TNF	Tumor necrosis factor
TP53	Tumor protein p53
3' UTR	3' Untranslated regions
V	Volt
WHO	World health organization
Wnt	Wingless-related integration site
XPO1	Exportin 1
μL	Microliter
μg	Microgram

## 6 Introduction

### 6.1 Overweight, obesity and type 2 diabetes mellitus

The ubiquity of overweight and obesity is a globally escalating serious plight. A problem initially linked to well developed countries, obesity is currently widespread in developing countries. This is due to change in life style, less physical activity and a high supply of unhealthy diets, as a result of urbanization (1).

World health organization (WHO) defines overweight and obesity as abnormal or excessive fat accumulation that presents a risk for health, where body mass index (BMI –  $\text{kg}/\text{m}^2$ ) is used as a guideline to designate obesity. The organization categorizes overweight as a BMI greater than or equal to  $25 \text{ kg}/\text{m}^2$  and obesity is a BMI greater than or equal to  $30 \text{ kg}/\text{m}^2$  in adults (2). According to a recent update from Centers for Disease Control and Prevention (CDC), obesity exposes individuals to dangers of critical long term diseases and elevates the chances of serious illnesses, such as type 2 diabetes, coronary heart disease, stroke, high blood pressure, cancer, musculoskeletal disorders such as osteoarthritis, and mental illnesses such as depression, and anxiety (3).

Statistics from WHO show that obesity has hit an epidemic scale where not less than 2.8 million people lose lives annually as an overweight or obese consequence. In an analysis done in 2015, circa 4 million deaths globally occurred as a consequence of excessive BMI, where over 70 % of the deaths were as a result of cardiovascular diseases (4).

In the opinion of WHO, the cause of obesity and overweight is an energy imbalance between calories consumed and calories used. Other factors such as physical inactivity and consumption of unhealthy foods containing high content of fat, sugar and salt can also cause obesity and overweight (Figure 1). A Living Conditions Survey done in 2015 in Norway showed that a difference in the level of education and socioeconomic status, did contribute towards overweight and obesity levels, in that there was a higher obesity level in individuals with low education compared with those with higher education (5). This indicates that education about the serious dire consequences of inactivity and poor eating habits can contribute toward reduction in obesity and overweight. Suggestions made by the Norwegian Institute of Public Health (NIPH) states that mental disorders might lead to obesity, since they

can affect the will power to self-control and regulation of the desire for food, which might lead to overeating and consumption of poor diets (2, 5). This shows that it is not only nutrition, but several other factors that play a role in development of overweight and obesity.

Diabetes mellitus is grouped in two categories namely type 1 and type 2 diabetes, where type 1 entails a damaged and dysfunction to the beta cells in pancreas accompanied with low or no insulin production, while type 2 diabetes is as a result of insulin resistance combined with an altered insulin secretion (6). In 2014, statistics from WHO suggested that about 422 million adults had diabetes globally (7). Complications that accompany diabetes include diabetic retinopathy, macrovascular issues, and kidney diseases (8).

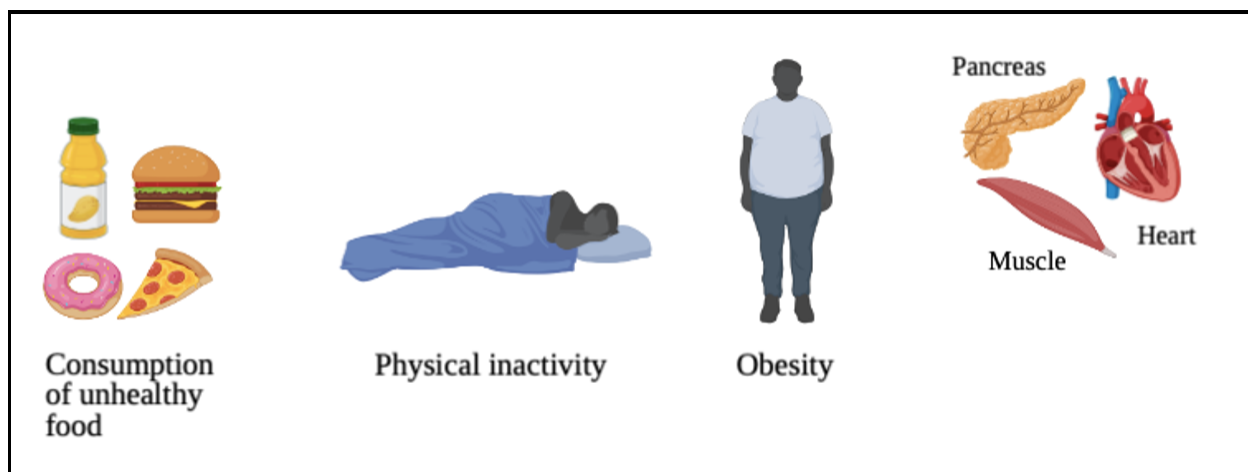


*Figure 1: Imbalance between calories consumed and calories used. Consumption of unhealthy foods with less physical activity can lead to obesity which is associated with insulin resistance in for example the pancreas, skeletal muscles and the heart. This can lead to diabetes and cardiovascular diseases. Figure designed by the thesis writer.*

## 6.2 Obesity and type 2 diabetes mellitus

Adipose tissue (AT) is a tissue that takes part in the regulation of glucose and metabolism of lipids, it is also involved in inflammation (9). It is divided into brown adipose tissue responsible for thermogenic activity and white adipose tissue responsible for storage of fat. The white adipose tissue consists of fibroblast and macrophages among adipocytes (10). In the course obesity development, the expansion of AT leads to adipocyte hypertrophy. And an increase in the AT and adipocyte volume leads to a decrease in insulin-mediated suppression and reduces the catecholamine stimulation of AT lipolysis. This might lead to elevated plasma levels of free fatty acids and an ectopic accumulation of lipid in insulin sensitive tissues such as liver, pancreas, skeletal muscle, the heart and kidney (11).



Another link to multisystem effects of obesity is the imbalance in homeostatic and proinflammatory immune responses (12). Obesity has been found to trigger the inflammatory pathways in adipose tissues and brain, that alters the physiological responses that play a role in the preservation of insulin and leptin sensitivity (12). The type of inflammation is a chronic low-grade activation of the immune system that affects the metabolic homeostasis over time. The hypertrophic-hyperplastic adipocytes facilitate the infiltration of monocytes to visceral adipose stroma which instigates the proinflammatory cycle between adipo- and monocytes (10).

The development of insulin resistance and type 2 diabetes mellitus is strongly associated with white adipose tissue (AT). As mentioned above, AT is known as an energy storage organ, but it is also an endocrine organ, that regulates whole-body homeostasis via a release of adipokines, lipids, metabolites, non-coding RNA, and extracellular vesicles (EVs). These signaling factors act on other metabolic tissues and regulate lipid and glucose homeostasis. This is what happens in healthy individuals. In individuals with obesity, the adipocyte-specific factors secretion has a defect and as a consequence it leads to low-grade chronic inflammation and insulin resistance (13, 14).

### 6.3 Skeletal muscles

In lean men and women, the skeletal muscle represent circa 40 % of the body weight and thus considered the largest organ in non-obese individuals (15). The vital cells in mature muscles are myocytes which develop from myoblasts to form muscles in a myogenesis process (16). These myocytes are in numerous forms with well-defined properties, and they include cardiac, skeletal and smooth muscle cells.

Skeletal muscle converts chemical energy into mechanical energy to generate force and power that maintains posture and mobility and enhances health. It contributes to the basal metabolic rate and acts as a storage for amino acids and carbohydrates required for maintenance of blood glucose levels during starvation (17). Skeletal muscles have a high capability of adapting and reacting to various environmental conditions, for example exercises or sedentarity, and physiological challenges such as inflammation and different forms of nutrition, by changing fiber composition and size (18). In addition to be a storage, skeletal muscles consume energy. This consumption is high during contraction by the molecular

motors which are the myosin heads and ion pumps (sarcoplasmic reticulum (SR)). The immediate source of energy during muscle contraction is ATP, but other metabolic pathways are activated to avoid ATP depletion if the muscle is fully activated. These pathways are divided into anaerobic (dominates during high-intensity physical exercise) and aerobic pathways (dominates during prolonged submaximal exercise) (19).

Insulin resistance is a feature in type 2 diabetes mellitus, and skeletal muscle is the main site of insulin-mediated glucose uptake site. It has been shown that skeletal muscle insulin sensitivity can be improved by contractile activity, since contraction among other mechanisms induces translocation of glucose transporters (GLUT4) from an intracellular location to the plasma membrane (20). In addition, it has been shown that exercise has beneficial effects such as secretion of myokines like IL-6, an anti-inflammatory cytokine, as a response to muscle contraction (21). A repeated homeostatic challenge induces cardiorespiratory and skeletal muscle adaptations which improve athletic performance. Furthermore, resistance exercise promotes muscle fibre growth and aerobic training increases the number of mitochondria or density and hence the oxidative capacity of muscles (22).

### 6.3.1 Skeletal muscle cells in cell culture

Adult skeletal muscle has the capacity to regenerate and adapt to physiological changes such as growth, training and injury and this adaptation is attributed to satellite cells *in vivo* (23). In addition to regeneration, satellite cells play a role in myofiber hypertrophy and remodeling where it was shown that they can expand acutely as a result of hypertrophy-inducing exercise *in vivo* (24). Satellite cells originate from adult skeletal muscles and are normally in a quiescent state, but after an injury, caused by for instance heavy exercise, the satellite cells are activated and can fuse with existing fibers and contribute to repair and growth. These satellite cells can be isolated from muscle biopsies, and *in vitro* they can proliferate into myoblasts which in turn can differentiate into myotubes and generate a cell culture model of primary human skeletal muscle cells (25). Satellite cells were first identified in a skeletal fiber of a frog in an electron microscopy study by Mauro A. et al., (26) and were found to be located between the sarcolemma and basal lamina (23).

It is a challenge to distinguish between genetic and environmental factors in *in vivo* studies, since they are generally very complex systems. Cultured myotubes represent a well-characterized *in vitro* model system of the skeletal muscle, where the extracellular

surroundings can be controlled and kept constant. The model is a vital system since, as observed in some studies, it displays the genetic background of the cells they originated from, and this provides possibilities for study of the innate features of the donor (27), thus identified for study in this thesis.

Even though cultured myotubes are proposed as a vital tool for study, the model has several limitations. They lack the *in vivo* microenvironment and communication available with other cells via direct contact and bioactive substances. Another limitation is that glucose uptake *in vivo* is regulated by its delivery, transport and metabolism unlike in cultured myotubes where it allows the studies of its transport and metabolism. Furthermore, in comparison to *in vivo*, in primary human myotubes, the insulin-stimulated glucose uptake is comparatively low, which might be as a result of a low expression of the insulin-responsive glucose transporter GLUT4 (25). In addition to the above mentioned, myoblast proliferation become exhausted as a result of increased passage numbers and this can affect the optimal function of the myotubes, for example the passages can result into reduced insulin sensitivity for glycogen synthesis and glucose oxidation (28). Age of the donors has been demonstrated to affect myotubes, where in older donors, the fusion capacity was shown to decrease, and the morphological aspects (thinner with few myonuclei) were affected compared to the myotubes obtained from young donors (29).

To be able to understand skeletal muscles in terms of their role in cell-to-cell communication, a cell culture that represents a model system for intact human skeletal muscle and one that can be modulated *ex vivo* is required. In order to create such a model, satellite cells isolated from skeletal muscle biopsies can be used (25). For the stimulation, a developed model that mimics muscle contraction *in vitro* (electrical pulse stimulation (EPS)) was used for the induction of muscle contraction in the cultured skeletal muscle cells. The model entails use of chronic, low-frequency EPS to stimulate the myotubes, over a decisive period of time and voltage. EPS has a robust effect that can cause metabolic and genetic adaptations *in vitro* where this has been investigated before in murine C2C12 cells (30-32). The investigation showed that there was an induction of contraction of myotubes, and effects caused *in vivo* as a result of muscle contraction like activation of the AMP-activated protein kinase (AMPK), glucose uptake stimulation and insulin sensitivity improvement were observed. Induction of several myokine expressions released from contracting skeletal muscles were observed as well. It was also observed that C2C12 and primary rat skeletal muscle cells cultures had a

good response to EPS and indicate that they were good models for the study of contraction-induced changes and mechanisms (33).

### 6.3.2 Skeletal muscle as a secretory organ

Skeletal muscles being an endocrine organ entails cells that are suggested to mediate communication between cells. Skeletal muscles do release molecules like lipids, amino acids, proteins, metabolites, small RNAs, and myokines among others, that contribute to cells communication (16). The cytokines and other peptides that are expressed and released have been classified as myokines by Bente Kiens et. al. (15). Myokines play a role in metabolic regulation, inflammatory processes, angiogenesis, and myogenesis (16). The muscle secretome, including the myokines, are believed to provide communication with other organs like liver, adipose tissues, brain, pancreas, bone and also cause autocrine effects (15).

Physical activities play a crucial role in creating a balanced secretion of myokines. A sedentary lifestyle is thought to push the secretion into a more pro-inflammatory direction (34). Physical inactivity in turn leads to visceral fat accumulation, which is a high-risk factor for cardiovascular diseases, diabetes, dementia, depression (Figure 2). These can be prevented by the skeletal muscle mediated protective effects via myokine secretion that might counterweigh the destructive effects of pro-inflammatory factors (15).

IL-6 is thought to induce anti-inflammatory and immunoregulatory effects where it was discovered to inhibit endotoxin-induced tumor necrosis factor (TNF, a pro-inflammatory factor) level in circulation of healthy individuals (35). The other anti-inflammatory effects are stimulating the secretion of anti-inflammatory cytokines IL-1ra and IL-10. These effects inhibit the pro-inflammatory factors that contribute to the low-grade inflammation seen in chronic diseases such as obesity, type 2 diabetes and coronary artery disease. Other effects caused by physical activity are the secretion of myostatin, and brain-derived neurotrophic factor (BDNF) among others (36). Recent studies show that skeletal muscle also release extracellular vesicles (EVs) into circulation (37).

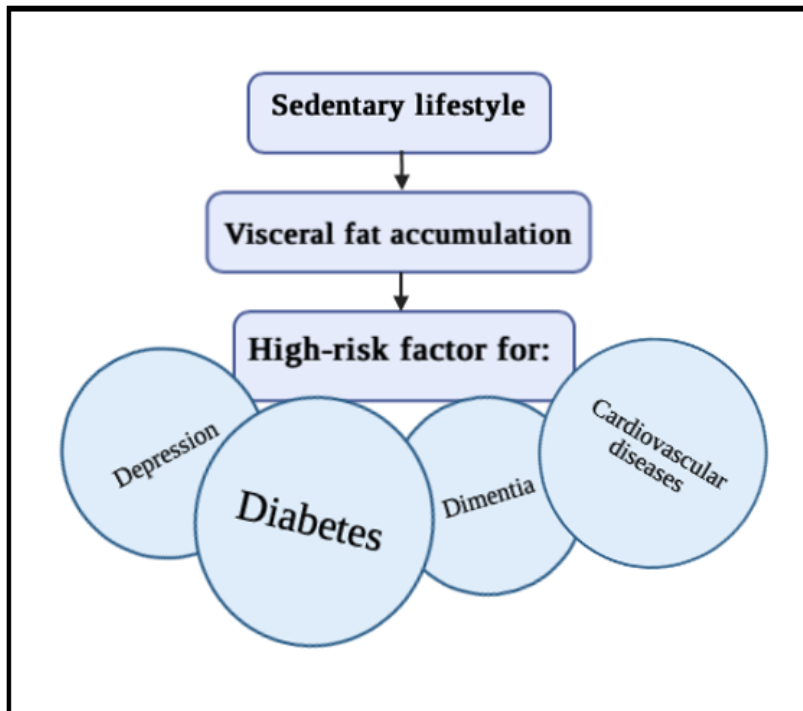


*Figure 2: Effects of physical inactivity. A sedentary lifestyle results into accumulation of fat that leads to infiltration of macrophage visceral fat. This in turn leads to a chronic inflammation that might lead to insulin resistance hence diabetes and other diseases. Figure designed by the thesis writer.*

### 6.3.3 Physical exercise

Evidence show that physical exercise activates signaling pathways that improve the functions of skeletal muscle. On the other hand physical inactivity poses a risk factor for chronic diseases like muscle atrophy and insulin resistance among others (38).

Exercise represents an exceptional complex alteration of homeostasis in numerous tissues that leads to an increase in metabolic demands of skeletal muscle contraction. The responses to exercises result in improved health and well-being.

Muscle contraction caused by physical exercise leads to a significant release of numerous molecules such as extracellular vesicles into circulation, whose effect has been demonstrated to be in various organs and tissues.

Regular physical activity has been suggested to improve numerous physiological and metabolic anomalies usually associated with T2DM, such as reducing body fat and an increase in muscle tissue, lowering blood pressure among others. This is an indicate that physical activity may play a critical role in the prevention and treatment of T2DM. T2DM

subjects have defects in insulin secretion from the beta cell, they have increased hepatic glucose production as a consequence of decreased insulin sensitivity in the liver, and a declined peripheral glucose utilization as a result of insulin resistance in skeletal muscles. Moderate to heavy intensity physical activity has proven to decrease blood glucose levels. This is as a result of the insulin-independent activation of glucose transport by physical activity and in addition an increased insulin sensitivity. Levels of GLUT4, an insulin-responsive glucose transporter have been shown to be increased in exercise-trained individuals and in T2DM individuals compared with sedentary individuals. This improves insulin sensitivity (39).

Muscle contraction has been suggested to release a number of important systemic factors into extracellular space such as EVs that contain a vast array of signaling molecules. These signal molecules have been suggested to have targets for various cells in organs for instance the brain and can prevent disease progressions (40).

Research has shown that in addition to an increase in circulating EVs, as a result of physical exercise, proteins encompassed in the EVs can also be upregulated (41). These increased proteins include ALIX (ALG-2 interacting protein-X), a protein associated with multi-vesicular body formation, rab proteins, and annexins, which are membrane trafficking proteins, and heat shock proteins, which are chaperones. Integrins and tetraspanins which are vesicle adhesion proteins are also increased (41).

Apart from being released into the extracellular space, there appears to be an uptake of these EVs into the recipient tissues (41). A vital function as this enables their transfer to target cells and the target specificity is mediated by adhesion proteins like integrins and tetraspanins found on the surface of the vesicles. This was demonstrated by Whitham M. et. al., when an isolation of EVs liberated into circulation after a 4-hour recovery from exercise were studied (41).

In addition, EVs have been suggested to play a role facilitating the myofiber repair and regeneration after a muscle injury. After an injury, there is a rapid influx of extracellular calcium which triggers vesicular activity internalization and non-vesicular reorganization, to repair the damaged area. These activities help the myofiber repair by securing the damaged areas of the plasma membrane into endosomal vesicles or shedding it through EVs (42).

## 6.4 Interleukin-6 (IL-6)

IL-6 is a cytokine classified as a myokine, which is released by muscle fibers from contracting skeletal muscles (21). Present studies show that IL-6 can be detected in plasma both in the course of and after a tough exercise (43). IL-6 functions are thought to vary between pro and anti-inflammatory activity (36). Low-grade systemic inflammation has been suggested to be linked to diabetes pathogenesis (44). A study by Aruna D. et.al., showed that increased levels of inflammatory markers (IL-6 and CRP (C-reactive protein) might possibly be associated with development of T2DM (44).

Numerous studies on physical exercise in humans have demonstrated that the contraction of muscles stimulates IL-6 mRNA synthesis (45). It has been proven that muscle contraction contributes towards IL-6 release into circulation. In this thesis IL-6 concentration was analyzed in the media from both unstimulated and stimulated (EPS) myotubes. Contraction of the muscles is thought to activate a series of signal pathways including AMP-activated kinase (AMPK), where a correlation between IL-6 and AMPK after 60 minutes of moderate intensity when muscle glycogen is low was found by MacDonald C. et. al. (46). AMPK activation is believed to stimulate other processes that escalate ATP generation, that encompasses fatty acid oxidation and glucose transport into skeletal muscles and switch off the ATP consuming pathways like fatty acid synthesis and cholesterol synthesis (47).

Studies have shown that an elevation of IL-6 might contribute to an increase of both cortisone and anti-inflammatory cytokines (IL-10 and cytokine IL-1 receptor agonist IL-1ra), which results in a delayed CRP increase in plasma. This demonstrates that IL-6 most likely has an anti-inflammatory effect whereby it induces an anti-inflammatory environment by inducing IL-1ra and IL-10 (36). Furthermore, investigations show that the plasma IL-6 concentration levels depends on the intensity of physical exercise (48).

In a previous master thesis (2019), IL-6 was determined in conditioned media. Differentiated myotubes were stimulated using electrical pulse stimulation (EPS), a model that induces contraction. This was to investigate and find out whether muscle contraction can lead to a release of IL-6 into the cell media. The results showed an increase of 23 % in IL-6 concentration in the media from the stimulated myotubes compared with the unstimulated (49).

## 6.5 Extracellular vesicles

For interaction and co-ordination both inside and outside remote organs that have significant functions in multicellular organs, effective intercellular communication is a necessity.

Extracellular vesicles (EVs) are recognized as potent conveyance of this communication.

They are a novel tool for communication by way of carrying their cargo components, a kind of “snapshot” of their cellular origin and releasing it into the extracellular environment by multicellular cells which causes physiological and pathological modifications to the recipient cell (50). Their first observation was as procoagulant platelet-derived particles in plasma by Chargaff, E and West, R in 1946 and were thought to be platelet dust (51).

Extracellular vesicles have been demonstrated to be released into the extracellular environment by cells from different organisms which includes eukaryotic and prokaryotic cells. As a result of this, together with other numerous groundbreaking discoveries like the presence of RNA in EVs (52), EVs have become an interest of study that has rapidly grown in the scientific research population in recent years. Extracellular vesicle, a name referring to particles naturally released from a cell delimited by a lipid bilayer that encompasses no useful nucleus, was endorsed by ISEV (International Society for Extracellular Vesicles) (53). They are a heterogenous class of membrane enclosed nanoparticles, whereby based on their postulated mechanisms of release from cells and their sizes, they are classified into divergent groups (54). The lipid bilayer membrane consolidated with proteins protect the EVs cargo from digestion or degradation by proteases and nucleases during their passage through the extracellular environment. EVs embodies bioactive receptors on the surface, cargo lipids, proteins and RNA (mRNA and non-coding RNA, microRNA and viral RNA among others) that interact with target cells (Figure 3). They have been isolated and can be detected in diverse biological fluids which includes; semen, blood, urine, saliva, breast milk, bile, amniotic fluid, and cerebrospinal fluid (55). Their detection in biological fluids has led to their promising function as sources of diagnostic disease biomarkers (56).



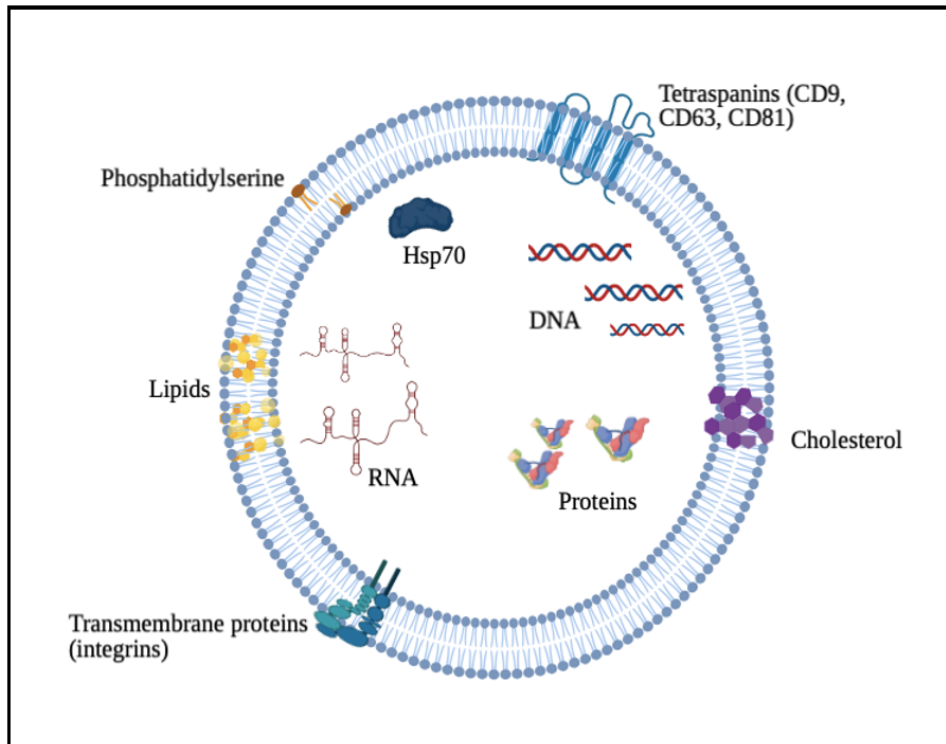


*Figure 3: Schematic representation of an extracellular vesicle (EV) and its cargo components. Cells release EVs that are membrane embedded and contain surface receptors, proteins, lipids and ribonucleic acids through which communication from parent cells to recipient cells occurs. Figure by the thesis writer, inspired by Yang J. et. al. (57). RNA (ribonucleic acid), DNA (deoxyribonucleic acid), Hsp70 (heat shock protein 70).*

### 6.5.1 Categorization of extracellular vesicles

The categorization of extracellular vesicles was before based on their size, biogenesis pathways and surface markers hence divided into three groups: exosomes, microvesicles (MV) and apoptotic bodies. The current guidelines provided by the International Society for Extracellular vesicles (ISEV), urges the use of operational terms for EVs subtypes that refer to; physical properties such as size (small EVs (exosomes), medium/large EVs (MV), biochemical compositions (CD63, CD81, annexin A5-stained etc.) and cellular condition description on which the cell originated from (apoptotic bodies, podocyte EVs etc.). This is believed to be as a result of the consensus not being able to come up with definite markers for EVs and the difficulties in their designation to a precise biogenesis pathway (53).

Despite their categorization, their common characteristic is a lipid bilayer membrane that protects the cargo biomolecules (50). EVs have a broad size range from 30 nm – 5 µm in diameter, with the lowest and most abundant vesicle in existence being exosomes at ~30 – 100 nm (54), followed by MV at ~100 – 1000 nm and the largest being apoptotic bodies at ~1000 – 5000 nm (Figure 4). Exosomes roughly overlay the viruses in diameter, while MV

do the same with bacteria and insoluble immune complexes, for instance protein aggregates. Apoptotic bodies have a diameter range of about the same size as blood platelets (58).

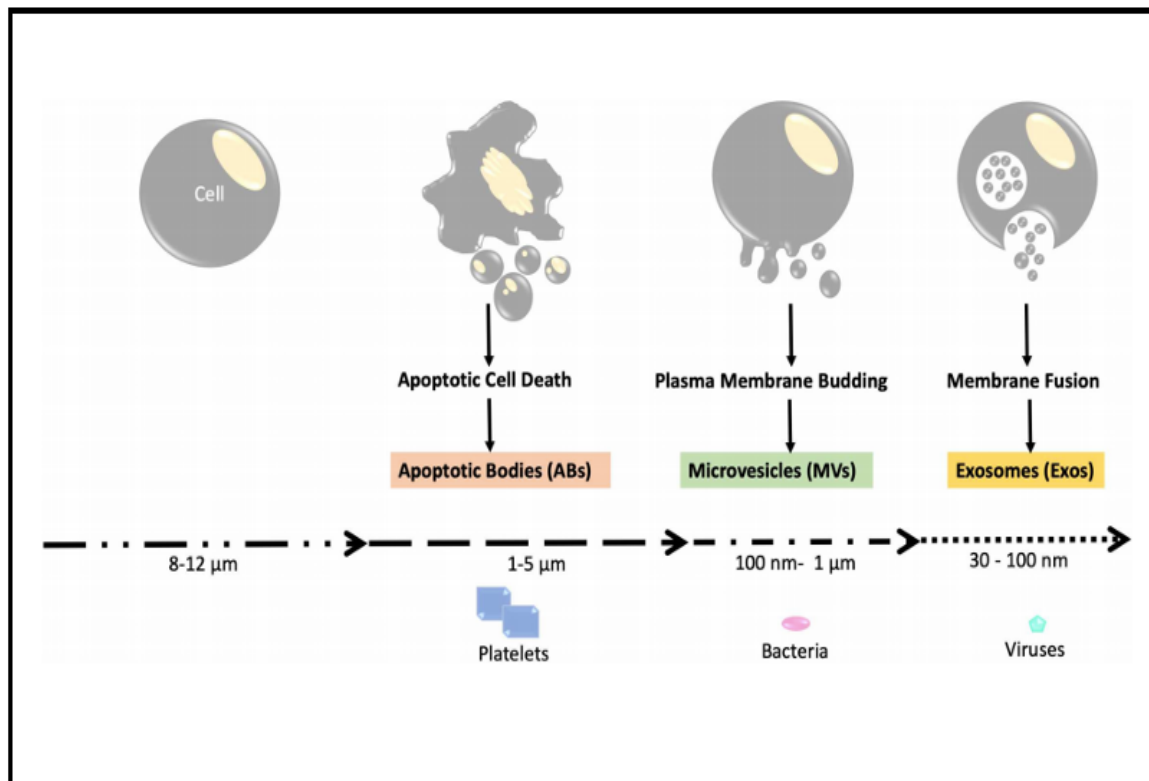


*Figure 4: Diameter ranges for extracellular vesicles. Overlaying the virus, exosomes range from ~30 nm - 100 nm, while microvesicles overlap with bacteria ~100 nm – 1000 nm and apoptotic bodies are almost the same size as blood platelets ~1000 nm – 5000 nm. Figure was used with permission from Yang Jing (59) .*

## 6.5.2 Biogenesis and composition of extracellular vesicles

### 6.5.2.1 Exosomes and their biogenesis

Secreted by numerous cell types into the extracellular expanse, exosomes are believed to be of an endosomal origin. They are bound by a bilayer of phospholipids rich with ceramide and cholesterol. They were discovered and described by Johnstone et al. in 1983 while examining reticulocytes' maturation into erythrocytes, where it was presumed to be a way by which plasma membrane proteins were discarded in maturing reticulocytes (60).

Exosomes emerge through 3 distinct phases; first, from the plasma membrane where the endocytic vesicles are formed and create the early endosomes that mature into late endosomes, second, an inward budding of endosomal membranes which ensues in a gradual increase of intraluminal vesicles (ILVs) within large multivesicular bodies (MVBs). ILVs constituents are from the cytosol. Fusion of MVBs with the plasma membrane and secretion

of the vascular constituents into the extracellular environment is the third phase (Figure 5). The MVBs contain different biochemical properties that determine their fate. Relying on this, they can be transported to the plasma membrane where they either can fuse with the plasma membrane and secrete their components (exosomes) into the extracellular environment (exocytosis), or they can be destined for protease degradation in the lysosomes (61, 62).

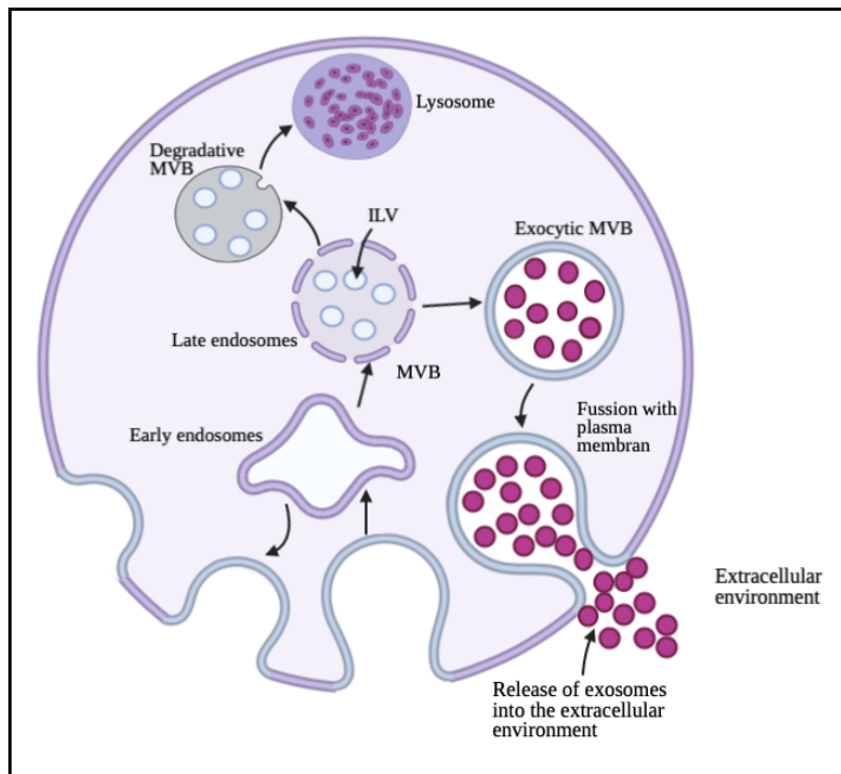


**Figure 5: The biogenesis of exosomes.** The exosomes are formed through different stages. The endocytic vesicles are formed from the plasma membrane and create the early endosomes that mature into late endosomes. This is followed by inward budding of the endosomal membrane that leads to a gradual increase of intraluminal vesicles (ILVs) within multivesicular bodies (MVBs). MVBs fuse with the plasma membrane resulting into the release of its constituents into the extracellular environment which are exosomes. Figure designed by the thesis writer inspired by Mathivanan S. et. al. (61). ILV (intraluminal vesicles), MVB (multivesicular bodies)

According to various studies, the synthesis of exosomes has been proposed to be through two pathways. The first is where the formation of exosomes (MVBs and ILVs) and protein sorting by application of a molecular machinery known as ESCRT (Endosomal sorting complex required for transport) take place. This machinery encompasses of four complexes of proteins; ESCRT-0, -I, -II and -III. All these four complexes have critical functions in different stages of exosome synthesis (37, 63). The second is an ESCRT-independent pathway where MVBs are formed without the presence of ESCRT constituents. This pathway is centered on the conversion of sphingomyelin into ceramide, which leads to the formation of lipid rafts. Due to a structural imbalance in the ceramide rich regions, an inward bending of

the membrane is caused, and MVBs are created (50, 62). In addition, the transmembrane proteins, for example tetraspanins, that merged into the invaginating membrane have been suggested to be involved in the secretion of exosomes through the ESCRT-independent pathway. However different the pathways are, it is believed that they might function synergistically with the end result being exosome synthesis (64).

Another thing worth mentioning is, it has been proposed that cellular homeostasis might play a role on whether MVBs ends up being degraded or end up in lysosomes. Or whether they will be secreted into the extracellular space. This is as a result of numerous studies showing that there is an increase of exosome release as a consequence of cellular stress even though the reason behind the exosome release response by the cells is not known. But it is assumed that it might be one of the elimination methods of the waste products where the exosomes are destined for degradation by phagocytes or a means of cell-to-cell communication about the cellular stress through an increase in exosome secretion (64).

#### 6.5.2.2 Composition of exosomes

The components of exosomes are postulated to be of luminal cargo or of endosomal origin. The luminal cargo mainly consists of protein, lipids, and nucleic acid. During exosome synthesis, the proteins found in exosomes are incorporated into exosomes for a cell-to-cell communication function (62). The protein cargo of exosomes consists of; membrane transport and fusion protein (e.g GTPase, annexins and flotillin), heat shock proteins (e.g heat shock protein Hsp90 and heat shock cognate Hsp90), tetraspanins (e.g CD9, CD 63, CD81 and CD82) and proteins associated with MVBs biogenesis (e.g Alix and TSG101(Tumor susceptibility gen 101)). Other proteins incorporated in exosomes are thrombospondin, CD55, CD59 and lactadherin (65). Depending upon the cell of origin, exosomes contain numerous lipid compounds identified to play a role in exosomes synthesis, and this includes phosphatidylethanolamine, phosphatidylcholine, phosphatidylserine, ceramide, cholesterol, sphingomyelin among others (62). The lipids have biophysical properties to exosomes that detects the rigidity and delivery efficiency. The exosomes nucleic acids cargo includes microRNA(miR), messenger RNA (mRNA), and different non-coding RNA. These nucleic acids play different functions in that, the mRNA transferred by exosomes from the parent cell to the recipient cell can be translated into proteins. MicroRNA and non-coding RNA regulate gene expression.

### 6.5.2.3 Microvesicles and their biogenesis

Microvesicles were first described as a precipitating factor likely to create thrombin in platelet free plasma by Chargaff and West in 1946. They are larger than exosomes, but similar to exosomes in terms of the membrane bound feature and a shared overlap in size ranges. The nomenclature is not standardized and different names have been proposed to identify MV, thus referred to as shedding vesicles for tumor cells, ectosomes for neutrophils and fibroblasts, shedding bodies for neurosecretory cells, microparticles and MV (a name often used in literature) among others depending upon their cell of origin (66).

Microvesicles are formed through outward budding of the plasma membrane (Figure 6). The distribution of proteins and phospholipids within the plasma membrane is not symmetric, and the distribution is regulated by aminophospholipid translocases (67), which are proteins that transfer phospholipids from one leaflet to another. These translocases are known as flippases (transfer phospholipids from outer to inner membrane leaflet) and floppases (transfer phospholipids from inner to outer membrane leaflet).

An increase in intracellular  $\text{Ca}^{2+}$  and activation of enzymes that degrade proteins leads to the breakdown of the cytoskeleton which in turn separates the plasma membrane from the cortical cytoskeleton. Simultaneously the lipid translocases, enzymes involved in the maintenance of the membrane asymmetry, are activated to induce changes within the membrane bilayer. This is whereby the phosphatidylserine, by the help of floppase, translocate to the outer membrane leaflet. This leads to an unstable structural within the lipid bilayer hence the budding of the membrane (50). For the membrane detachment, there are several proteins involved. The GDP-binding protein ADP ribosylation factor 6 (ARF6) commences the signal cascade (68). Phospholipase D (PLD) is activated, and PLD hydrolyses phosphatidylcholine (PC) resulting in membrane-bound phosphatidic acid (PA), which in turn recruits extracellular-signal-regulated kinase (ERK). ERK phosphorylates and activates myosin light-chain kinase (MLCK) that phosphorylates and activates myosin light chain. This in turn leads to the contraction of the cytoskeletal structures (actin-myosin interaction) followed by abscission of MV (Figure 6) (69).

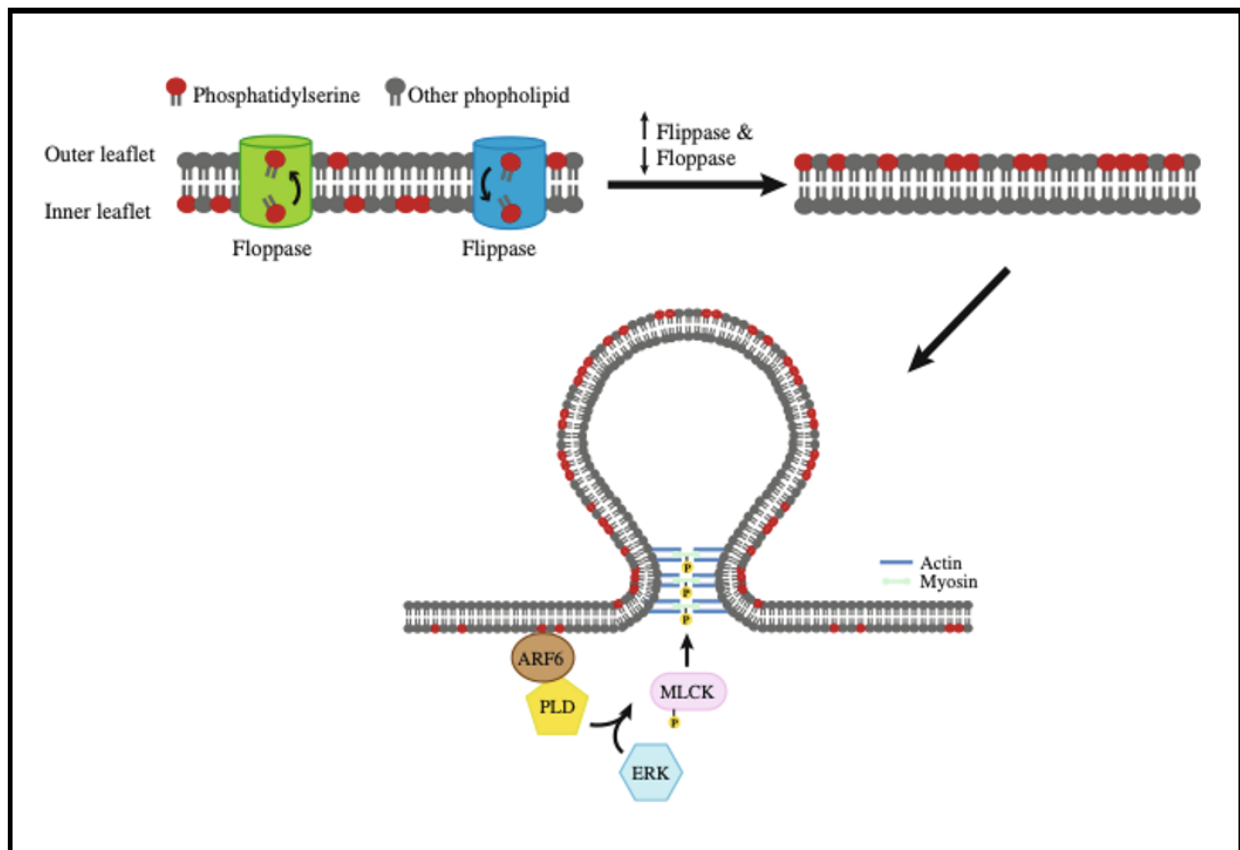


**Figure 6: Microvesicle formation.** The plasma membrane is not symmetric, and the protein and phospholipid distribution is regulated by aminophospholipid translocases which include flippase, that translocates phospholipids from the outer membrane leaflet to the inner membrane leaflet, and floppase, that transfers phospholipids from the inner membrane leaflet to the outer membrane leaflet. For the outward budding of the microvesicles to occur, several proteins are involved where ADP-ribosylation factor 6 (ARF6) instigates the signaling cascade. Phospholipase D (PLD) is activated, and this recruits extracellular signal-regulated kinase (ERK) to the plasma membrane. ERK phosphorylates and activates myosin light-chain kinase (MLCK), whose phosphorylation and activation of myosin light chain leads to abscission of microvesicles. Figure used is from (69) and a request for permission was registered on Springer Nature Permission Providers.

#### 6.5.2.4 Composition of microvesicles

Unlike the exosomes, whose plasma membrane is identical to the parent cells, the MVs' plasma membrane is not, since certain changes are created upon nucleation and budding of the plasma membrane. Their cargo contents depend upon the cell of origin, just like in exosomes, and the determination of their cargo contents is an ongoing research process. The components of cargoes in MV might be similar to that of exosomes generally in terms of proteins, lipids (e.g cholesterol) and RNA contents, but not all are identical. The major protein markers for MV are integrins, selectins and CD40 ligand, and they too contain phosphatidylserine (70, 71). In addition, they contain annexin V binding protein. According to a search done in Vesiclepedia, the MVs' molecular composition is heat shock protein HSP90B1, receptors (e.g EGFRvIII a mutated form of epidermal growth factor receptor that

is tumor specific, GPR150-G protein-coupled receptor) among others. As for nucleic acid, mRNA, and RNA have been detected in serum MV (72).

#### 6.5.2.5 Apoptotic bodies and their biogenesis

The expression “apoptotic bodies” was invented by J. F. R. Kerr in 1972 and which was described as a controlled deletion mechanism in the animal cell population regulation (58, 73). Apoptosis is a programmed cell death mechanism for both normal and cancerous cells. Argued as the largest EVs, they are ~1000 – 5000 nm in diameter and overlap with MV in size ranges. Apoptotic bodies are formed by blebbing of the plasma membrane during apoptosis.

One thing that makes apoptotic bodies different from the rest of EVs is that they are thought to contain cell organelles and fragmented genomic DNA (55).

#### 6.5.3 Extracellular vesicles' interaction with recipient cells and uptake

The revelation that EVs had the ability to influence and cause physiological changes in target cells via transferring of functional cargo components, created a humongous interest in the research population. This was because EVs created a numerous number of possibilities as a result of cell-to-cell communication for example, the potential of a possible conversion of EVs into vehicles, that can transfer and deliver therapeutic compounds and drugs (74, 75). Studies have shown evidence of functional mRNA and RNA transfer from a parent cell to a recipient cell, where protein from a mouse were able to be identified in the target human cells (76). In addition, as a result of SARS-CoV-2 (Covid-19), SARS-CoV-2 mRNA vaccines were developed based on EV principles and are currently in use (77). The process entailed in the EVs uptake or internalization by the target cells is still debatable, though numerous EVs uptake mechanisms have been suggested (37, 75, 78).

It is postulated that receptors and ligands exposed on the plasma membrane surface accounts for EVs transportation and deliverance of cargo components. On the other hand, the uptake of the cargo components by recipient cells depends upon the type of target cell, plus other various crucial elements such as signaling status of the target cell (51, 79). Being highly abundant on the surface of EVs, tetraspanins have been suggested to play a crucial function with regard to internalization of EV in the recipient cells. Tetraspanins such as CD9, CD63 and CD81 are the popularly known exosome biomarkers, and CD9 and CD81 have been

proven to participate in oocyte-spermatozoa fusion (75, 80). This is where an investigation was performed and egg fusion protein, upon associating with CD9, changed conformation and interacted specifically with a sperm fusion protein (81).

Several experiments have been done to demonstrate EVs uptake and internalization via endocytosis, an example being clathrin-mediated endocytosis (Figure 7). This is a process whereby the clathrin-coated vesicles, damage the membrane which collapses into a vesicular bud, matures and pinches off. The intracellularly vesicle undergoes clathrin un-coating and fuses with the endosome where it releases its cargo. Macropinocytosis is another suggested alternative way through which cargo is transferred and received. This is through the ruffle membrane invagination that is then pinched off intracellularly. Phagocytosis is another process performed by macrophages where there is the invagination of the target material that are marked (by phosphatidylserine) to be internalized for example apoptotic bodies. Phagocytosis is known to apply mainly to larger particles, but studies have shown that this can apply to smaller particles too, hence there is a possibility of EVs internalization via phagocytosis (75). Macropinocytosis and phagocytosis mechanisms have been suggested to be clean-up mechanisms (82).



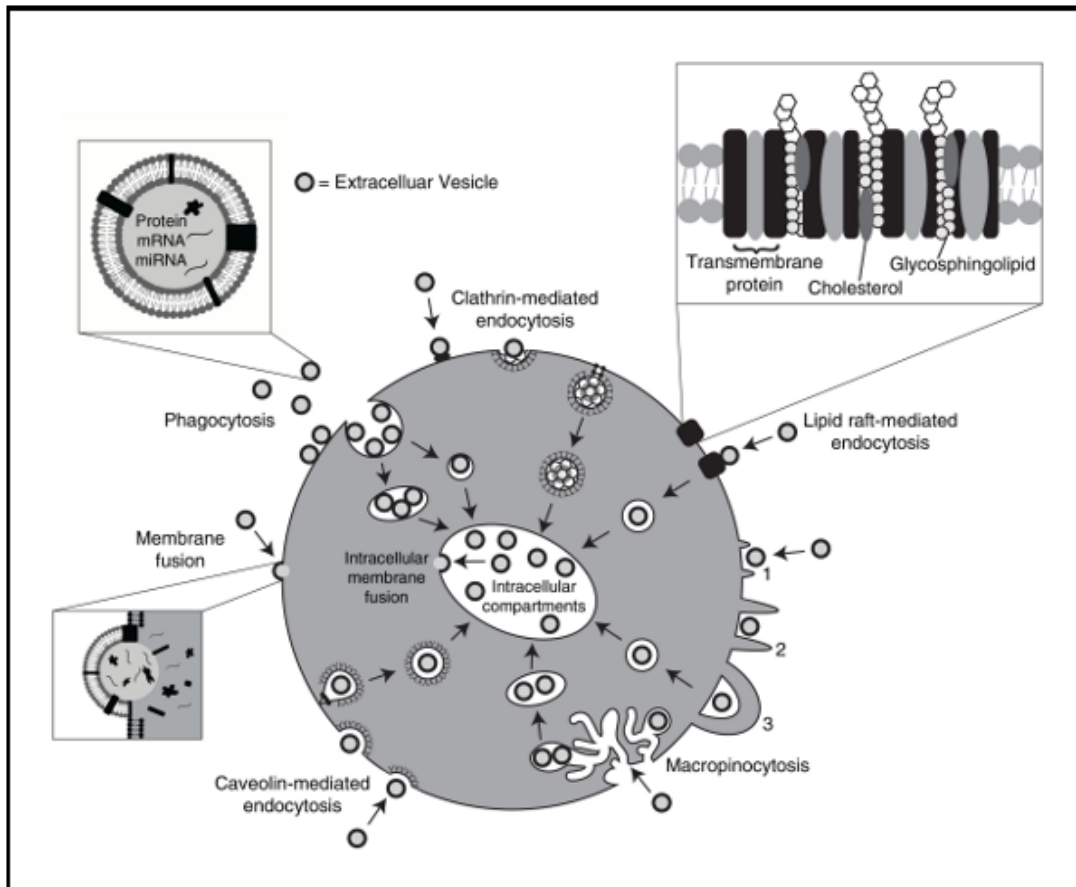


**Figure 7: Extracellular vesicles (EVs) uptake.** After secretion of EVs into the extracellular environment and transported to the target cell, EVs are internalized into the target cells via numerous mechanisms. This includes phagocytosis, endocytosis, and macropinocytosis among others. Figure from (75) and a request for permission was registered on USJournalPermissions.

#### 6.5.4 Extracellular vesicles in type 2 diabetes mellitus and obesity

Obesity has been shown to be associated with an increase in circulating EVs amount, where women with severe obesity were found to have higher number of plasma EV compared to a normal-weight control group (83). In a previous study, there was a higher level of plasma EVs in obese individuals compared to the healthy weight in where it wasn't clear whether the increase in plasma EVs was as a result of an increase in exosomes, MV or both (84). The plasma level increase of EVs in this individuals was also found in excessive weight (BMI = or > 25 kg/m<sup>2</sup>) (84). In another study the expression of exosomal microRNAs were different when compared between those with visceral obesity and lean individuals (85). TGF-beta and Wnt/beta-catenin signaling were found to be the top canonical pathways targeted by miR-23b, miR-148b, miR-4269, and miR-4429, the miRs that differed between the lean and obese individuals (85).

Complications associated with obesity are as a result of induction of inflammation in major metabolic organs (liver, adipose tissue and skeletal muscle). In another study it was found that exosomes released from adipocytes stimulated the differentiation of monocytes into active macrophages and induced increased pro-inflammatory cytokine secretion like IL-1 and TNF (86) suggesting a pro-inflammatory role of exosomes. However, in another investigation, exosomes were found to have anti-inflammatory roles where adipose-derived stem cells secreted exosomes that inhibited adipose inflammation (87). Exosomes have been shown to regulate insulin sensitivity through different mechanisms, one of them being by modulating inflammation and the second by direct interaction with insulin-response organs. The human adipose tissue derived EVs regulate hepatic and skeletal muscle insulin signaling by interacting with signaling molecules like serine/threonine kinase Akt (83).

Two previous master theses performed at OsloMet compared myotube cultures from severely obese donors with diabetes (T2DM) and normal glucose tolerance (NGT), with an aim of establishing whether EVs from these two groups are different and determine the protein and RNA (microRNA) profile of the EVs (49, 88). Transcriptomics analysis showed that 160 different miRNAs were present in both diabetes and NGT groups. A bioinformatic filter demonstrated that 6 miRNAs were significantly different between T2DM and NGT. This included miR-23a-3p, miR-663a, miR-6789-5p, miR-6808-3p, miR-4674 and miR-7641 (88). A proteomic analysis detected 604 proteins that appeared in exosomes from both diabetes and NGT myotubes, of which 204 appeared in significantly different amount (49). Glycolysis was the top bio-functional pathway in which proteins were involved (88).

#### 6.5.5 Extracellular vesicles and training

Training stimulates a release of various bioactive molecules into the extracellular space, where for example inter-tissue signaling for example proteins are deduced to be vital mediators of adaptations to exercise. Some of these proteins have been suggested to be packed in extracellular vesicles (41).

In addition to myokines, EVs have been suggested to encompass microRNAs and other bioactive molecules that are released into the extracellular environment, as other mechanisms through which physical exercise benefits are relayed to other tissues (89).

The biomolecules entailed in EVs include different non-coding RNA, and it has been established that there are skeletal muscle specific microRNAs (miRNAs) myomiR. Their function is believed to be down-regulation of expression of mRNAs and proteins and that their expression depends on physical activity level or intensity. Some of these muscle specific myomiR include miR-1-3P, miR-133a, miR-133b, miR-206, miR-208b, miR-486, and miR-499 and hence the name myomiRs (89) (38).

In addition to microRNA, EVs encompass adhesion proteins that mediate localization of EVs to specific tissues. The emergence of these proteins has been suggested to vary, where it was shown by proteomics that there was a wide range of protein increase in the systemic circulation with exercise compared to at rest (41).

In an earlier master thesis at OsloMet, a proteomic analysis was performed on electrically stimulated skeletal muscle cell derived EVs. In this thesis, it was demonstrated that EVs do contain proteins and EPS changed the content of 75 proteins in exosomes, 51 were increased and 24 decreased. Pathway analysis of the affected proteins based on the fold change, suggested biological pathways as Eukaryotic initiation factor 2 (EIF2) signaling, regulation of eukaryotic translation initiation factor 4E (eIF4) and 70-kDa ribosomal protein S6 kinase (p70S6K) signaling, integrin-linked kinase (ILK) signaling, and ras homolog family, member A (RhoA) signaling to play a role (49).

#### 6.5.6 Isolation and characterization of extracellular vesicles

So, much has been done in the EV field in terms of EVs biology and biogenesis and more is yet to be discovered, since this is such a deep field that is continually expanding. In spite of that, there is a major limiting factor that still creates holes to be filled. This is with regard to how much knowledge there is about EVs, this factor is EVs isolation. One of the reasons is no census for a standardized method for EV isolation. The international Society for Extracellular Vesicles (ISEV) has made an effort to address this through various articles such as the minimal experimental requirements for definition of EVs and their function (90), extracellular vesicles RNA analysis and bioinformatics (91) and applying extracellular vesicles based therapeutics in clinical trials (92, 93). Even so, minimal information is available about what is practiced on the ground. This is as a consequence of different EVs isolation and varying protocols applied. Ultracentrifugation is the method appraised as a gold standard method. It comprises of varying repeated centrifugal forces where EVs are separated based

on their buoyant density by centrifugation, gel filtration and in addition washing in between these centrifugations, thus a necessity for standardized methods. An introduction of newer methods like precipitation with polyethylene glycol came about as a result of utilization of the solubility and aggregation of EVs (55).

The characterization of EVs was meant to certify that what was recovered from previous EV preparations were indeed EVs. Extracellular vesicle characterization methods that are commonly used are nanoparticle tracking analysis (NTA), western blotting and flowcytometry. In line with ISEVs guidelines, the minimal requirement for EVs characterization include a minimum of 2 varying technologies. Electron microscopy (transmission electron microscopy) or atomic force microscopy which shows EVs images, and for size and concentration assessment, nanoparticle tracking analysis (NTA) (93).

## 6.6 MicroRNA

EVs have been proven to contain RNA, and the existence of functional or non-coding RNA in EVs were first reported between 2006 and 2007 (76, 94).

MicroRNAs (miRNAs) ~22 nucleotides (nt) long, are a wide family of short, highly conserved, single-stranded non-coding RNA molecules, that modulate the expression of protein-coding genes negatively. They are presumed to be found in body fluids and are released from cells encapsulated inside extracellular vesicles (EVs). The discovery of this expression modulation was established in 1990s. miRNA's class founding member *Caenorhabditis elegans* gene *lin-4* and *Let-7* identified by Lee et al., in the 1990s was found to activate the translational repression of specific target mRNAs, by binding to the 3'-untranslated region (UTR) (95, 96).

The transcription of majority miRNAs is from genome DNA to precursor molecules as primary transcripts (pri-miRNAs) performed by RNA polymerase II. The transcripts carry hairpins which encompasses a double strand stem (stem-loop structure) in which lies miRNA and have a 5' cap and 3' poly-A tail (97). A microprocessor complex comprising of RNase III enzyme Drosha (catalyzes the excisions) (98), and DGCR8 (Di George Syndrome Critical Region Gene 8), a protein binding double-stranded RNA, locates the excision area on 5' and 3' overhangs bound to the stem-loop). The complex then cleaves and releases the hairpins and pri-miRNA are converted into precursor miRNAs (pre-miRNA), which are ~70 nucleotides

long. Following exportation of pre-miRNA from the nucleus to the cytoplasm by exportin 5, an additional complex encompassing of RNase III enzyme, Dicer binds to pre-miRNAs, cleaves off the loop from the hairpin where a miRNA duplex with an average of ~22 nucleotides in length is generated. The double stranded duplex contains two strands: miRNA passenger strand and mature miRNA guide strand. The guide strand is integrated into the RISC (RNA-induced silencing complex) that contains RNA-binding protein family such as argonaute (Ago 2) that promotes the binding of mature miRNA to the target mRNA. This leads to inhibition of translation or degradation of the target mRNA by binding to the 3' untranslated region. The passenger strand is degraded by nucleases (97, 99) (Figure 8).

Cardiac and skeletal muscle development are postulated to be controlled by miRNA. The miRNA expressions are activated by myogenic transcription factors that regulate the expression of genes that take part in muscle growth, differentiation and contractility. Numerous miRNAs are expressed specifically in cardiac and skeletal muscle, and these include members of miR-1, miR-206 and miR-133a, miR-133b families. Mir-206 and miR-133b are expressed mainly in skeletal muscle. In an *in vitro* investigation on C2C12 skeletal muscle cells, mirR-1 was found to repress the expression of histone deacetylase 4 (HDAC4), which is a negative regulator of differentiation and an inhibitor of the myocyte enhancer factor (MEF2) transcription factor. Which means that the inhibition of HDAC4 by miR-1 initiates a positive feed-forward loop, where the upregulation of miR-1 by MEF2 leads to additional HDAC4 inhibition and increases MEF2 activity which drives myocyte differentiation. In C2C12 myoblasts, miR-206 was shown to promote *in vitro* where there was an induction of differentiation through inhibition of a subunit of DNA polymerase alpha (Pola1), connexin 43 (Cx43), among others (100).

As mentioned above, miRNAs do regulate gene expression negatively at a post-transcriptional level by binding of miRNAs to the 3'-untranslated region (UTR) of distinct mRNA sequences. This is through miRNA's 2 – 8 nucleotides (representing a seed area) base pairing. This results in a protein expression decrease, where mRNA translation is repressed, and mRNA is degraded. Among protein-coding genes, an estimated over 60 % is believed to be regulated by miRNAs. In addition, miRNAs can bind and regulate more than one target gene. This is as a consequence of miRNAs ability having numerous binding sites into a 3'UTR, leading to a synergistic interaction with effective repression and later degradation of mRNA (95, 101).

Extracellular vesicles are considered as novel tools for cell-to-cell communication through mediation of biological information to other cells. As a result of detection of their presence extracellularly and in body fluids, EVs components i.e miRNAs have been thought to play a critical function in their use as biomarkers for diagnosis and prognosis of various human diseases. In an investigation done by Wang Q. et. al., there was a high expression of miR-377 in a mouse diabetic nephropathy model and through stimulation with TGF-beta. Stimulation by TGF-beta led to an increase in expression of miR-377 (102). The upregulation of this miRNA in mesangial cells lead to an increase in fibronectin. MiR-377 targets and inhibits p21 protein and a knock down of this protein increases fibronectin production (102), a glycoprotein which takes part in cell-adhesive interactions.

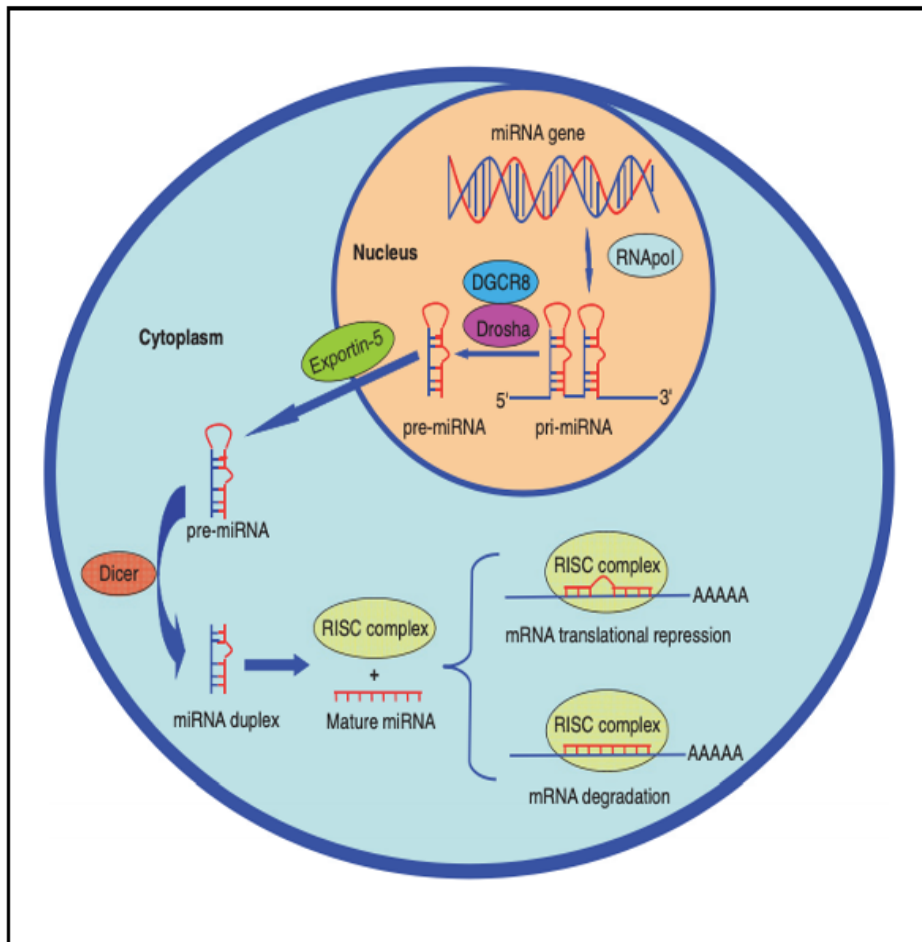


**Figure 8: Biogenesis of miRNA.** The transcription of pri-miRNA (immature primary microRNA) is performed by RNA polymerase (RNAPol). Before maturation, the Drosha and DGCR8 (microprocessor complex) cleaves pri-miRNA generating a precursor miRNA (pre-miRNA). This is followed by exportation of pre-miRNA from the nucleus to the cytoplasm where the hairpin is cleaved off by Dicer, and a double-stranded RNA duplex is formed. Argonaute 2 (Ago 2) protein plays a role in the separation of the double stranded, and a single-stranded mature RNA is generated followed by the binding of the mature miRNA with RISC. This results into regulation of the target gene expression. DGCR8 (DiGeorge Critical Region 8), RISC (RNA-induced silencing complex), mRNA (messenger RNA) Modified from (103) and was registered as used on [permissionsaacr.org](http://permissionsaacr.org).

## 7 Aim of the study

Physical exercise has numerous beneficial effects not only on the muscles that train but on other organs in the body such as the liver, adipose tissues, heart and respiratory system among others. These beneficial effects are mediated through various signaling pathway systems such that they lead to intracellular responses. Earlier studies done on skeletal muscle cells using proteomics illustrated that skeletal muscle stimulation by EPS (electrical pulse stimulation) had a significant effect on protein levels encompassed in EVs released by skeletal muscle cells. This fueled interest in finding out more about the potential of EVs cargo components. MiR another EV component that have been found to be enriched in skeletal muscles, whose role and function was not fully known or understood captured an interest to study.

In this study, EPS, a training model that mimics muscle contraction *in vivo* and satellite cells, cells that can be isolated from muscle biopsies, activated to proliferate into myoblasts and differentiate into myotubes in culture were used. This is because the cell cultures constitute a model system for intact human skeletal muscle and can be modulated *ex vivo*. Furthermore, the model provides relevant genetic background for studies where extracellular environment can be controlled. Using these two, we wished to study and characterize the cargo contents of extracellular vesicles which included exosomes and MV isolated from the unstimulated and stimulated (EPS) myotubes. This was with an aim of finding out:

- Whether skeletal muscle cell release microRNA into extracellular environment, if yes, is there any difference between microRNA found in EVs derived from unstimulated myotubes and stimulated (EPS) myotubes?
- Does EPS have any effects on EVs in terms of size and concentration after stimulation of myotubes?

## 8 Methods and material

### 8.1 Materials and ethics

Specimens used in this project were kindly provided by Oslo Metropolitan University in conjunction with Vestfold Hospital Trust in Tønsberg. The cells used in the study were primary human skeletal muscles cells, isolated from abdominal muscle biopsies (the inner oblique abdominal muscles) of severely obese donors. The sample materials were acquired during a gastric by-pass surgery from severely obese women donors (n=6) aged 34 – 60 years with T2DM during a gastric by-pass surgery (Table 1). Each donor was assigned with a unique identification code that contained two letters and a double digit, that referred to the cells for anonymity in accordance with given guidelines. The cells were later stored in an established muscle biopsy samples cell bank. An informed written consent was obtained from all donors before the onset of the research project and the project was approved by the Regional Committees for Medical and Health Research Ethics (REK) (Reference S-09078d,2009/66) (Appendix 1 & 2). The project was performed as a co-operation between Oslo Metropolitan University and The Blood Cell Research Group, Section for Research, Development and Innovation, Department of Medical Biochemistry, Oslo University Hospital.

**Table 1: Presentation of cell donors characteristics**

Donor	Age (years)	BMI (kg/m <sup>2</sup> )	HbA1c (%)	Total Cholesterol (mmol/L)	HDL (mmol/L)	LDL (mmol/L)	Triglycerides (mmol/L)
<b>0/6</b>	49	45.0	7.0	5.0	1.1	2.8	2.1
<b>Men/women</b>	(±12.00)	(±5.0)	(±1.2)	(±1.3)	(±0.4)	(±1.1)	(±0.9)

*The donors' characteristics presented as mean ± standard deviation (SD). BMI=Body Mass Index(kg/m<sup>2</sup>), HbA1c = Glycated Hemoglobin A1c (%), HDL = High Density Lipoprotein Cholesterol (mmol/L), LDL = Low Density Lipoprotein Cholesterol (mmol/L).*

### 8.2 Study design

To be able to define, identify and confirm the existence and functions of EVs isolated from myotubes, a criterion of a number of minimal requirements identified by Lötvall et al., from the International Society for Extracellular Vesicles (ISEV) were observed (104). Figure 9 shows an overview of different methods and processes done from the seeding of the cells to characterization of EVs.



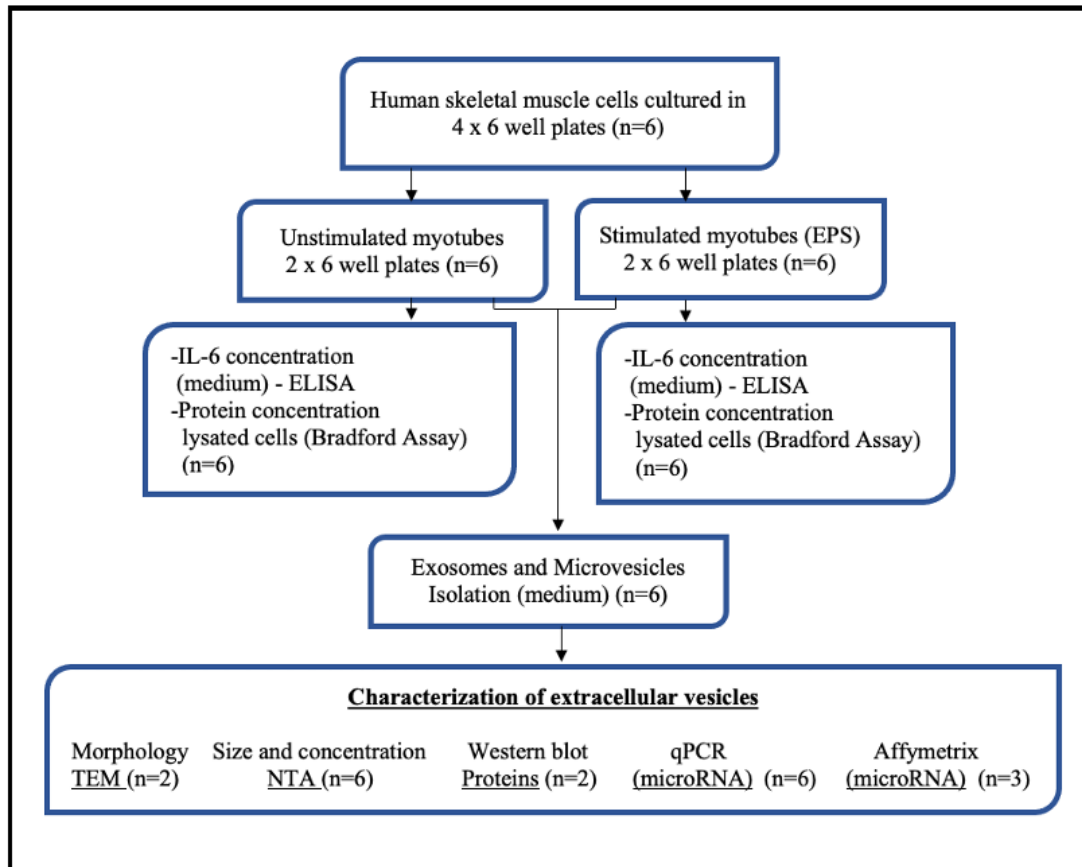


**Figure 9: An epitome presentation of the study.** Muscle cells from 6 different donor (n) were each seeded in a set of 4 extracellular matrix (ECM)-gel coated 6 well plates. Two of the plates were stimulated with Electrical Pulse Stimulation (EPS) for 24 hours, while the two remaining plates were unstimulated. The media from both conditions were collected for interleukin-6 (IL-6) determination using enzyme-linked immunosorbent assay (ELISA). The myotubes were then incubated in serum free medium (SFM) for 24 hours and the media collected and centrifuged. After media collection the myotubes were washed with PBS, lysed and protein quantitation performed thereafter by Bradford Assay. The media collected after incubation was centrifuged to isolate extracellular vesicles (EVs) before separating exosomes and microvesicles by centrifugation and ultrafiltration followed by characterization. Transmission electron microscopy (TEM) analysis was performed on freshly harvested EVs. The EVs concentration analysis was done using nanoparticle tracking analysis (NTA), real-time quantitative polymerase chain reaction (qPCR) and Affymetrix was used to measure the expression of microRNA (miRNA). Western blotting was used to identify characteristics of EV biomarkers.

## 9 Cell cultures

Appendix 7 contains details of reagents/chemicals and equipment used. For the samples, isolation of satellite cells from the donors' abdominal muscle biopsies were first done. The satellite cells were then activated to proliferating myoblasts and allowed to differentiate into multi-nucleated myotubes in culture, which constituted mature skeletal muscle cells. These were later used in the research project and grown according to a modified protocol by Gaster et al., (105).

### 9.1.1 Pre-coating of the well plates with extracellular matrix (ECM) gel

A number of 6 well plates with a lock (Costar®(Corning)) were coated manually with extracellular matrix (ECM) gel and allowed to dry before use to enable cell adhesion. Frozen ECM-gel was thawed in a water bath (Sab Aqua Pro Water bath) and diluted in DMEM (Dulbecco's modified Eagle medium) at a ratio of 1:4. Using a pipette, 1 mL was applied on one well, sucked out and applied onto the next well until all the wells were equally coated with ECM-solution, and cell suspension added.

For the cells' growth and expansion, appropriate amount of medium solution was prepared beforehand. FCS (Foetal Calf Serum), gentamicin, amphotericin, Ultrosor G and insulin were added into DMEM medium and mixed well before use (appendix 3-5).

### 9.1.2 The cell seeding

The muscle cells were seeded using an aseptic technique in a Laminar Air Flow (LAF)-bench. The frozen human myoblasts were thawed at 37 °C in a water bath before transferring the cell suspension into a 50 mL centrifugation tube (Corning). A volume of 5 mL seeding medium (M1-medium, appendix 3) kept at room temperature (RT) was dripped on the cells carefully to avoid temperature shock for the cells. Centrifugation of the suspension at 1500 rotations per minute (rpm) for 7 minutes was performed in a Hettich ROTOFIX 32 centrifuge. The supernatant was discarded, the cell pellet resuspended first in 5 mL M1-medium, and then mixed before adding appropriate volume of M1-medium for seeding. A cell suspension of 1 mL was added in each 6-well plate. The cells were then incubated at 37 °C with 5 % CO<sub>2</sub>.

### 9.1.3 Cell proliferation and differentiation

To determine the cell growth and their morphology, a light microscope was used (Motic AE31 microscope). After 24 hours the initial seeding medium was changed to a cell proliferation medium (M2-medium, appendix 4). M2-medium was changed twice a week (every 2-3 days) until the cells obtained an optimal confluence of approximately 80 - 90 %. Since the cells' growth varied widely, confluence was reached from 14 to 19 days (Figure 10). At 80 - 90 % confluence, the medium was changed to differentiation medium (M3-medium, appendix 5) to induce differentiation of myoblasts into myotubes. M3-medium was changed every 2 - 3 days until day 6 of differentiation.

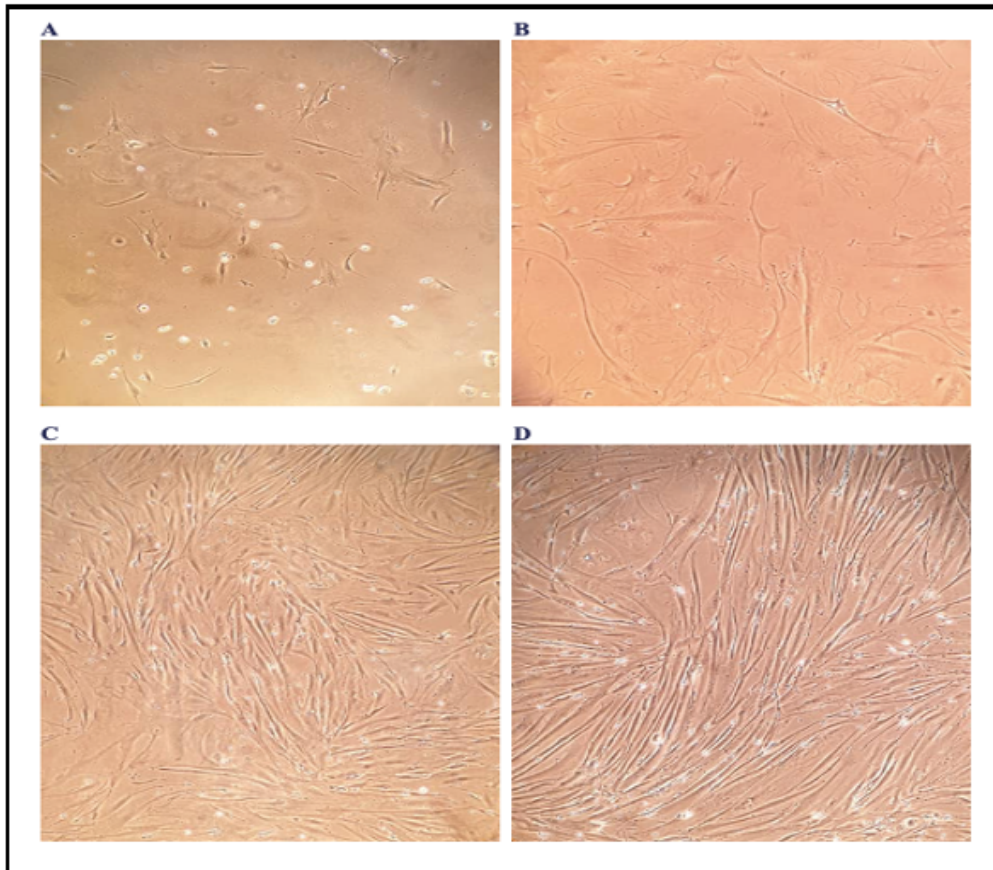


**Figure 10: Human skeletal muscle cells at different growth phases.** The human skeletal muscle cells were seeded in extracellular matrix (ECM) gel coated 6 well plates, where different media with different functions was used at different phases. The cells were allowed to develop from myoblasts and further into mature myotubes in culture over a period time. **A.** Muscle cells in the seeding medium after 24 hours. **B.** Muscle cells in proliferation medium after 6 days. **C.** Myotubes after 5 days in differentiation medium. **D.** Myotubes in differentiation medium right before media harvesting on the 7<sup>th</sup> day after electrical pulse stimulation. Photograph: By Samsung Galaxy S9 mobile camera through a light microscope lens (n=1).

## 9.2 Electrical pulse stimulation (EPS)

EPS is a training model system that mimics the activation of muscle fibers by motor neuron *in vivo*. It has been in use for a while and was applied for the stimulation and induction of muscle contraction in the human skeletal muscle cells in culture. The protocol employed was developed by Nikolić N. et al., (31, 106). In this study, a chronic low-frequency electric pulse stimulation (EPS) was applied to the adherent differentiated myotubes in culture for 24 hours.

### Procedure

On the 6<sup>th</sup> day of differentiation old M3-medium was discarded and new M3-medium (2.2 mL) added to the ECM-coated 6 well plates with multinucleated myotubes. The electric pulse stimulation was applied through the rod carbon electrodes fixed inside the C-Dish™ lid (commercially available from IonOptix, Dublin Ireland). The rod carbon electrodes were

descended into the M3-medium in 2 of the ECM-coated 6 well plates meant for stimulation and connected to the pulse generator (developed by Electronic Laboratory University of Oslo). The stimulator was connected to and controlled by a self-developed software on a data machine (Figure 11). The assembled C-Dish/rod carbon electrodes connected to the pulse generator were transferred into the incubator (37 °C and 5 % CO<sub>2</sub>). Bipolar pulses of 2 milliseconds (ms), 11 volt (V) and 1 Hertz (Hz) was applied continuously for 24 hours. The total volume of the cell medium from the stimulated (EPS) and unstimulated cells wells were collected in separate 50 mL Falcon tubes, marked and frozen at -20 °C for later determination of interleukin-6 (IL-6).

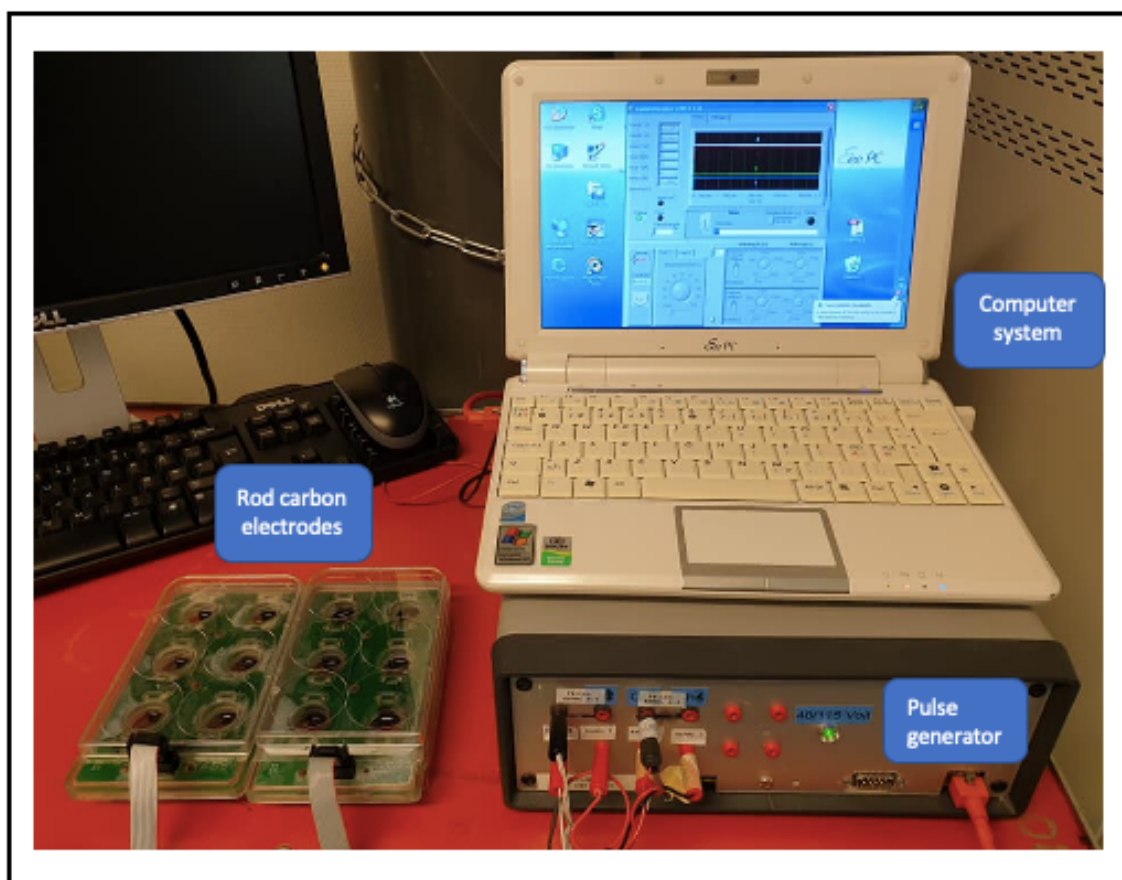


**Figure 11: Completely assembled model for electrical pulse stimulation of the muscle cells.** At 80 – 90 % confluence, myotubes in the two of the four 6 well plates were stimulated for 24 hours using electrical pulse stimulation (EPS). A volume of 2.2 mL of the differentiation media (M3-medium) was added into the wells. The rod carbon electrodes were descended into the M3-medium in two ECM-coated wells and the C-Dish/rod carbon electrodes were then connected to the pulse generator. A computer system connected to the pulse generator was used to control the frequency (1 Hertz), voltage (11 volt), pulse rate (2 milliseconds) and stimulation time (24 hours). Photograph: By Samsung Galaxy S9 mobile camera.

### 9.2.1 Harvesting of the conditioned medium

On the 7<sup>th</sup> day of differentiation, 24 hours after cell stimulation (EPS), the cells in both the stimulated (EPS) and unstimulated ECM-coated 6 well plates were washed twice with 1 mL serum-free M3-medium (S-free medium, appendix 6). A volume of 1 mL S-free M3-medium was added thereafter, and the cells were incubated for another 24 hours before the cells and medium containing EVs were separated. The media (12 mL) from stimulated (EPS) and unstimulated cells were collected and transferred into two separate 50 mL Falcon tubes and centrifuged at 1500 rpm for 7 minutes. The supernatants were then transferred into new Falcon tubes, marked and frozen at -20 °C on the 7<sup>th</sup> day after initiation of differentiation and later used for EV isolation.

### 9.2.2 Skeletal muscle cell collection

The remaining cells in the ECM-coated 6 well plates were washed with 1 mL phosphate buffered saline (PBS), 0.5 mL (0.1M NaOH) was added, and the cells were left for approximately 10 minutes before collecting the cell lysate suspension in a 15 mL Falcon tube, marked and frozen at -20 °C. These cell lysates were later used for protein concentration analysis.

## 9.3 Protein quantitation

### 9.3.1 Protein measurement using Bradford's method

The assay used to evaluate the protein concentration in the cell lysate was initially described by Marion M. Bradford in 1976 (107). The assay depends on the binding of the dye Coomassie Brilliant Blue G-250 to proteins and upon binding of the dye to the protein, it rapidly changes the color with an absorption maximum from red (465 nm) to blue (595 nm) in acidic conditions. Using a protein stock solution, with known concentration, one is able to measure and analyze unknown protein concentrations in a given sample.

### **Procedure**

Appendix 8 contains a detailed overview of the chemicals/reagents and equipment used. Protein quantity measurement was performed on the cell lysates from (paragraph 3.2.3). A stock solution, used to create a standard curve, had been prepared earlier and frozen at 20 °C. The stock solution was prepared using bovine serum albumin (BSA) diluted in 0.1 M NaOH at a concentration of 5 mg/mL, and from this a standard curve was designed (0, 0.01, 0.025,

0.05, 0.1, 0.2 and 0.3) mg/mL in 0.1 M NaOH. Cell lysates and the standards were first thawed. Bio-Rad Protein Assay Dye Reagent Concentrate was diluted in distilled water 1:4 before filtering the solutions through a 0.20 µm filter to remove unwanted particles. An amount of 10 µL of the standard and samples were pipetted in duplicates into a 96-well flat-bottom plate. A volume of 200 µL Bio-Rad protein assay dye reagent was added in each well. Bubbles formed during pipetting were removed to avoid any interference with the path length in the spectrophotometer. The well plate was then loaded into the PerkinElmer 1420 Multilabel Counter VICTOR3™ Spectrophotometer for analysis. The standards and sample protein concentration results were analyzed in pairs and the absorbance values measured at optimum absorbance at 595 nm. Requirement for an R<sup>2</sup>-value for the standard curve was >0.95.

### 9.3.2 Interleukin-6 (IL-6) analysis

IL-6 was used as a marker for cell contraction in the EPS model. Cell release of IL-6 was measured in both unstimulated and stimulated (EPS) cells. ELISA an *in vitro* enzyme-linked immunosorbent assay was used to quantitatively measure IL-6.

#### **Procedure**

The Human IL-6 ELISA kit contained all the reagents used in the procedure (appendix 9). Reagents to be used and samples (from paragraph 9.2) were first brought to room temperature before dilution. The assay diluent B was diluted at ratio of 1:5, biotinylated detection antibody at 1:80, HRP-Streptavidin at 1:600 and samples at 1:3 as instructed in the Human IL-6 ELISA kit (Sigma-Aldrich®) protocol (108, 109). For the target proteins to bind to the antibodies in the wells, 100 µL standard (lyophilized human IL-6 protein) and samples were pipetted into the IL-6 antibody-coated ELISA 96 well plate. The wells were gently shaken during incubation overnight at 4 °C.

After incubation the solution was discarded and each well washed 4 times with 300 µL wash buffer. An amount of 100 µL antibodies (Biotinylated Human IL-6 detection antibody) was then added into each well and incubated for 1 hour at room temperature with moderate shaking. After 1 hour of incubation the solution was discarded, and the wells washed 4 times with 300 µL wash buffer. A volume of 100 µL HRP-Streptavidin solution was added into each well before incubation for 45 minutes at room temperature with moderate shaking. The principles of IL-6 analysis are shown in figure 12.

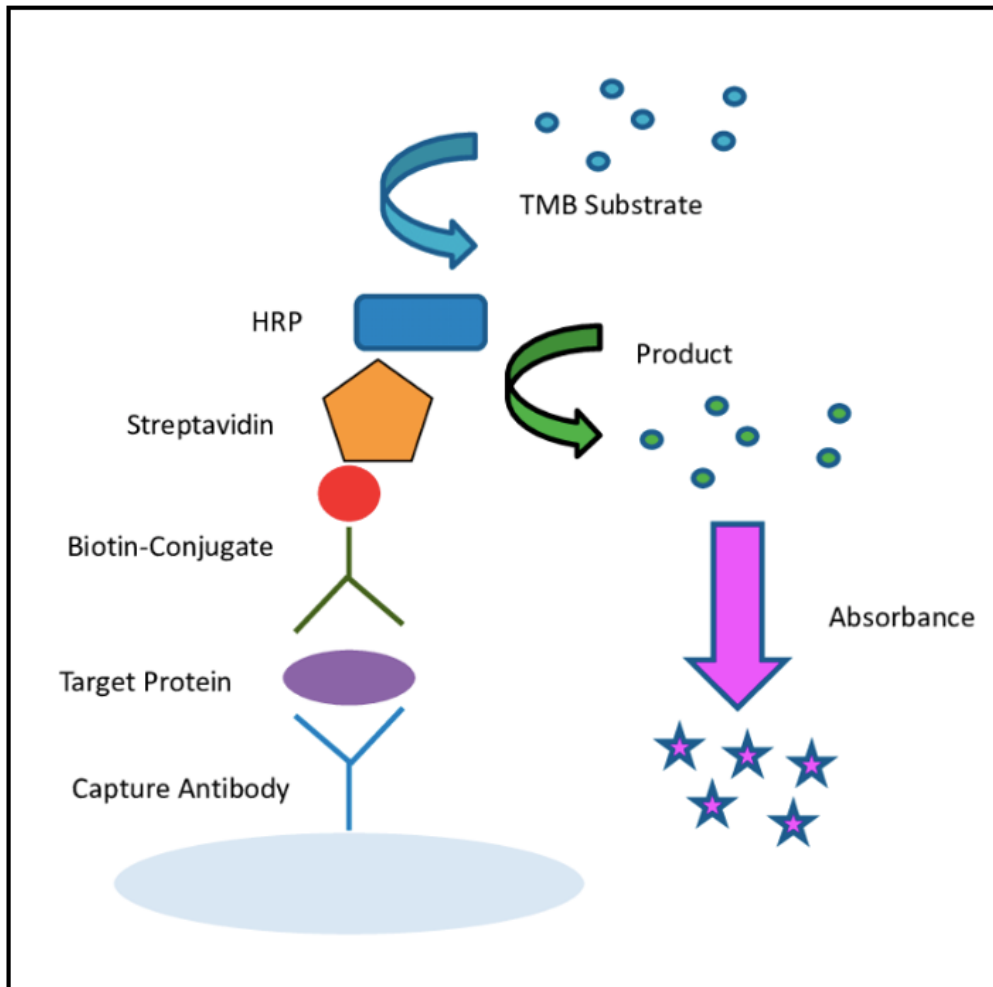


**Figure 12: The principles of the Interleukin-6 analysis.** The concentration of interleukin 6 (IL-6) was measured in the medium that was harvested and cleared by centrifugation from both the unstimulated and stimulated (EPS) myotubes. Standards and samples were pipetted in duplicates onto the 96 IL-6- antibody coated well plates before incubation. After incubation, unbound standards and samples washed off and biotin added, then incubated. The unbound biotin was washed off and biotin-labeled secondary antibody added before incubation. After incubation the unbound secondary antibodies were washed off, and horseradish peroxide (HRP)-conjugated streptavidin was added. The unbound HRP-conjugated streptavidin was washed off before adding a HRP and incubated in a dark environment. At the end of incubation period, a stop solution was added. The 96 well plate was then loaded onto Perkin Elmer 1420 Multilabel Counter Victor3™ system for analysis. Figure is from (110). No permission was required to reuse part or all article published by MDPI including figures and tables.

At the end of 45 minutes, the solution was discarded, and the wells washed 4 times with 300  $\mu\text{L}$  wash buffer. For color development, 100  $\mu\text{L}$  of ELISA Colorimetric (tetramethylbenzidine) TMB reagent was added in each well. The plate was then covered with aluminum foil to create a dark environment followed by incubation for 30 minutes at room temperature with gentle shaking. A volume of 50  $\mu\text{L}$  of Stop Solution was added after incubation to change the color which was immediately read at 450 nm on Perkin Elmer 1420 Multilabel Counter Victor3™ system (Figure 12).

## 10 Isolation of muscle derived extracellular vesicles

There are numerous different methods for EV isolation. The methods used in this thesis were a combination of centrifugation and ultrafiltration through columns with different filter sizes, which were performed according to Konoshenko M. et al., protocol (55). Figure 13 shows the principles followed.

### Procedure

Appendix 10 comprises the details of chemicals/reagents and equipment used in the procedure. The cell media assumed to carry EVs (harvested as described in paragraph 9.2.1) from unstimulated and stimulated (EPS) cells, and S-free medium (negative control) were thawed at 37 °C in a water bath. The media were then divided into 31 mL Sorvall tubes, weighed for equal balance and centrifuged at 17000 g for 30 minutes (RC5C Plus centrifuge) at room temperature to separate MV (~100 – 1000 nm) and exosomes (~30 – 150 nm). As a result of microvesicles' heavier weight and size, they sediment as a pellet after centrifugation, while exosomes remain in the supernatant. The supernatant from each Sorvall tube contained exosomes was transferred into 15 mL Falcon tubes.

#### 10.1.1 Isolation of microvesicles

After the initial centrifugation and removal of the exosome-containing supernatant a residue of supernatant (~2 mL) was used to resuspend the cell pellet presumed to contain MV. The suspension of MV was then transferred into a 4mL AmiconUltra-4 centrifugal filter, 100 kDa (kilodalton) (Merck Millipore). The column was centrifuged at 4000 g for 10 minutes at room temperature in a Hettich® ROTINA 420R centrifuge. The filtrate that ends up at the bottom of the filter column was discarded, and the fragments remaining on the filter were washed with pre-filtered (0.02 µm) 2 mL PBS and centrifuged at 4000 g for 10 minutes at room temperature. The solution assumed to contain MV located in the bottom of the filter column was carefully collected and transferred into a new Eppendorf tube. In order to collect all the MV, the filters were rinsed with PBS along the two filter walls, and the solution was transferred into the Eppendorf tubes. The total volume of the collected MV and PBS solution from both stimulated (EPS) and unstimulated cells were aliquoted (à 10 – 20 µL) into Eppendorf tubes and frozen at -80 °C for further downstream analysis. However, the quantity of MV was low and therefore not included in the subsequent analysis except concentration



measurement using nanoparticle tracking analysis (NTA) and transmission electron microscopy (TEM).

#### 10.1.2 Isolation of exosomes

After the 17000 g centrifugation, the supernatant was transferred into a 15 mL Falcon tube for exosome isolation. The supernatant was filtered through a 0.22  $\mu\text{m}$ -filter into a Centricon® Plus-70 Centrifugal Filter Units, with 100 kDa Kit (Merck Millipore) using a syringe. The column was then centrifuged at 3500 g for 15 minutes at room temperature in a Hettich® ROTINA 420R centrifuge. The exosomes were assumed to be collected on the column filter, and the column filter was washed with prefiltered 20 mL PBS and centrifuged at 3500 g for 10 minutes at room temperature. The filter column was then placed upside down (reverse spin) in a collection cup and centrifuged at 1000 g for 2 minutes at room temperature, where the exosomes were collected at the bottom of the cup. The total volume of the collected exosomes and PBS solution from both unstimulated and stimulated (EPS) cells were aliquoted (à 20  $\mu\text{L}$ ) into Eppendorf tubes and frozen at -80 °C for further analysis. Figure 13 shows the procedures done.

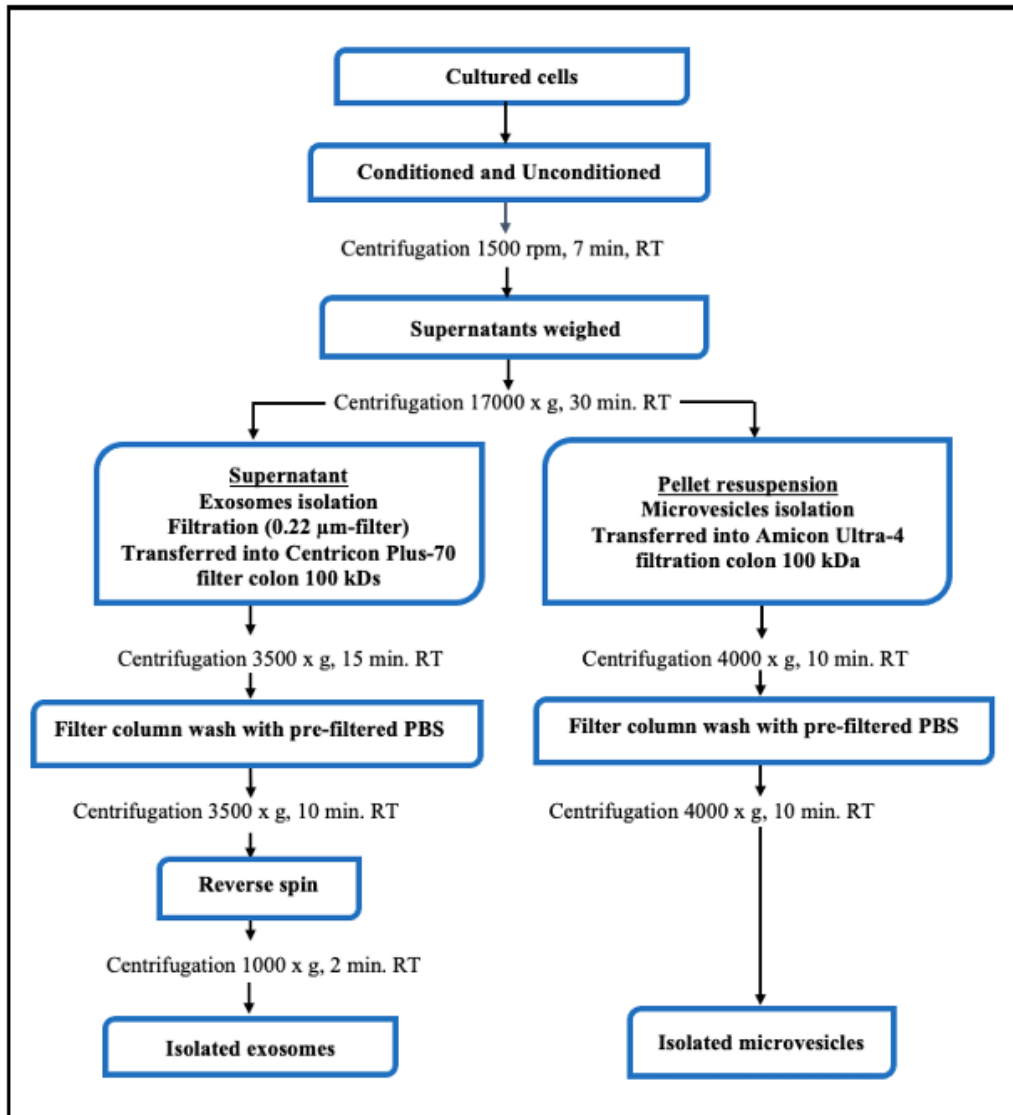


*Figure 13: Principles through which extracellular vesicles (EVs) were isolated. Media from both conditions were collected and centrifuged before EVs isolation. Media containing exosomes was transferred into Falcon tubes and the remaining supernatant used to resuspend microvesicle pellet before transferring into filtration column and centrifugating. This was followed by more centrifugations and washing procedures of the separated EV containing media, which was then aliquoted and stored at -80°C. n=6. Rpm (revolutions per minute), g (gravitational force), RT (room temperature).*

## 11 Characterization of extracellular vesicles (EVs)

For verification, identification and confirmation that the end results obtained were indeed intact EVs isolated from the differentiated human myotubes, transmission electron microscopy (TEM), western blotting and nanoparticle tracking analysis (NTA) were used for characterization. Real-time reverse transcription quantitative polymerase chain reaction RT-qPCR, and microarray (Affymetrix) were used to quantify nucleic acids (microRNA) present in EVs, and to ascertain the differences between EVs from unstimulated and stimulated (EPS) myotubes.

### 11.1 Transmission electron microscopy (TEM)

TEM is a gold standard method used for imaging purposes, and the technique is whereby an image is created by transmitting electrons through an extremely thin sized specimen. The technique was invented by Max Knoll together with Ernest Ruska Z, and because of its high resolution, it can be used to detect EVs' morphology in terms of size and border distinctions (111).

Freshly isolated EVs were stored at 4 °C overnight and taken to The Electron Microscopy Laboratory, Department of Molecular Biosciences, University of Oslo. As a result of the Covid-19 pandemic, we were not allowed to take part in the TEM process. The process was performed by Professor Norbert Roos, University of Oslo.

### 11.2 Sizing and enumeration of extracellular vesicles by nanoparticle tracking analysis (NTA)

Nanoparticle tracking analysis (NTA) is a unique and useful study technique that is used to characterize nanoparticles in terms of size and concentration. NTA merges and utilizes the two qualities of laser light scattering and Brownian motion, an irregular movement of suspended particles in a medium, to acquire size dispersal of particles in liquid suspensions. It has a capacity to measure the particle size from 50 nm to 1000 nm (54). The implement entails a syringe pump in which samples are injected into the fluid chamber where the sample particles are illuminated by a centered laser beam that transverses through particles in the specimen suspension. The particles then scatter light that is collected by a lens on an optical microscope which focuses the light onto a sensitive digital camera that records the videos of the scattered light which is displayed on a screen. The particles are envisioned when they are in the lane of the laser beam and scatter the light, which is immediately picked up by the microscope and recorded with a digital camera. A video of the particles' Brownian motion is captured by the digital camera and enables a real-time visualization of the particles. NTA software analyzes massive numbers of particles one by one at the same time, by tracking their mean square displacement (MSD), which measures the particles' fluctuation position in relation to the starting point (54).

## Procedure

Details of chemicals/regents used in the procedure see appendix 11.

The instrument used for NTA was NanoSight NS500, and the software program was version 3.4. The instrument was equipped with a laser type 488 nm CW, with a high sensitivity scalable complementary metal-oxide semiconductor (sCMOS) camera which was adjusted to a level of 15 (scale of 12 - 15) for better particle visualization light. The syringe pump speed was 20 and the detection threshold was 4 (scale of 1 to 4) to avoid the presence of noise in the observed end results. Routinely, the apparatus was calibrated before use, and 100 nm diameter standard polystyrene latex microsphere beads were used for this purpose.

An aliquot of the isolated exosomes and MV frozen at -80 °C were first thawed at room temperature before diluting 1:50 with filtered phosphate buffer saline (PBS) (0.02 µm filter). This dilution was selected since it gave the required optimal concentration area of  $1-10 \times 10^8$  -  $1-10 \times 10^{10}$  particles/mL. The diluted EV-solutions were then transferred into an Eppendorf tube and vortexed, before 1 mL was drawn into a syringe and air bubbles eliminated by tapping on the syringe. The syringe was then fit onto the injection pump tube carefully avoiding introduction of bubbles or air into the system, before the camera was started. To start off, approximately 0.2 – 0.3 mL of the diluted sample was slowly and carefully injected into the system until particles were observed on the screen and the syringe mounted onto the syringe pump. Infusion rate was instilled to 20 and the system was set to run. The particle concentrations (particles/mL) and particle sizes (nanometer) in all the samples were analyzed, and an average of three recordings per sample was calculated. Figure 14 shows the instrument used in NTA.

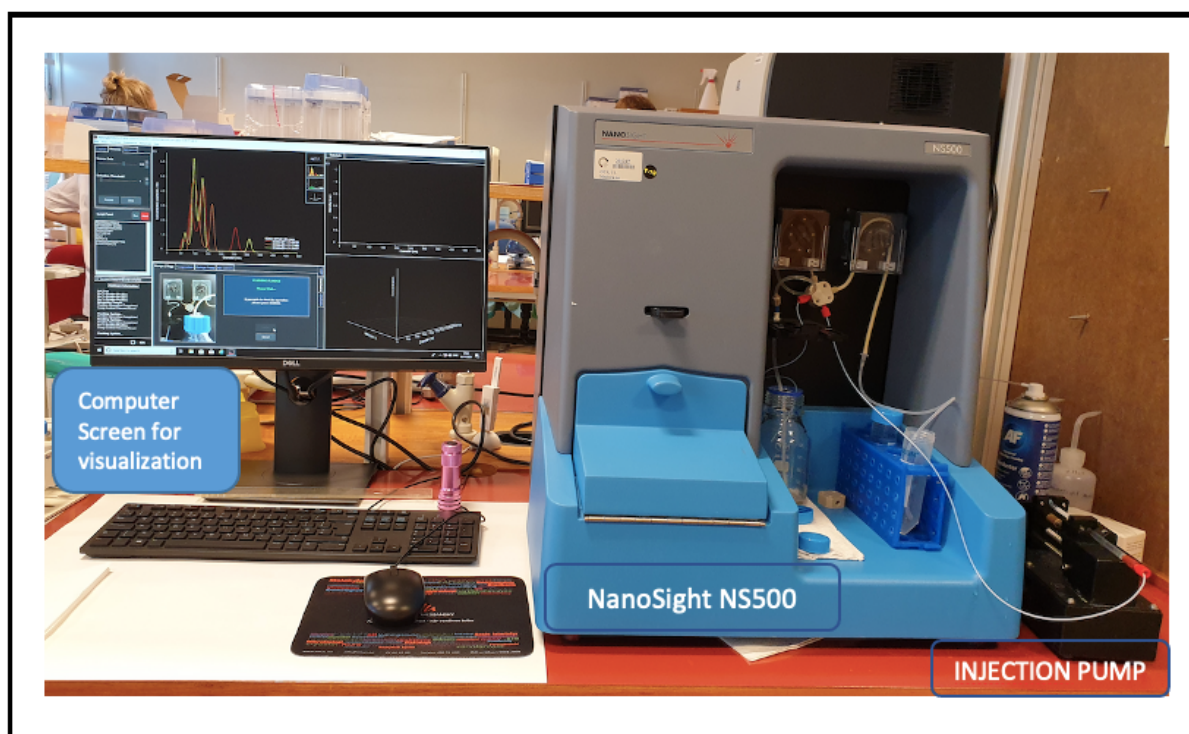


**Figure 14: The nanoparticle tracking analysis instrument (NTA) (NanoSight NS500):** The isolated extracellular vesicles (EVs) (exosomes and microvesicles) were characterized using NTA. NanoSight instrument is connected to an injection pump where the syringe that is used to inject the samples into the fluid chamber is mounted. After injecting the samples in the fluid chamber, the sample particles are illuminated by a laser that passes through the sample particles and the particles scatter light. The light is then captured by a lens from an optical microscope which then focuses the light onto a sensitive digital camera that records the scattered light that is then displayed on a screen. Photograph: By Samsung Galaxy S9 mobile camera.

### 11.3 Quantification of proteins in extracellular vesicles on NanoDrop One spectrophotometer

The protein content in isolated EVs was quantified using the NanoDrop technique to measure the concentration and control the protein quality.

#### Procedure

The protocol applied was described in the NanoDrop One user guide (112). Use of gloves was mandatory to avoid ribonuclease (RNase) contamination. The upper and lower optical surfaces were cleaned before selecting the right application and correct absorption spectrum ratio (A260/A280) chosen. Blanking was performed and the samples applied on the lower optical surface before closing the lever arm. The concentration and purity were then analyzed.

### 11.4 Western blotting

Western blot was used for identification of EV biomarkers which included heat shock proteins (Hsc70/Hsp70) and the tetraspanins CD63 and CD9. In addition, calnexin which is a

negative control for exosome was determined while a cancer cell line 480 was used as a positive control.

### **Procedure**

After exosome isolation, a sample volume of 20  $\mu\text{L}$  was used in the biomarkers determination. An amount of 6  $\mu\text{L}$  RIPA 5x buffer (Thermo Fisher Scientific) and 2.25  $\mu\text{L}$  protease inhibitor (cOmplete, Mini, EDTA-free Protease Inhibitor Cocktail 25x, Roche), was added to the samples. This was then sonicated for 20 seconds and lysed on ice for 15 minutes. A volume of 10  $\mu\text{L}$  LDS (lithium dodecyl sulfate) Sample Buffer (Invitrogen) was added. An amount of 4  $\mu\text{L}$  Bolt Sample Reducing Agent was added to Hsc70/Hsp70. A volume of 4  $\mu\text{L}$  PBS was then added to CD9 before all lysates were heated for 10 min at 70 °C. The proteins were separated on Bolt 4-12 % Bis-Tris Plus Gels with Bolt MES SDS (sodium dodecyl sulfate) Running Buffer (both Invitrogen) and were transferred to 0.2  $\mu\text{m}$  PVDF Blotting Membranes (Invitrogen). Membranes were then blocked with 1 % casein (Western Blocking Reagent, Sigma Aldrich) in tris-buffered saline with 0.1 % Tween 20 (TBS-T) for 1 hour at RT, followed by incubation with primary mouse monoclonal antibodies overnight at 4 °C (anti-CD9, 1062D diluted at 1:5; anti-CD63, 10628D diluted at 1:5; Hsc70/Hsp70, Enzo, ADI-SPA-820 diluted at 1:50; anti-calnexin, MA5-15389 diluted at 1:50 all from Invitrogen). The membranes were then washed three times for 20 minutes with TBS-T before incubating with horseradish peroxidase-coupled secondary antibody (Mouse TrueBlot Ultra, Rockland Immunochemicals, Pottstown, USA) for one hour at RT. A triplicate washing was performed with TBS-T. The blots were then imaged using SuperSignal west Dura Extended Duration Substrate (Thermo Scientific) and Amersham Imager 600 (GE Healthcare, UK).

## **12 Quantification of microRNA**

RNA expression varies considerably between living cells, and the same applies to microRNA(miRNA) levels in EVs. In this thesis, RNA quantification was used to determine miRNA levels in EVs secreted from myotubes (isolated from individuals with diabetes) with an objective to find out whether there is any difference in expressions in unstimulated and stimulated (EPS) groups.

## 12.1 Total RNA extraction from exosomes

RNA is an unstable molecule that is prone to degradation. This is due to its structure with focus on the hydroxyl group on the C2 of the sugar that is vulnerable to both enzymatic (RNase) and non-enzymatic degradation (113). A crucial requirement for potent and conclusive results acquired in gene expression analysis using real-time reverse transcription quantitative polymerase chain reaction (RT-qPCR) is high-quality RNA. As a result, total RNA should be free of protein and organic contaminations with no degradation for better downstream application results. Thus, it is mandatory to use gloves and a laboratory coat and aseptic technique to avoid RNA contamination during any RNA analysis.

For total RNA extraction, Qiagen Quick-Start protocol (114) was used as instructed in the guidelines and a miRNeasy Micro Kit was used for the procedure, with a few adjustments (115).

### **Procedure**

For an overview of reagents and equipment used in total RNA extraction refer to appendix 12. The RNA extraction was performed in a fume chamber to avoid inhalation of toxic organic fumes produced by QIAzol during the analysis. Before adding 1000  $\mu\text{L}$  QIAzol (phenol and guanidine thiocyanate) cell lysis reagent, the frozen samples were thawed at room temperature and a volume between 60 – 100  $\mu\text{L}$  of the sample was pipetted into a 2 mL sample tube. The volumes varied because of variable yield of the exosome extractions, and due to use of extra samples in NTA and NanoDrop analysis, while optimizing analysis of EV size and concentration. The solution was rigorously homogenized by shaking for 1 minute before incubating for 5 - 10 minutes at room temperature. A volume of 200  $\mu\text{L}$  chloroform was added to the tube containing the homogenate and shook vigorously for 15 seconds before incubating for 2-3 minutes at room temperature. Centrifugation at 12000 g for 15 minutes at 4 °C followed thereafter in an Eppendorf centrifuge 5415 R. A two-phase layer was formed, an overlying colorless aqueous phase and an underlying red organic phase separated by a thin interphase layer. The overlying colorless aqueous phase encompassing RNA was carefully transferred into a new collection tube using a pipette and avoiding touching the interphase and the red organic phase. An amount of 525  $\mu\text{L}$  100 % ethanol (1.5 x colorless aqueous phase volumes) was added and mixed rigorously with a pipette. From the total volume, 700  $\mu\text{L}$  of the lysate mixture was pipetted into a Qiagen RNeasy MinElute spin column placed in a 2 mL

collection tube and centrifuged at 12000 g for 15 seconds at room temperature. After discarding the filtrate, the same procedure was repeated with the surplus volume of the lysate. The RNeasy MinElute spin column was then washed with 700  $\mu$ L buffer RWT and centrifuged at 12000 g for 15 seconds at room temperature, before discarding the flow-through. A volume of 500  $\mu$ L buffer RPE was pipetted into the RNeasy MinElute spin column and centrifuged at 12000 g for 15 seconds at room temperature prior to discarding the filtrate. This was then followed by pipetting 500  $\mu$ L of 80 % ethanol into the RNeasy MinElute spin column and centrifuged at 12000 g for 2 minutes at room temperature. The RNeasy MinElute spin column was gently taken out from the collection tube and placed into a new 2 mL collection tube. Both the collection tube and filtrate were discarded. The cap on RNeasy MinElute spin column was opened and the column was centrifuged at 12000 g for 5 minutes at room temperature to dry the membrane. Ultimately, the RNeasy MinElute spin column was transferred into a new 1.5 mL collection tube, where RNA was eluted after 14  $\mu$ L RNase-free water was pipetted on to the membrane and the cap carefully secured before centrifuging at 12000g for 60 seconds at room temperature. The collection tube containing the elute encompassing of total-RNA from exosomes was then marked and stored at -80 °C for further analysis (NanoDrop One, Bioanalyzer and Qubit).

## 12.2 Quantification of total RNA from exosomes

### 12.2.1 NanoDrop One

NanoDrop One technique applied in protein quantification (11.3) was also applied in microRNA quantification.

NanoDrop One analysis determines the concentration and purity of nucleic acid by measuring the absorbance of ultraviolet light. The sample purity is indicated by absorbance values of 260 nm versus 280 nm ( $A_{260}/A_{280}$ ) for RNA and 260 nm versus 230 ( $A_{260}/230$ ) for contaminants. The contaminants include salts, proteins and phenol among others. RNA samples with over 1.8 for  $A_{260}/A_{280}$  ratio and  $A_{260}/230$  ratio are considered highly purified and suitable for use in succeeding analysis.

### **Procedure**

The protocol applied was described in the NanoDrop One user guide (17). To make sure that the surface/area of work was RNase free, the upper and lower optical surfaces were cleaned



by wiping using laboratory wipe moistened with RNase free water. The correct settings were selected and samples (1.5  $\mu\text{L}$ ) was carefully applied on the lower optical surface and the lever arm closed. The concentration and purity were automatically calculated, and results availed on the screen.

### 12.3 Agilent 2100 Bioanalyzer

Agilent 2100 Bioanalyzer is a semi-quantitative analysis. It performs integrity checks and sample quantitation of biomolecules such as RNA molecules. It is a bio-analytical device that uses microfluidics technology to create an electric field which separates charged particles. RNA molecules are negatively charged and are therefore drawn towards the positive terminal. In this manner, the RNA samples are separated with respect to their molecular weight, which are detected by a laser-induced fluorescence and then visualized as electropherograms. The measured detections correspond to the RNA size in the sample and gives an estimate of RNA quality (RIN-RNA integrity number) and quantity (RNA concentrations ( $\text{pg}/\mu\text{L}$ )) (116). In this thesis, Agilent 2100 Bioanalyzer was used to control the integrity of RNA.

#### **Procedure**

For more details about the reagents/chemicals and equipment used see appendix 13. The protocol applied was one described in the Agilent RNA 6000 Pico Kit Quick Start guide (117). The reagents used were equilibrated to room temperature for 30 minutes, while samples were thawed on ice. A 65  $\mu\text{L}$  aliquot of filtered gel was prepared in an Eppendorf tube beforehand and stored at 4  $^{\circ}\text{C}$ . After equilibration, 1  $\mu\text{L}$  RNA dye concentrate was vortexed and spun to bring the contents down before pipetting 1  $\mu\text{L}$  into the Eppendorf tube containing 65  $\mu\text{L}$  aliquot of filtered gel. This was vortexed thoroughly and spun at 13000 g for 10 minutes in an Eppendorf Centrifuge 5415 R at room temperature. The plunger on the chip priming station was positioned at 1 mL before mounting an RNA chip and loading in the gel-dyes, conditioning solutions, ladder, and samples in their appropriate wells (Figure 15). On the chip, 9  $\mu\text{L}$  of gel-dye mix was pipetted into the G well before pressing the plunger that was held in place by a clip and waiting for 30 seconds. The plunger was then released and was let to stay for 5 seconds before slowly pulling it back to original. Another 9  $\mu\text{L}$  of the gel-dye mix was pipetted in the next two G wells.

A volume of 9  $\mu\text{L}$  of the RNA conditioning solution was pipetted into a CS marked well. Thereafter 5  $\mu\text{L}$  RNA marker was added to the 11 sample and ladder wells followed by 1  $\mu\text{L}$  of samples into their respective wells avoiding creating bubbles. All samples were placed in a thermomixer for heat denaturation at 70  $^{\circ}\text{C}$  for 2 minutes prior to pipetting into the sample wells. The RNA chip was then vortexed at 2400 rpm on an IKA vortexer for 1 minute before loading on the Agilent 2100 Bioanalyzer instrument for analysis. Figure 15 shows the priming station used for holding the RNA pico chip and pump used for pumping the dye gel. The results (RNA integrity number – quality and RNA concentrations ( $\text{pg}/\mu\text{L}$ )) were displayed on a PC screen connected to Agilent 2100 bioanalyzer.

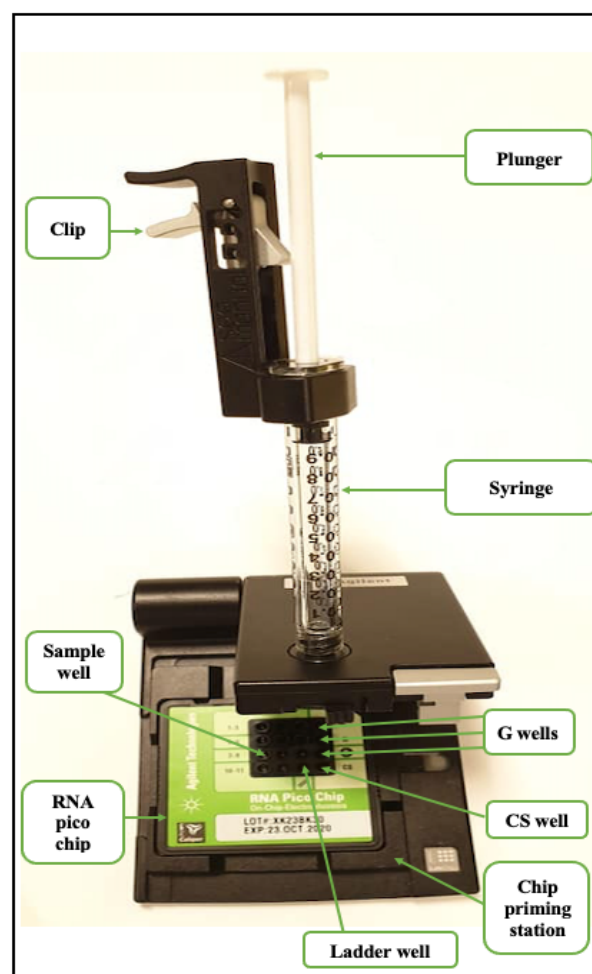


*Figure 15: Agilent 2100 Bioanalyzer chip priming station with a plunger that expels gel-dyes. The quality and quantity of RNA was determined using RNA pico chip. RNA pico chip encompassing wells was mounted onto the priming station and small amounts of recommended gel-dyes, conditioning solutions, RNA marker and samples were loaded into appropriate (11) wells before placing the chip into the Agilent ChipReader for analysis. PHOTO: Mobile camera Samsung Galaxy S9.*

## 12.4 Qubit microRNA assay

Qubit microRNA assay is a quantitative assay which is exceedingly sensitive. It is a method used to accurately quantitate low levels of RNA samples. The assay uses dyes that fluoresce only when bound to RNA an indicate of selectivity for RNA, which minimizes effects of contaminants in the sample. It gives accurate results since it gives a report of only RNA concentration and not the contaminants. In our analysis the method was used to measure the RNA concentration in each sample, to check whether there was enough RNA for further downstream applications.

### **Procedure**

Appendix 14 entails details of reagents/chemicals and equipment used.

The protocol applied was described by Qubit® microRNA Assay Kits (118). Reagents, standards and buffer were equilibrated to room temperature while the samples used were thawed on ice. Appropriate Qubit working solution was prepared by diluting the reagent (Qubit® microRNA reagent) in a buffer (Qubit® microRNA buffer) at 1:200 and mixed in an Eppendorf tube. A volume of 199  $\mu\text{L}$  of the working solution was pipetted into each PCR tube meant for samples and 1  $\mu\text{L}$  of the samples were added (to give a final volume of 200  $\mu\text{L}$ ) in the appropriate PCR tubes before vortexing for 2-3 seconds. Two standards (Qubit® microRNA Standard #1 and #2) were used to calibrate the fluorometer. Each standard was prepared separately by pipetting 190  $\mu\text{L}$  Qubit working solution into standard labeled PCR tubes and later 10  $\mu\text{L}$  of the standards were added (to give a final volume of 200  $\mu\text{L}$ ) into appropriate tubes followed by vortexing for 2-3 seconds. These were left to incubate at room temperature. After 2 minutes, the standards and samples were ready to be loaded onto Qubit® 2.0 fluorometer starting with the standards for calibration. Standards and samples were analyzed for 3 seconds, and the results displayed on a sample screen.

## 12.5 Real-time reverse transcription quantitative polymerase chain reaction

### (RT-qPCR)

The RT-qPCR procedure commences by generating complementary DNA (cDNA) from total RNA. Figure 16 shows the principles followed in cDNA synthesis from RNA.

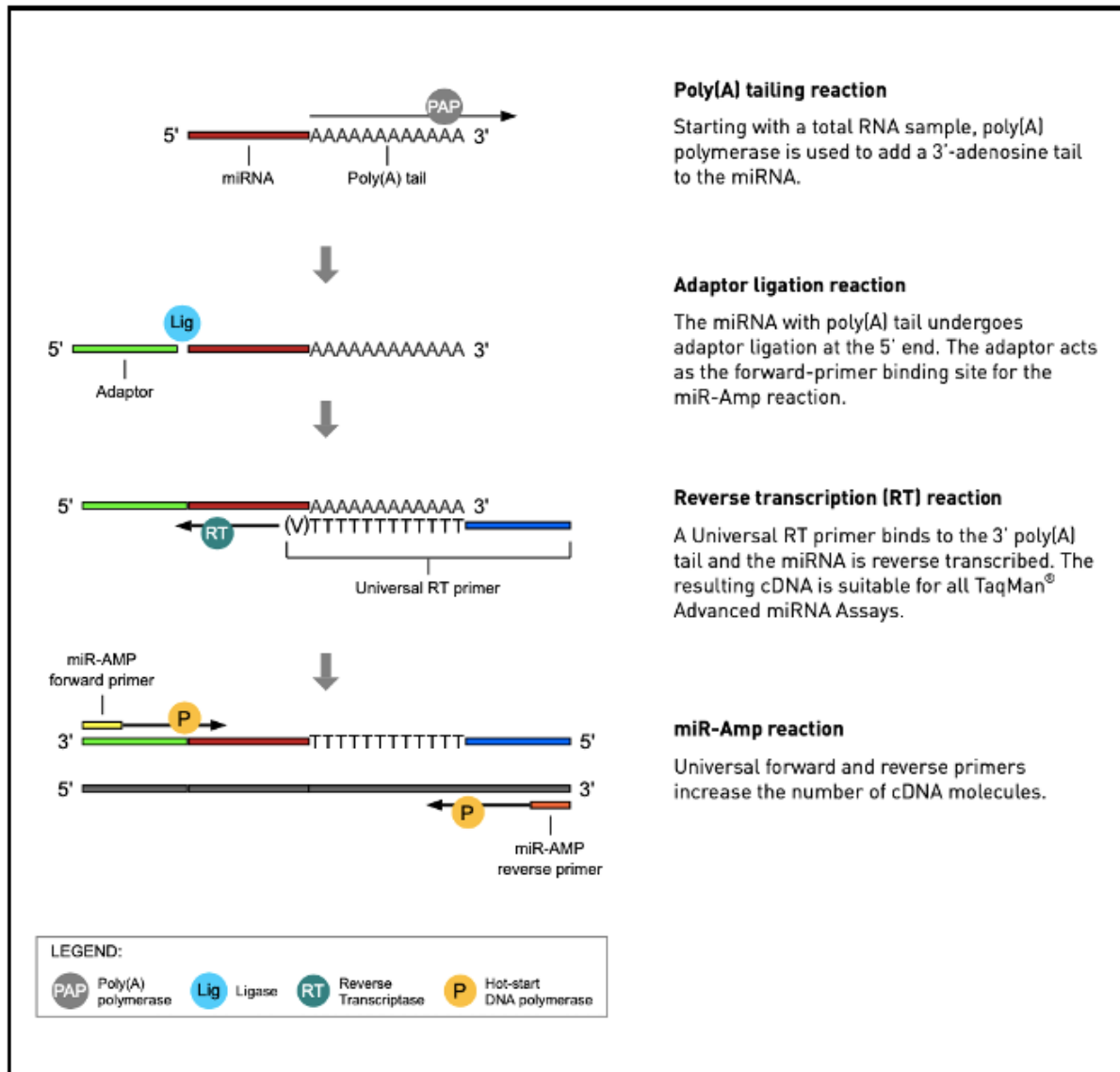


**Figure 16: Processes entailed in cDNA synthesis from RNA.** After total RNA extraction from the exosomes, total RNA was quantified to determine the microRNA(miR) levels. This commenced with mature microRNA modification by addition of poly(A) tail to extend the 3' end and lengthened by an adaptor ligation on the 5' end. This was followed by complementary DNA (cDNA) generation from single stranded RNA using reverse transcription (RT) assisted by reverse transcriptase. The cDNA was then amplified to generate more cDNA molecules. Figure modified from TaqMan<sup>®</sup> Advanced miRNA Assay user guide (119)

The mature miRNA modification was conducted through a poly(A) tail addition assisted by poly(A) polymerase enzyme to the 3' end of miRNA. The extended miRNA went through adaptor ligation to the 5' end to elongate, followed by reverse transcription (RT). Reverse transcription was executed by binding of the universal RT primer to the 3' poly(A) tail, from where the miRNA was reversely transcribed. This was then followed by a miR-amplification reaction, which is a PCR-reaction where the multiplication of the cDNA quantity is performed using universal forward and reverse primers.

The specific amplification of cDNA occurs during the quantitative real-time polymerase chain reaction (qPCR) where gene specific primers and probes are used. The forward and reverse primers bind along the denatured cDNA template strands. The forward primers anneal to the adaptor regions, the reverse primers partially bind to both the poly(A) tail and miRNA regions while the probes (labeled with a fluorescent reporter and a quencher) bind to the target sequence (miRNA) between the primers. A detachment of the reporter dye from the probe separates the reporter dye from the quencher dye. This leads to a fluorescence signal from the reporter dye, which corresponds to the amount of amplified miRNA in the sample that is later quantified.

## 12.6 Complimentary DNA (cDNA) template generation

cDNA synthesized from total RNA was performed in four separate phases: Polyadenylation, adaptor ligation, reverse transcription and miR-Amp reaction.

### **Procedure**

Appendix 15 contains a detailed overview of the reagents/chemicals and equipment used in the procedures.

### **Poly adenine tail synthesis (Poly(A) tail)**

RNA samples and cDNA synthesis reagents were thawed on ice and centrifuged for 2-3 seconds. Adequate poly(A) reaction mix for poly(A) synthesis was prepared in a reaction tube according to a table provided in the TaqMan® Advanced miRNA Assays User Guide (24).

The poly(A) reaction mix was rigorously mixed by vortexing and centrifuged for a few seconds. A volume of 2  $\mu$ L of each RNA sample was pipetted into separate PCR tubes and 3  $\mu$ L of poly(A) reaction mix added. The tubes were then spun for a few seconds before incubating in a thermal cycler (Veriti® 96-Well Thermal Cycler) according to the user guide as shown in table 2.

Table 2: Polyadenylation conditions

Step	Temperature	Time
<b>Polyadenylation</b>	37 °C	45 minutes
<b>Stop reaction</b>	65 °C	10 minutes
<b>Hold</b>	4 °C	Hold

### **Adaptor ligation reaction**

An adequate ligation reaction mix was prepared in a reaction tube and thoroughly vortexed after thawing on ice. The air bubbles were removed by centrifuging the reaction mix for a few seconds. An amount of 10 µL of the ligation reaction mix was transferred into each PCR tube that contained the poly(A) tailed reaction product. The PCR tubes were carefully locked and vortexed for a few seconds before spinning and putting the reaction into a thermal cycler for incubation under conditions shown in table 3.

Table 3: Adaptor ligation conditions

Step	Temperature	Time
<b>Ligation</b>	16 °C	60 minutes
<b>Hold</b>	4 °C	Hold

### **Reverse transcription reaction**

Reagents used in the preparation of reverse transcriptase reaction (RT), generating cDNA from the modified RNA templates, were thawed on ice. Enough reaction mix was then transferred into a reaction tube followed by vortexing and centrifuged for a few seconds. A 15 µL volume of the reaction mix was then pipetted into each PCR tube holding the adaptor ligated reaction product and locked carefully before vortexing and spinning for a few seconds. The tubes were then incubated in a thermal cycler under the setting conditions shown in table 4.

Table 4: Reverse transcription conditions

Step	Temperature	Time
<b>Reverse transcription</b>	42 °C	15 minutes
<b>Stop reaction</b>	85 °C	5 minutes
<b>Hold</b>	4 °C	Hold

### miR-Amp reaction

An acceptable amount of miR-Amp Reaction Mix was prepared in a reaction tube, after thawing the reagents on ice. This was then vortexed and centrifuged before transferring 45  $\mu$ L into new reaction tubes and adding 5  $\mu$ L of cDNA product. The reaction tubes were then sealed, vortexed for a few seconds before spinning and putting in the thermal cycler for incubation under the right setting conditions in the PCR shown in table 5.

Table 5: Polymerase chain reaction (PCR) (miR amplification) conditions

Step	Temperature	Time	Cycles
<b>Enzyme activation</b>	95 °C	5 minutes	1
<b>Denature</b>	95 °C	3 seconds	14
<b>Anneal/Extend</b>	60 °C	30 seconds	
<b>Stop reaction</b>	99 °C	10 minutes	1
<b>Hold</b>	4 °C	Hold	1

### 12.7 Pilot real-time polymerase chain reaction (RT-qPCR)

Some miRNAs, known as myomiRs, have been shown to be selectively expressed in muscle cells (28). Three selected myomiRs, miR-1-3p, miR-133a and miR-206 were examined on RT-qPCR as a test to determine whether the skeletal muscle-derived EVs contained these miRNAs.

#### Procedure

A detailed overview of the reagents/chemicals and equipment used are in appendix 15. The assay reagents and the generated cDNAs from the combined RT/miR-Amp reaction was thawed on ice before vortexing to rigorously mix then spined for a few seconds. A dilution of 1:10 was prepared by adding 5  $\mu$ L of miR-Amp reaction product (cDNA) to 45  $\mu$ L 0.1xTE buffer (Tris-EDTA buffer). TaqMan® Fast Advanced Master Mix was delicately shaken

without bottle inversion to mix. In 4 different reaction tubes a separate PCR reaction mix was prepared for each microRNA (miR-1-3p, miR-133a, miR-206 and miR-223). This was then vortexed and spanned to remove air bubbles. A volume of 15  $\mu$ L PCR reaction mix and 5  $\mu$ L of the diluted cDNA template, both in duplicates, were pipetted in each well of a 96 wells PCR reaction plate before sealing the plate carefully and spinning the contents down using Eppendorf centrifuge 5430 R. The reaction plate was then loaded into the ViiA7 real-time PCR instrument after an input of the right settings as shown in table 6.

Table 6: Real-time PCR (qPCR) conditions and cycles

Step	Temperature	Time	Cycles
<b>Enzyme activation</b>	95 °C	20 seconds	1
<b>Denature</b>	95 °C	1 second	40
<b>Anneal/Extend</b>	60 °C	20 seconds	

### **Integrity and concentration of RNA**

As a result of poor integrity and low yield, several methods were used to control the integrity and RNA concentration without any success. A new RNA extraction was performed on the small remaining volumes of the isolated exosomes. This was to enable a decision of how much concentration of RNA would be used in the Affymetrix microarray analysis. The concentration and integrity of the new extracted RNA was analyzed using NanoDrop One, Qubit 2.0 assay and Agilent 2100 Bioanalyzer.

## 12.8 Pilot Affymetrix microarray

### 12.8.1 Pilot Affymetrix trial

Microarray Affymetrix analysis was done at The Blood Cell Research Group, Section for Research, Development and Innovation, Department of Medical Biochemistry, Oslo University Hospital. Due to concerns around Covid-19 pandemic I was not allowed to actively participate in the pilot Affymetrix microarray analysis but got a summary of what had been done underway from the research team. For details of chemical/reagents used refer to appendix 16.



Flash Tag™ Biotin RNA Labeling Kit and the GeneChip™ miRNA 4.0 were used for analysis of microRNA isolated from EVs.

As a result of low RNA yields from the isolated exosomes in this study, a pilot Affymetrix microarray was performed. This was to find out how low RNA concentrations can be used in Affymetrix microarray analysis. Several methods were used to quantify the amount of RNA (see paragraph 12.2.1 (NanoDrop One), 12.3 (Agilent 2100 bioanalyzer) and 12.4 (Qubit microRNA assay)).

Known as a standard tool in genetic research, Affymetrix microarray, a complex technique, was used to deduce microRNA levels in EVs derived from skeletal muscle cells. The protocol used in the analysis was Flash Tag for Affymetrix (Appendix 16). The cells from donors that had emerged with better exosomes concentrations (particles/mL) on nanoparticle tracking analysis (NTA), NanoDrop One (total RNA), and Qubit (total RNA) assay analyses were selected for the pilot analysis.

ATP was diluted into different concentrations depending on the amount of RNA, using nuclease-free water, and added to RNA samples of (25, 10, 5, 1 ng and 100 ng of a reference control for miRNA-targeted QRT-PCR experiments (Agilent cat. 750700)).

#### 12.8.2 Poly (A) tailing

Spike control oligos and poly(A) tailing master mix including cel-miR-39 were prepared and added to RNA sample. This was gently vortexed and micro-centrifuged before incubating in a 37 °C heat block for 5 minutes.

#### 12.8.3 FlashTag biotin HSR ligation

After incubation, the tailed RNA was micro-centrifuged and placed on ice. An amount of 5x flashTag biotin HSR (hidden-surface removal) ligation mix was added to each sample to label the samples, thereafter T4 DNA ligase was added before mixing gently and micro-centrifuging. This was then incubated at RT for 30 minutes. At the end of 30 minutes the reaction was stopped by an addition of HSR stop solution, before mixing and micro-centrifuging and kept at -20 °C until hybridization of the mixture on the GeneChip 4.0 array.

#### 12.8.4 Hybridization

To the FlashTag™ Biotin HSR RNA labelled samples hybridization cocktail was added and incubated at 99 °C for 5 minutes, then 45 °C for 5 minutes. The mixture was then injected into the upper right septum room tempered and marked arrays. The arrays were placed into the hybridization oven trays. The arrays were then incubated with a 60 rpm for 18 hours at 48 °C before washing and staining. After hybridization, the arrays were removed from the oven and the hybridization cocktail extracted from each array and transferred into Eppendorf tubes. The arrays were then filled with array holding buffer and allowed to equilibrate to RT before washing and staining in a fluidics station using washing buffers and Stain Cocktail 1 and 2. The arrays were checked for air bubbles, dust and other particles before scanning in a GeneChip Scanner 3000.

Data from scanned arrays were transferred to the Expression Conesole software for summarization, normalization, and quality control. To evaluate the labelling protocol and array processing, the spike in control probe sets should have signal greater than or equal to 1000. The spike in-controls consisted of oligos 3, 23 and 29 which are RNA and confirm the poly(A) tailing ligation. Oligo 31 is poly(A) RNA and confirms ligation. Oligo 36 is poly(dA) DNA and confirms ligation and the lack of RNases in the RNA sample. In addition, 200 amol/μL cel-miR-39 was added to each sample.

#### 12.9 Ingenuity pathways analysis (IPA)

Ingenuity pathway analysis (IPA) is an online, web-based software application used in analysis of raw data from microRNA and proteomics among others. It is used to enable an understanding of the role of microRNA, their targets and function in cells. It identifies signal pathways that are regulated by microRNA. In this thesis the method was used to predict the targets and biological functions in which miRNA were involved.

#### 12.10 Data and statistical analyses

A paired Student's T-test was used for statistical analysis and p-value <0.05 was considered statistically significant. The presentation of data is as mean with standard error of the mean ( $\pm$  SEM) or standard deviation ( $\pm$  SD). N indicates the number of donors, each with at least duplicate measures. Linear regression analysis was used to determine the relationship between signal value in Affymetrix analysis of RNA amounts. The programs used were

Ingenuity pathways analysis (IPA), Partek, prism9 GraphPad, and in addition SPSS and Excel were used when required.

## 13 Results

### 13.1 Concentration of IL-6 in cell medium

To determine whether there was any muscle contraction during electrical pulse stimulation (EPS) of myotubes in culture, IL-6 concentration in the conditioned cell media was analyzed by ELISA. The results indicated a 37 % ( $\pm 17$  %) increase in IL-6 concentration after EPS (Figure 17). This might demonstrate that EPS have had an effect on the myotubes, even though not statistically significant ( $p = 0.11$ ). All, except one donor, responded to EPS by increasing the release of IL-6.

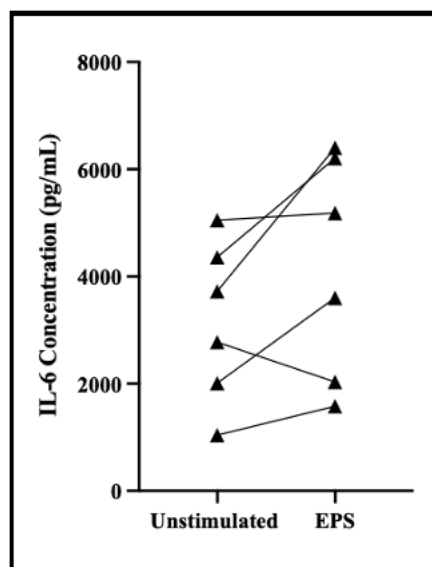


*Figure 17: Interleukin-6 (IL-6) concentration.* The IL-6 concentration was measured in the media from the myotubes cell culture after 24 hours with and without electrical pulse stimulation (EPS) using enzyme-linked immunosorbent assay (ELISA). Each point is an average concentration of duplicates measures.

### 13.1 Protein quantification

Figure 18 shows a determination of whether there was any difference in total cell protein concentration with or without stimulation with EPS to establish whether cell content was affected by EPS. The analysis showed that there was no significant difference between unstimulated and EPS ( $p > 0.05$ ).

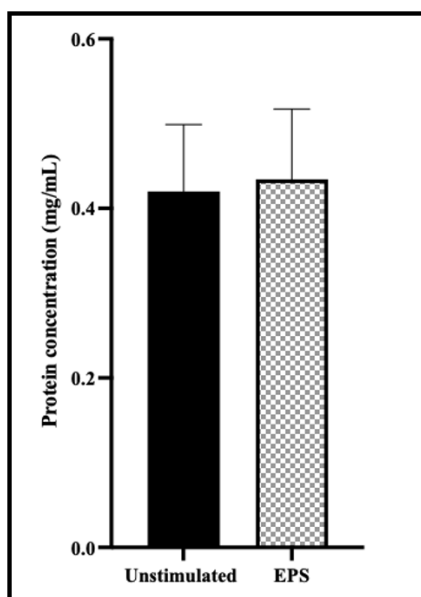


**Figure 18: Protein concentration measurement in lysed myotubes.** The mature myotubes were either unstimulated or stimulated for 24 hours with electrical pulse stimulation (EPS), lysed using 0.1M NaOH and then protein concentration determined according to Bradford (107). The measured data is presented as mean  $\pm$  SEM, n=6.

## 13.2 Characterization of extracellular vesicles

The characterization of EVs was determined using transmission electron microscopy (TEM), nanoparticle tracking analysis (NTA), and western blotting analysis, according to ISEVs guidelines for the minimal requirements for EVs characterization (90) (120).

### 13.2.1 Transmission electron microscopy (TEM)

To assess the morphology of EVs TEM technique was utilized. The pictures of EVs (Figure 19) show a spherical morphology and a cup formed shape, typical EV characteristics.

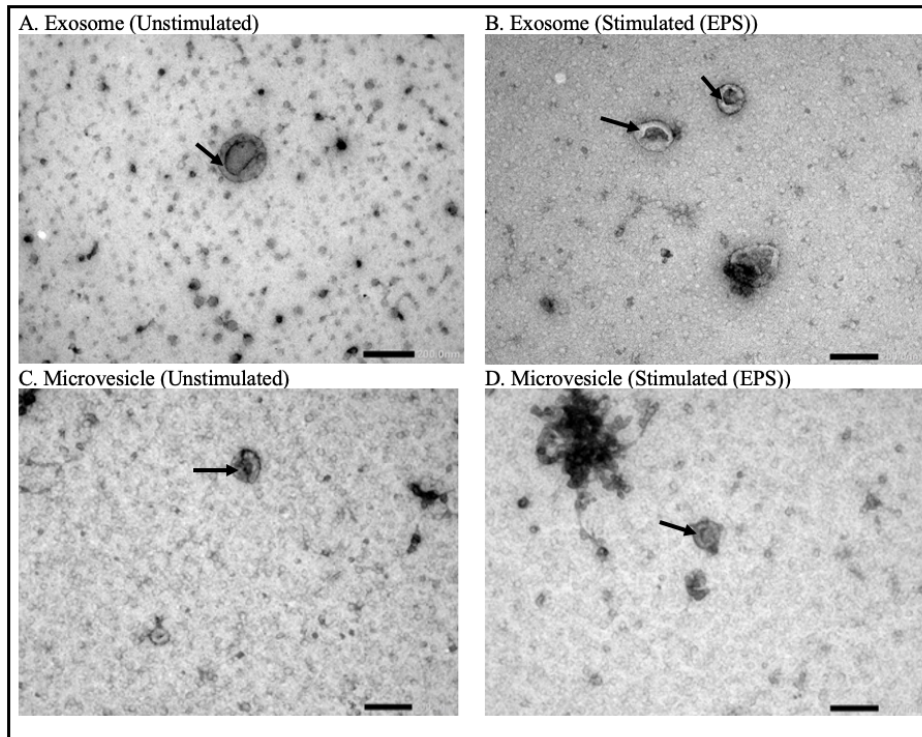


**Figure 19: Morphology of extracellular vesicles (EVs)** After harvesting conditioned media, freshly isolated EVs were sent in for transmission electron microscopy (TEM) analysis. A & B; The spherical morphology of exosomes, C & D the microvesicle' morphology. A & C are from the unstimulated myotubes, while B & D are from the stimulated (EPS) myotubes. The dark arrows point at EVs. The scale bar sizes are 200 nm. The analysis and image capturing were done at, The Electron Microscopy Laboratory, Department of Molecular Biosciences, University of Oslo by Professor Norbert Roos. EPS (electrical pulse stimulation) (n=2).

### 13.2.2 Size and concentration of extracellular vesicles

The particle size distributions and concentrations of EVs released by myotubes with and without EPS were measured using nanoparticle tracking analysis (NTA).

Mean size for exosomes was 139 nm for unstimulated and 141 nm for stimulated (EPS), whereas MV had a mean size of 158 nm for unstimulated and 164 nm after EPS (Figure 20 A). Mode size for exosomes was 126 nm for unstimulated and 127 nm for EPS, while for the MV the mode size was 138 nm for unstimulated and EPS had 141 nm (Figure 20 B). Using a Student's paired t-test, there was no statistically significant difference in size after EPS for exosomes neither was there for MV. However, there was a statistically significant difference in size between exosomes and MV for mean when put together (unstimulated and EPS for exosomes against MV,  $p = 0.02$ ), but no statistically significant difference in size between exosomes and MV when assessed by mode,  $p = 0.13$ .

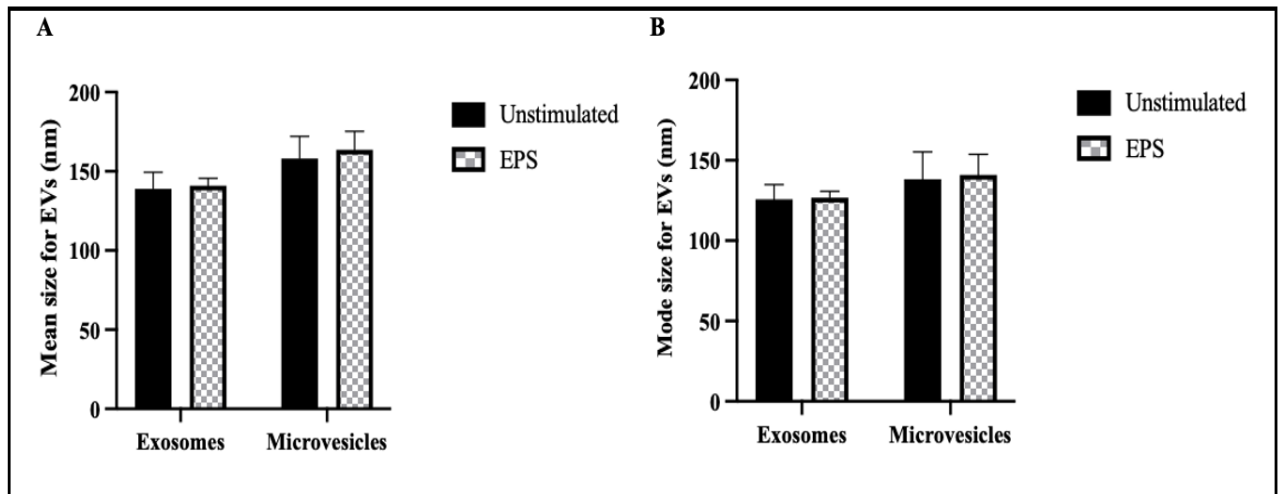


**Figure 20: Characterization of extracellular vesicle (EV) size using nanoparticle tracking analysis (NTA).** The myotubes were either unstimulated or stimulated for 24 hours with electrical pulse stimulation (EPS) and incubated for another 24 hours in serum free media. The media was then collected and EVs isolated before analyzing to determine the EV size. A number of 3 videos at 60 seconds per sample were captured, and the results are reported as an average of 3 videos. (A) Mean size presentation of EVs and (B) mode size presentation of EVs, both with  $\pm$  SEM. nm (nanometer). N=6.

The average concentration of exosomes derived from unstimulated myotubes was  $2.97 \times 10^9$  particles/mL, and  $3.34 \times 10^9$  particles/mL after EPS (Figure 21, Table 7). MV had an average concentration of  $8.93 \times 10^9$  particles/mL for unstimulated and  $1.09 \times 10^{10}$  particles/mL after EPS (Figure 21, Table 7).

Overall, the total average concentrations of EVs (exosomes + MV) without EPS was  $1.19 \times 10^{10}$  particles/mL, while after EPS it was  $1.42 \times 10^{10}$  particles/mL. However, there was no significant difference in particle concentrations with or without EPS.

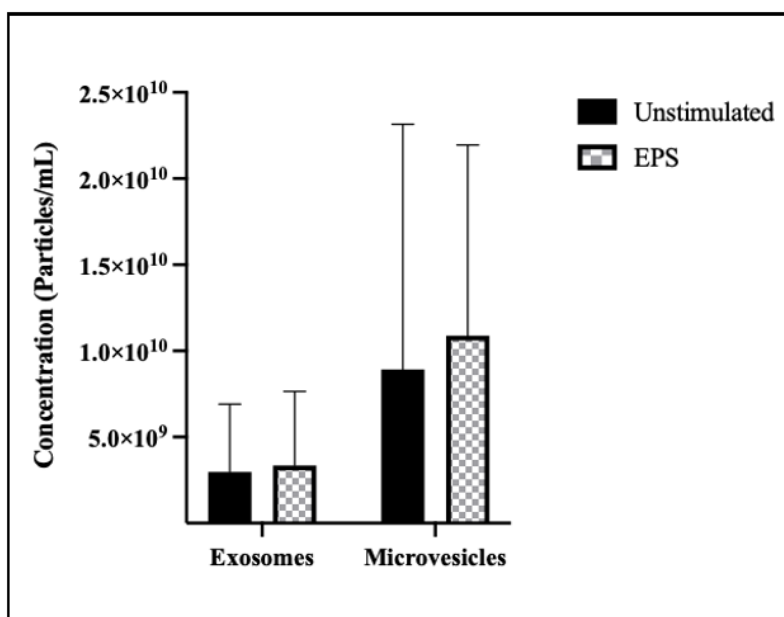


**Figure 21: Characterization of extracellular vesicle (EV) concentrations using nanoparticle tracking analysis (NTA).** After electrical pulse stimulation of myotubes for 24 hours, the cells were incubated in serum free medium for another 24 hours. These media were collected ready for isolation of EVs followed by NTA to determine the EV concentration. A number of 3 videos at 60 seconds per sample were captured and the results are reported as the average of 3 videos. The measured data are presented as mean  $\pm$ SEM, EPS (electrical pulse stimulation.)  $n=6$ .

To determine the total yield of extracellular vesicles obtained from the media, calculation of the total number of EVs was performed. This was to find out the exact amounts of each EVs obtained after isolation from the media. The total outcome of number of exosomes was very similar to number of MV (Table 7).

**Table 7: Average concentrations, volumes and total number of extracellular vesicles recovered**

Extracellular vesicles	Exosomes		Microvesicles	
	Unstimulated	Stimulated (EPS)	Unstimulated	Stimulated (EPS)
<b>Concentrations (Particles/mL)</b>	2.97 x 10 <sup>9</sup> $\pm$ (1.61 x 10 <sup>9</sup> )	3.34 x 10 <sup>9</sup> $\pm$ (1.76 x 10 <sup>9</sup> )	8.93 x 10 <sup>9</sup> $\pm$ (5.81 x 10 <sup>9</sup> )	1.09 x 10 <sup>10</sup> $\pm$ (4.52 x 10 <sup>9</sup> )
<b>Volume (mL)</b>	0.197	0.228	0.087	0.082
<b>Total number</b>	5.85 x 10 <sup>8</sup> $\pm$ (3.17 x 10 <sup>8</sup> )	7.62 x 10 <sup>8</sup> $\pm$ (4.23 x 10 <sup>8</sup> )	7.77 x 10 <sup>8</sup> $\pm$ (5.84 x 10 <sup>8</sup> )	8.94 x 10 <sup>8</sup> $\pm$ (3.62 x 10 <sup>8</sup> )

The results are presented as means  $\pm$  SEM. EPS (electrical pulse stimulation).



As a negative control, EVs were also isolated from serum free media that had not been in contact with cells. This was to control for a possible contamination with serum-derived extracellular vesicles from M3-differentiation media used in cell culturing. NTA confirmed the presence of particles in the serum free medium (SFM). In comparison to the conditioned media from donor samples, SFM contained much lower concentrations ( $1.66 \times 10^8$  particles/mL) for exosomes and ( $3.14 \times 10^8$  particles/mL) for MV. This means that there was 20-fold higher concentration of exosomes and a 35-fold higher concentration of MV in conditioned media from myotubes.

### 13.2.2.1 Characterization of exosomes by western blot analysis

Western blotting indicated the presence of CD63 and Hsc70/Hsp70 in the skeletal muscle cell derived exosomes from all the analyzed donors, whereas CD9 and the negative control calnexin were not detected (Figure 22). No obvious differences between unstimulated and EPS-stimulated exosomes were observed. In the positive control, lysate of cell line SW480, all the markers were detected (Figure 22).

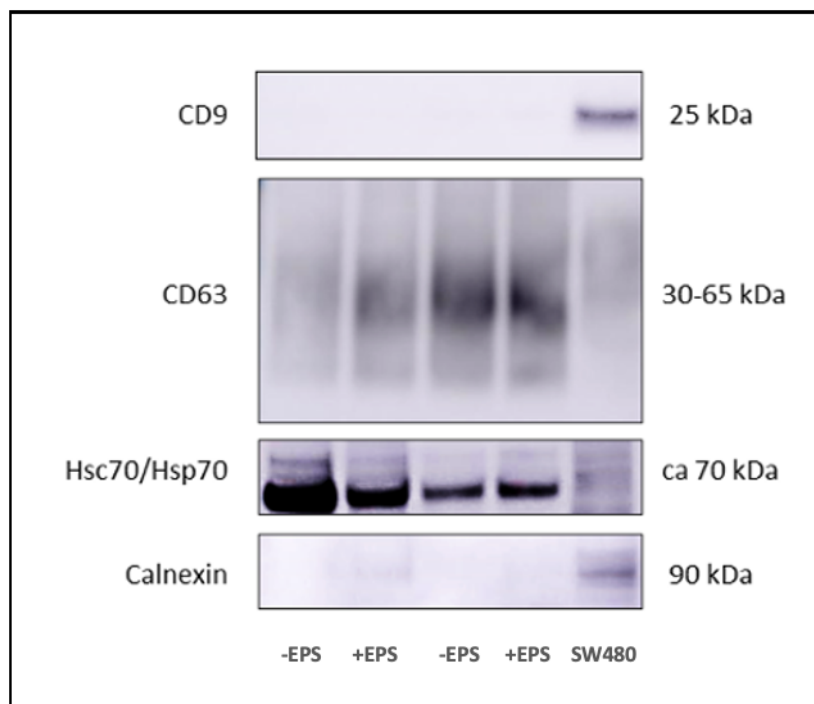


**Figure 22: Western blotting analysis.** Western blotting analysis was done on exosomes isolated from unstimulated and electrical pulse stimulated (EPS) cell's conditioned media. This was done to determine the biomarkers encompassed in exosomes, CD9, CD63 and Hsc70/Hsp70. Calnexin was used as a negative control (marker of endoplasmic reticulum). The cancer cell line SW480 was used as a positive control. Two randomly selected donors are shown. -EPS (unstimulated), +EPS (stimulated), CD (cluster of differentiation), ca(circa), kDa (kilodalton), Hsc/Hsp (heat shock protein), cell line SW480 (colorectal cancer cell line).

### 13.3 Quantification of miRNA.

#### 13.3.1 Real-time RT-qPCR of miR from exosome derived RNA

Three previously identified human miRNAs (myomiR) miR-1-3p, miR-133a, and miR-206 were analyzed using RT-qPCR (Table 8).

This was performed as a combined study of the quality and quantity of the isolated total RNA from EVs, to confirm that these miRs were enriched in muscles and could be detected in skeletal muscle cell derived EVs.

Real-time RT-qPCR analysis was utilized to quantify the levels of the selected miRs in all the 6 donors using the same volume of exosome derived total RNA (2  $\mu$ L). The crossing point (cycle threshold (Ct)) values were recorded, and the results showed that the three myomiRs were able to be fully read in only 3 of the 6 donors (Table 8).

**Table 8: RT-qPCR of myomiR**

miR type	miR-1-3p		miR-133a		miR-206	
Cycle threshold	Ct		Ct		Ct	
Donors	<i>Unstimulated</i>	<b>EPS</b>	<i>Unstimulated</i>	<b>EPS</b>	<i>Unstimulated</i>	<b>EPS</b>
<b>1</b>	24.9	23.7	27.6	25.8	27.1	27.1
<b>2</b>	22.8	29.4	23.5	28.2	22.7	25.7
<b>6</b>	21.4	22.5	22.7	24.1	21.9	23.7

*miR (microRNA), Ct (cycle threshold), EPS (electrical pulse stimulation)*

There was a considerable variation in Ct values ranging from 21.4 to 29.4, implying a need for quantification of RNA concentrations before Affymetrix.

#### 13.3.2 Quantification of isolated RNA

Given the above results, quantification of total RNA to control the concentration and purity was performed using different quantification methods; NanoDrop One, Agilent Bioanalyzer and Qubit fluorometric quantification method. NanoDrop One showed that RNAs were not

clean (Table 9). The concentrations varied considerably among donors, and the low RN ratios confirmed the presence of impurities since the ideal ratio is 2.0 or above (Table 9).

**Table 9: Control of RNA concentrations and purity using NanoDrop One**

Donors	RNA concentration NanoDrop One (ng/ $\mu$ L)		RNA ratio (A260/A280)	
	<i>Unstimulated</i>	EPS	<i>Unstimulated</i>	EPS
<b>1</b>	12.50	24.00	1.44	1.46
<b>2</b>	14.90	71.50	1.47	1.91
<b>3</b>	13.20	17.10	1.61	1.47
<b>4</b>	13.80	13.60	1.49	1.47
<b>5</b>	322.40	9.30	1.45	1.44
<b>6</b>	58.90	9.20	2.00	1.72

*EPS (electrical pulse stimulation)*

### 13.3.2.1 Agilent 2100 Bioanalyzer

Agilent 2100 Bioanalyzer was the second RNA quantification method that was used to check RNA concentrations and integrity, since this was important knowledge to generate before the downstream analysis. The Agilent 2100 Bioanalyzer results confirmed that the RNA integrity was poor (Figure 23). The concentrations measured were unreliable due to low levels and the bands were not easy to read. There were numerous small RNA molecules encompassed in the isolated total RNA from exosomes. Since microRNA have a size of circa 22 nucleotides, the strong bands in the electrophoresis were expected to start from around the green line between 20 and 25 (Figure 23), an indication of impurity in the samples.

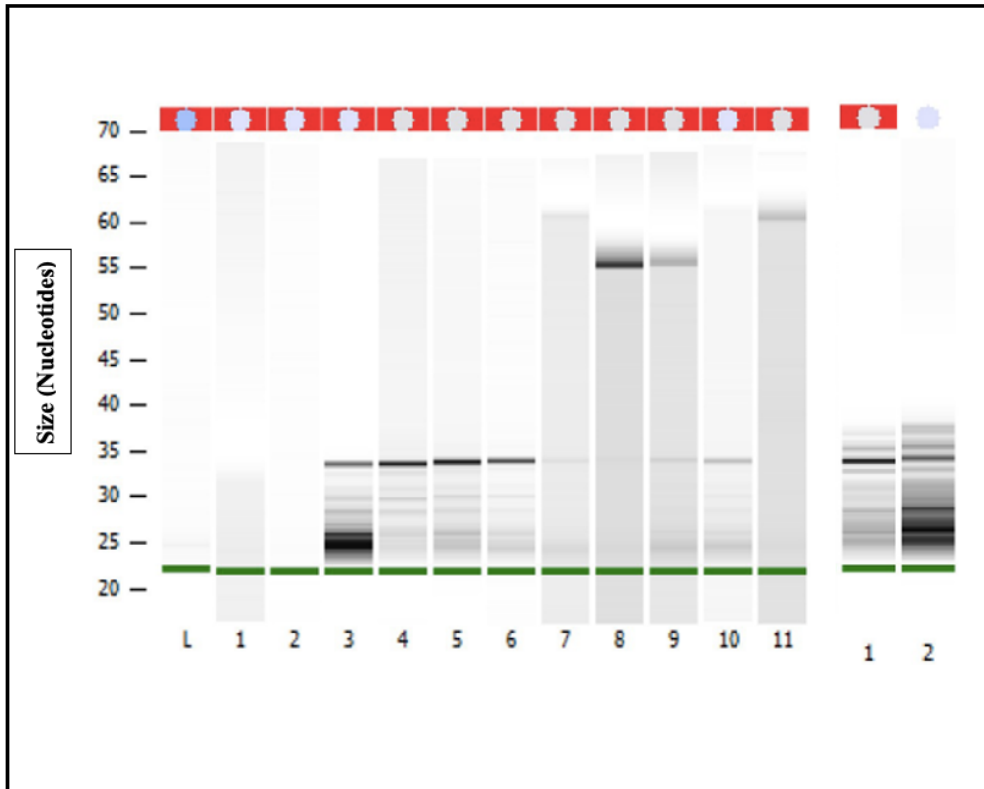


*Figure 23: Agilent 2100 Bioanalyzer analysis of total RNA extracted from exosomes for all donors. After reagents, samples and ladder pipetting into the chip priming station, the RNA pico chip was loaded into the Agilent 2100 Bioanalyzer for analysis. The ladder was used as a calibrator. RNA pico chip allows a maximum of 10 samples to be analyzed at a time but samples to be analyzed were 12 in total, thus the analysis was performed twice with different ladders. Unstimulated are denoted by even numbers and stimulated (EPS) by odd numbers and lane 11 is a ladder. L (Ladder).*

The low RNA yield and poor integrity led to a search for a solution for new quantifications, kits and positive controls that could be analyzed in parallel with other samples. Qubit fluorometric quantitation method for microRNA and spike-in controls such as ath-miR-159a miR39 and a reference miR, were bought and analyzed to provide information from exosomes derived miR results that were expected after NanoDrop One, Agilent 2100 Bioanalyzer and Qubit microRNA analysis.

### 13.3.2.2 Qubit microRNA assay

It was concluded to perform a new isolation of total RNA on the remaining small volumes of exosome samples to provide RNA for further analysis. New measurements by NanoDrop One together with a third, highly sensitive RNA quantification method, Qubit 2.0 assay, were performed on the newly extracted RNA. This was done to ascertain reliable concentration measurement for RNA samples with low levels. The total RNA yields still varied and were quite low (Table 10).

**Table 10: Total RNA concentration analyzed by NanoDrop One and Qubit 2.0**

<b>Donors</b>	<b>RNA concentration NanoDrop One (ng/<math>\mu</math>L)</b>		<b>RNA concentration Qubit 2.0 (ng/<math>\mu</math>L)</b>	
	<i>Unstimulated</i>	<b>EPS</b>	<i>Unstimulated</i>	<b>EPS</b>
<b>1</b>	35.04	57.93	5.94	0.26
<b>2</b>	31.36	87.34	4.78	44.0
<b>3</b>	54.64	33.80	0.40	0.35
<b>4</b>	37.58	34.27	0.38	0.20
<b>5</b>	25.43	18.18	0.52	0.21
<b>6</b>	42.74	26.43	11.60	1.09

*EPS (electrical pulse stimulation).*

### 13.3.2.3 Second Agilent 2100 Bioanalyzer performed

The integrity of the new RNA was controlled using Agilent 2100 Bioanalyzer (Figure 24). This was to decide whether the new RNA had a satisfactory quality to be used in Affymetrix microarray analysis. Only two donors were used in this analysis, both were from unstimulated cells (Table 10 and Figure 24). From figure 24 it can be seen that the bands start at around 20 - 25. The bands were tightly close to each other, and evenly distributed around the size of nucleotides of microRNA, a pattern expected of EV derived RNA, with good integrity. Lanes 3 and 4 are reference RNA from cell derived total RNA, which were used to compare the RNA patterns from cells with EV derived total RNA. Cell derived RNA have two distinct high molecular bands representing ribosomal RNA that are enriched in cells.

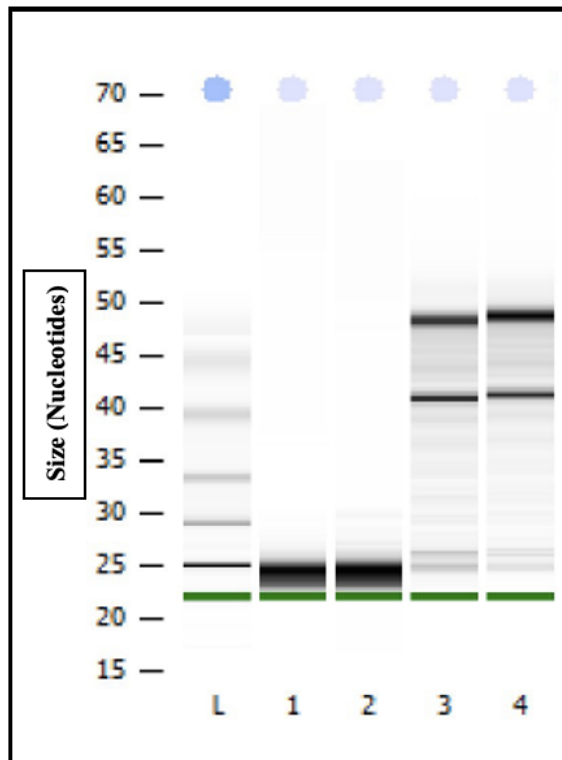


*Figure 24: Total RNA analysis on Agilent 2100 Bioanalyzer. As a result of poor integrity and low RNA yield, new total RNA was extracted from the remaining exosomes and the integrity and concentrations controlled. The donors are in lane 1 and 2, RNA from unstimulated exosomes. Lanes 3 and 4 are reference total RNA from reference samples, commercially available cells.*

### 13.3.3 Affymetrix microarray

Affymetrix microarray technology was used to determine what types of miRNA are found in skeletal muscle cell derived EVs from diabetes individuals and to determine whether muscle stimulation with EPS changes the miRNA-pattern.

#### 13.3.3.1 Pilot dilution experiment on Affymetrix microarray - determination of total RNA input from exosomes.

Flash Tag™ Biotin RNA Labeling Kit and the GeneChip™ miRNA 4.0 were used for analysis of total RNA isolated from donor exosomes. This kit is designed for analysis of total RNA from cells, and a pilot experiment was performed to determine the amount of RNA from exosomes that was needed to achieve optimal and reproducible data. Trials of the Affymetrix microarray analysis were performed with different amounts of total RNA to ascertain the optimal input of RNA. This information was critical to achieve before the final Affymetrix analysis was performed, since this would enable the comparison of the two groups (unstimulated and EPS) and find out whether EPS had any effect on the miR cargo content of exosomes.

**Pilot analysis to determine input of total RNA from extracellular vesicles in the Affymetrix analysis**

Table 11 shows a screen shot of a pilot Affymetrix microarray analysis performed on donors where results were sorted based on reduced signal values. The array analysis illustrated that 1 to 10 ng RNA input from exosomes gave satisfactory results with good signal values, while lower signals were achieved for amounts above 10 ng. It was illustrated that skeletal muscle cell derived exosomes contained different types of small non-coding RNA.

**Table 11: Screen shot results from pilot Affymetrix microarray analysis.**

			Normale tall											
			1 ng			5 ng			10 ng			25 ng	100 ng ref RNA	
Species St	Transcript	Array Des	Pr4_exo4	Pr7_exo5	Mean	Pr3_exo4	Pr6_exo5	Mean	Pr2_exo4	Pr5_exo5	Mean	Pr1_exo4	Pr8_refRN	100ng_(m
Homo sapiens	hsa-miR-3665		3548	6847	5198	8744	10137	9440	9346	10550	9948	5460	3163	
Homo sapiens	hsa-miR-3960		2865	5859	4362	7549	9907	8728	8419	10198	9308	5074	3281	
Homo sapiens	hsa-miR-6089		2952	5479	4216	7405	9454	8429	7978	10088	9033	5118	2832	
Homo sapiens	hsa-miR-6090		2944	5263	4104	6957	8252	7605	7805	8689	8247	4455	2541	
Homo sapiens	hsa-miR-4497		1530	3122	2326	4992	7337	6164	6612	9365	7988	6180	858	
Homo sapiens	hsa-miR-8069		2004	4127	3066	5797	7507	6652	6903	7895	7399	3754	1159	
Homo sapiens	hsa-miR-7704		2187	4361	3274	5653	7340	6497	6117	7168	6642	3408	2334	
Homo sapiens	hsa-miR-4787-5p		1916	4342	3129	5348	6875	6111	6037	6908	6473	3031	2264	
Homo sapiens	hsa-miR-6125		1437	3235	2336	4607	6106	5356	5516	6795	6156	3176	1414	
Homo sapiens	hsa-miR-6087		1621	3585	2603	4515	6323	5419	5227	6842	6035	3550	1754	
Homo sapiens	hsa-miR-4466		1602	3258	2430	4344	6024	5184	5053	6208	5630	2931	1130	
Homo sapiens	hsa-miR-224-3p		625	760	693	2493	2905	2699	4675	5116	4896	5377	3	
Homo sapiens	hsa-miR-6088		1332	2264	1798	3448	4964	4206	4157	5464	4810	2276	1332	
Homo sapiens	hsa-miR-6729-5p		1279	2659	1969	4028	4907	4467	4228	5244	4736	2393	1202	
Homo sapiens	hsa-miR-1915-3p		1467	2629	2048	3741	4652	4197	4298	5004	4651	2259	1034	
Homo sapiens	hsa-miR-4488		1303	2750	2027	3401	4931	4166	3652	4986	4319	2264	663	
Homo sapiens	hsa-miR-638		1046	2430	1738	3121	4490	3806	3720	4735	4227	2043	966	
Homo sapiens	hsa-miR-4516		1417	2288	1853	3650	3934	3792	3982	4336	4159	1990	759	
Homo sapiens	hsa-miR-6869-5p		1583	2658	2121	4186	3760	3973	4126	4160	4143	2105	1635	
Homo sapiens	hsa-miR-6727-5p		1057	2312	1685	3001	4233	3617	3479	4605	4042	1910	770	
Homo sapiens	hsa-miR-2861		730	1712	1221	2441	3596	3018	3087	4296	3691	1815	720	
Homo sapiens	hsa-miR-3196		725	1886	1306	2227	3941	3084	2863	3857	3360	1651	624	
Homo sapiens	hsa-miR-1237-5p		723	1581	1152	2151	3810	2980	2789	3767	3278	1958	433	
Homo sapiens	hsa-miR-3656		496	1312	904	1775	3205	2490	2545	3598	3071	1728	581	

An amount of 1, 5, 10 and 25 ng total RNA from 2 donors and 100 ng reference RNA were applied to the Flash Tag™ Biotin RNA Labeling Kit and the GeneChip™ miRNA 4.0. The selected data shown are unfiltered and sorted in a descending order. Hsa (homo sapiens), miR (microRNA).

A correlation plot between the results generated using signal values from an input of 1 ng and 5 ng RNA, showed a good correlation with a coefficient of determination being ( $R^2 = 0.98$ ). Meaning that the signal values obtained with 1 ng correlated well with the signal values obtained with 5 ng RNA (Figure 25).

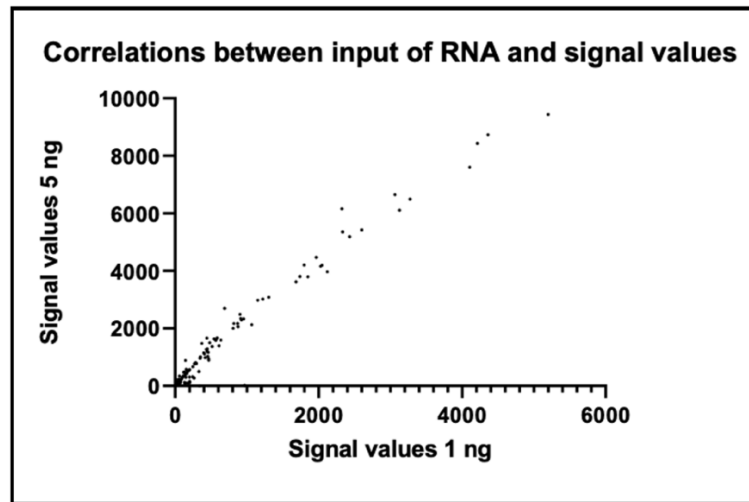


*Figure 25: Pilot Affymetrix microarray dilution analysis on two donors. Different RNA amounts were tested to find the amounts that gave the best signal values. A correlation plot was then generated based on 1 ng and 5 ng to find out if the signal values from the different amounts correlated  $R^2 = 0.98$ .*

### 13.3.3.2 Affymetrix microarray analysis of RNA

The final Affymetrix microarray was then performed on exosome derived RNA from three donors (2, 3 and 6), on both unstimulated and stimulated (EPS) exosomes. From the pilot Affymetrix microarray analysis, the results illustrated that there was a variation in the signal value generated depending on total RNA input. An input of 2.5 ng total RNA was assumed to give satisfactory results on the signal values, hence used in the analysis on the 3 donors.

An amount of 2.5 ng RNA from three donors before and after electrical pulse stimulation were applied to the Flash Tag™ Biotin RNA labeling Kit and the GeneChip™ miRNA 4.0. Following the Affymetrix microarray results, the results were then loaded in Partek Genomic for statistical analysis and in Ingenuity Pathway Analysis (IPA) for biological analysis. A descriptive analysis of RNA in the skeletal muscle cell derived exosomes was done on RNA from unstimulated myotubes only (Table 12). This was done to investigate which microRNA sequence types were present in exosomes. Based on signal values = or >5, 271 non-coding RNA transcripts were detected by IPA and out of the total 219 were miRNA. This illustrated that there were numerous divergent biological cargo components contained in muscle derived extracellular vesicles (Table 12).



**Table 12: Subtypes of non-coding RNA detected by Affymetrix microarray analysis**

Sequence type	Numbers	Signal values (range)
<b>5.8 rRNA (gi555853)</b>	10	5 - 316
<b>CDBOX (U43)</b>	3	5 - 53
<b>miRNA</b>	219	5 - 2700
<b>snoRNA</b>	14	5 - 465
<b>Stemloop miRNA</b>	25	5 - 200

rRNA (ribosomal RNA), CDBOX (U43), miRNA (microRNA), snoRNA (immature RNA/small nucleolar RNA), n = 3

The miR from unstimulated skeletal muscle cell derived EVs were found to be involved in diseases and functions such as inflammatory diseases, respiratory diseases, cardiovascular diseases, psychological disorders, hereditary disorders among others (Figure 26).

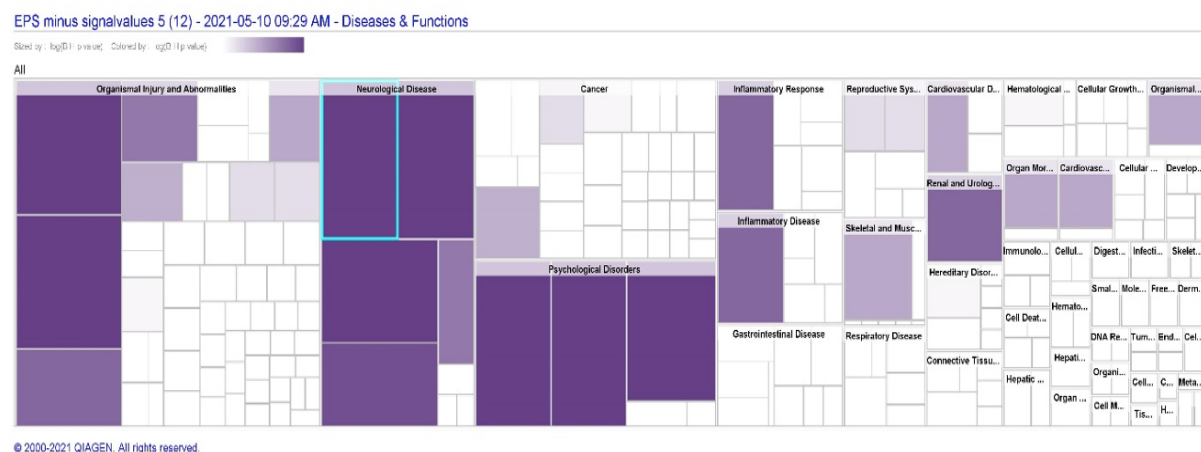


**Figure 26: MiRNAs' biological functions generated in IPA.** Top diseases and biological functions of miRNA in exosome derived from skeletal muscle cells.

The 271 transcripts were loaded into the Ingenuity Pathway Analysis (IPA) and it was illustrated that 236 of the transcripts were mapped with known ID and 35 were found unmapped, which means that 35 miRs could not be mapped to a corresponding protein.

Affymetrix microarray analysis was loaded in IPA and based on the following criteria, signal values  $>5$  and  $>1.5$  fold-change, IPA found that 12 miRs were significantly changed by EPS ( $p < 0.05$ ). Of these 12 miRs, 10 miR were found to be significantly upregulated while 2 miR were significantly down regulated (Table 13). MiR-1233-5p had the highest fold change with 3.29 and miR-1909-3p the lowest with 1.78 in the 10 upgraded miR (Table 13).

**Table 13: Analysis of Affymetrix microarray data of 271 transcripts in Ingenuity Pathway Analysis software. MiRs that were significantly changed by EPS with >1.5-fold-change and signal values >5.**

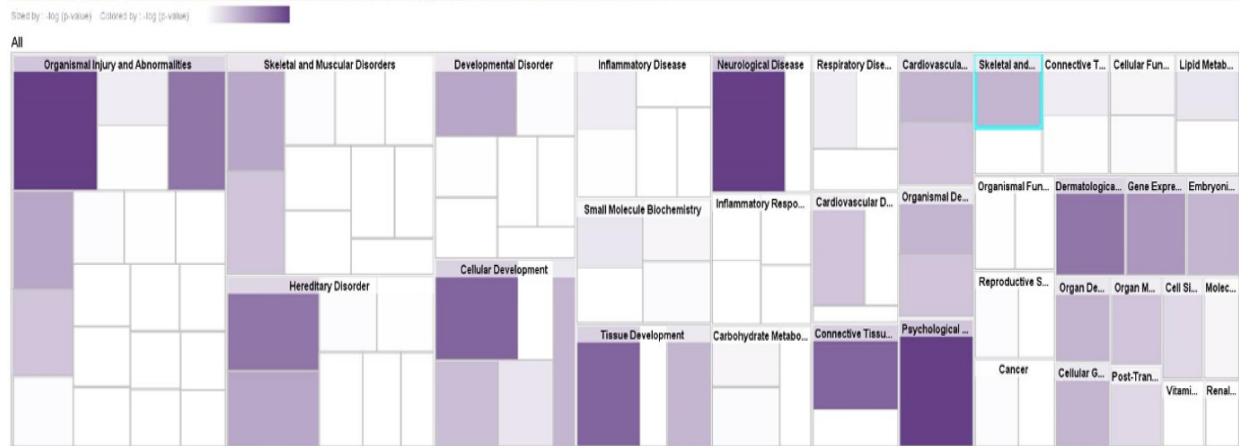
Molecules	Fold change
miR-1233-5p	3.29
miR-320b	2.81
miR-4532	2.52
miR-92b-5p	2.49
miR-3141	2.36
miR-4634	2.23
miR-4649-5p	2.02
miR-4467	1.98
miR-4433b-3p	1.89
miR-1909-3p	1.78
miR-6880-3p	-1.65
miR-10399-5p	-1.57

### 13.3.3.3 Ingenuity pathways analysis (IPA)

Pathway analysis in IPA showed which diseases, biological functions and physiological systems that are known to be associated with the miRs that were significantly changed by EPS (Table 14, Figure 27).

**Table 14: Top diseases and biofunctions of miR with significantly changed levels after EPS from skeletal muscle cell derived exosomes**

Molecular and cellular functions	p-value range
Cellular development	$3.31 \times 10^{-2} - 3.97 \times 10^{-4}$
Gene expression	$2.01 \times 10^{-3} - 2.01 \times 10^{-3}$
Cellular growth and proliferation	$4.19 \times 10^{-3} - 4.19 \times 10^{-3}$
Cell signaling	$8.37 \times 10^{-3} - 8.37 \times 10^{-3}$
Post-translational modification	$8.37 \times 10^{-3} - 8.37 \times 10^{-3}$
<b>Physiological system development and function</b>	
Connective tissue development and function	$3.31 \times 10^{-2} - 3.97 \times 10^{-4}$
Tissue development	$3.31 \times 10^{-2} - 3.97 \times 10^{-4}$
Cardiovascular system development and function	$5.76 \times 10^{-3} - 4.19 \times 10^{-3}$
Embryonic development	$4.19 \times 10^{-3} - 4.19 \times 10^{-3}$
Organic development	$4.19 \times 10^{-3} - 4.19 \times 10^{-3}$



© 2000-2021 QIAGEN. All rights reserved.

**Figure 27:** miRNAs' biological functions generated in IPA. MiRNA with significantly changed signal levels during EPS from skeletal muscle cell derived exosomes.

Table 15 shows upstream regulators involved in expression of the significantly affected miRs by EPS. AGO2 (argonaute RISC catalytic component 2) showed to be the most significant upstream regulator.

**Table 15: Prediction of top upstream regulators involved in expression of the miRNAs significantly changed by EPS**

Upstream regulators	p-value
AGO2	$3.54 \times 10^{-5}$
TGS1	$2.93 \times 10^{-4}$
MET	$2.05 \times 10^{-3}$
XPO1	$2.05 \times 10^{-3}$
TP53	$3.32 \times 10^{-2}$

IPA prediction showed that MET (MET Proto-Oncogene, Receptor Tyrosine Kinase) had an inhibiting effect while XPO1(Exportin 1), AGO2 (argonaute RISC catalytic component 2), TP53 (Tumor protein p53) and TGS1 (Trimethylguanosine synthase 1) had an activating effect on the involved miR (Figure 28).



## 14 Discussion

The main aims of this thesis were to find out if skeletal muscle cell derived EVs do encompass miRNA and evaluate changes that EPS can have on this miRNA. Several novel findings emerged. The key findings were that, following Affymetrix microarray performed on EVs from 3 donors 271 transcripts were generated by IPA of which 236 had a mapped ID and 35 unmapped, meaning that 35 transcripts had never been mapped before. A number of 12 miR were relevant (filtrations criterion which included  $p < 0.05$ , 5 or above signal values and 1.5 or above fold change) for our aim, which was to find out whether there was a difference in miR found in exosomes with and without EPS. The miRs significantly changed by EPS were miR-1233-5p, miR-320b, miR-4532, miR-92b-5p, miR-3141, miR-4634, miR-4649-5p, miR-4467, miR-4433b-3p, miR-1909-3p, miR-6880-3p and miR-10399-5p.

Further, EPS did not change the number or size of EVs neither exosomes nor MV. The number of exosomes and MV released from skeletal muscle cells were about the same, and the presence of EVs was confirmed by TEM while the presence of the specific surface markers CD63 and Hsc70/Hsp70 were identified by western blotting.

To further explore possible ways in which exercise could have had effects on miR in terms of changes in the miR levels of expression, the results from Affymetrix microarray analysis 271 were loaded into IPA. After EPS the levels of the following biofunctions of miR were found to be significantly changed; connective tissue development and function, cardiovascular system development and function, among others. The levels of molecular and cellular functions were also found to be changed and this included post-translational modification, cell signaling gene expression among others. It is reasonable to suggest that these pathways or molecular systems were affected by muscle contraction caused by EPS.

A prediction analysis was then run in IPA to determine the top upstream regulators involved in miR expression. Among the top regulators were AGO2, XPO1, TP53 and MET. According to IPAs prediction, MET had an inhibiting effect while AGO2, XPO1, TP53 and TGS1 had an activating effect on miR. A search in the Panther Classification System showed that AGO2 was a translation initiation factor and was defined as a non-ribosomal protein involved in translation initiation. XPO1 was found to be involved in RNA binding and transporter activity, where it was defined as a class of transmembrane proteins that allows

substances to cross plasma membranes far faster than they would be possible by diffusion alone. MET was found to be involved among others in RNA processing, including capping, polyadenylation and splicing. TP53 was found to be involved among others in the attachment of one cell to another cell via adhesion molecules.

The upstream regulators in IPA were an indicate that EPS can have an effect on some of the signal pathways in the skeletal muscles, where the consequences are a release of EVs loaded with active miRNA into the extracellular environment. In general, the activation of upstream regulators means that the gene expression changes where specific genes are affected. That means that EPS might cause an effect that leads to activation of gene expression. This is expected since muscle stimulation leads to a production of numerous components.

It was illustrated that skeletal muscles do release EVs into the extracellular environment as demonstrated by two master theses performed on the same donors by Qureshi S. and Abdullahi H. A (49, 88), in addition to the previous study by Bihan M. L et. al. (121). The released EVs were found to contain numerous cargoes, in which are divergent components that have important biological functions. The Affymetrix microarray analysis showed a detection of the following cargo components from skeletal muscle cell derived exosomes; 5.8 rRNA (gi555853) a ribosomal RNA, CDBOX (U43), miRNA, snoRNA and Stemloop miRNA. This illustrated that EVs does encompass other RNA components apart from miRNA. This was also illustrated in previous master studies by Qureshi S. and Abdullahi H. A, where a proteomics analysis on the same donors was performed and it was illustrated that EVs do entail proteins (49, 88).

Studies have shown that physical exercise induces changes in skeletal muscles and can modify the expression of miRNA in skeletal muscle (38, 41, 122). MiR-1, miR-206 and miR-133 have been found in skeletal muscles (123), and real-time RT-qPCR was performed in this work, using miR-1-3p, miR-133a and miR-206 to ascertain their presence in skeletal muscles. Physical activities can modify miR expression and their expression varies depending on the intensity, type of exercise and how long the exercise lasts (38). This was demonstrated in a study done on muscle cells by Nielsen S. et al. *in vivo*, where it was observed that repeated bouts of endurance exercise increased miR-133a while a 12-week high intensity endurance physical exercise downregulated miR-1, miR-133a and miR-206 (38). In another *in vivo* study by Nielsen. S et al. done on muscle cells, it was observed that miR-233 was upregulated

1 hour after an acute exercise bout (124). In this thesis, electrical pulse stimulation (EPS) was used to induce muscle contraction. This was found to have some effects on the contents of skeletal muscle cell derived exosomes, where 10 miR were found to be upregulated. This included miR-1233-5p, miR-320b, miR-4532, miR-92b-5p, miR-3141, miR-4634, miR-4649-5p, miR-4467, miR-4433b-3p, miR-1909-3p and downregulated miR-6880-3p and miR-10399-5p. Some of these miR were found to have previously been studied. In an *in vivo* study by Tsiloulis T. et. al. done to determine effects of training on adipocyte microRNA expression, a high expression of miR-4532 in gluteofemoral compared to abdominal subcutaneous adipocytes before exercise was shown (125). In another study done on patients with coronary artery disease showed that the expression of miR-92a and miR-92b had increased following cardiac rehabilitation (126).

Total RNA from EVs is very different from cellular total RNA. All the methodology within RNA work is based on cellular total RNA. As a result, all the quality and concentration analysis appear to be performing poorly for RNA extracted from EVs. In this thesis, using the pilot titration experiments, it was illustrated that it is possible to analyze total RNA from EVs with both low concentrations and poor integrity on the Affymetrix microarray and achieved satisfactory reproducible results. RNA extracted from EVs does not have poor integrity. It is perceived to have poor integrity because it fails to meet the requirements of the RNA standards set by the manufacturer. This is because the protocols and kits used are designed for analysis of cellular total RNA and not total RNA extracted from EVs. This opened up a good opportunity and an understanding that it is possible to analyze EV cargo in many contexts using low RNA concentrations with “poor integrity”.

#### 14.1 Effects of training on skeletal muscle cells

Obesity merged with lack of or no physical activity, is a high-risk factor for T2DM development. Physical inactivity can lead to accumulation of visceral fat which can lead to systemic low grade-inflammation (127), and the pro-inflammation activation (TNF) can lead to insulin resistance (128). Physical activities done regularly have beneficial effects with reference to prevention and enhancement of various chronic illnesses. Electrical pulse stimulation (EPS) is a model system that has been ensued to mimic the activation of muscle fibers by motor neuron *in vivo* (129). In this thesis, it was demonstrated that EPS had significant effect on miR where their levels of expression had been changed in their biological and physiological functions which included cellular development, gene expression, cellular

growth and proliferation, connective tissue development and function, tissue development and cardiovascular system development and function. This provides evidence that training has effects beyond the muscles that train since the exercise provokes widespread changes in numerous tissues and organs.

*In vitro* studies have demonstrated that as a result of physical exercise, insulin stimulated glucose uptake increases (130) and plasma concentration of IL-6 increases (131). IL-6, a cytokine released in the circulation in large amounts, can have effects on the liver and contribute to glucose homeostasis as a consequence of physical activities (132). The stimulation and induction of muscle contraction in the human skeletal muscle cells in culture, has been previously used *in vitro* to study metabolic undertakings in skeletal muscle cells (131). The model used was the one with a chronic low-frequency. There were two groups of cultured myotubes in this thesis, the unstimulated and stimulated (EPS). Half of the cultured myotubes were stimulated with while the other half was not. IL-6 concentration was then analyzed in the media collected after stimulation to determine the effects of EPS. This EPS model was demonstrated to be optimal enough to stimulate IL-6 secretion, where the IL-6 concentration tended to be increased by 37 % in the stimulated (EPS) media though not statistically significant. In line with this, we believe that EPS had an effect in the cells, since 5 out of 6 donors responded as expected. The unresponsive donor might have affected the end results. IL-6 concentration measurement might not be the best biomarker to determine whether EPS had an effect on the cells or not. However, it has been used in a previous master thesis where IL-6 concentration was significantly increased ( $p=0.01$ ) with 23 % in the EPS stimulated media.

After media collection, both cells from unstimulated and EPS myotubes were lysed and total protein concentration analyzed. This was to determine whether EPS had any effects on the total protein levels of the cells after 24 hours with EPS. The results showed that there was no significant difference in concentrations between the unstimulated and EPS myotubes. This demonstrated that the treatment regime applied had no obvious toxic effects on the cells, that might have caused damage or death to the cells. It also indicated that the treatment was a safe range for the cells. This was also demonstrated by Nikolić N. et. al., where EPS did not cause any leakage of enzymes out of the cells since no damages were caused on the cell membrane (31).



## 14.2 Characterization of extracellular vesicles

The size of EVs was determined using NTA. EPS didn't seem to have had any effects on the size and concentration of EVs since there was no statistically significant difference between the unstimulated and EPS group. This might be as a result of exosomes and MV having an overlap in diameter size as studied by Oliveira et. al. (133).

The conventional methods used to isolate EVs was by size using serial centrifugations and ultrafiltration in addition washing for purification (55). The separation method where the MV pellets are resuspended into the remaining supernatant that contains exosomes, might expose MV to contaminations.

As a negative control, a comparison of the conditioned media and the serum free medium were performed. The results showed that serum free media had particles but in lower concentrations ( $1.66 \times 10^8$  particles/mL) for exosomes and ( $3.14 \times 10^8$  particles/mL) for MV, compared to the average concentrations of exosomes (EPS) ( $3.34 \times 10^9$  particles/mL) and MV (EPS) ( $1.09 \times 10^{10}$  particles/mL). This demonstrated that there are particles in the serum free media, and they were detected by nanoparticle tracking analysis. This does not necessarily illustrate that they are EVs, since NTA only detects particles and has no capacity to differentiate EVs from other particles encompassed in the media. This might give inaccurate results of EV size and concentration which might affect the end results. This was demonstrated by Dagovic R A. et. al, where it was found that NTA is unable to determine the phenotype of the vesicles and differentiate them but allows a quantitative estimation of size distribution and concentration (134). In addition, a serum free concentration measurement done on Qubit 2.0 assay and Affymetrix microarray analysis showed no concentration of EVs (data not shown).

The total average concentrations of EVs (exosomes + MV) without EPS was  $1.19 \times 10^{10}$  particles/mL, while after EPS was  $1.42 \times 10^{10}$  particles/mL, an indication that EPS might have had some effect on EVs production and secretion even though not significant. This was though found significant in a study done by Oliveira G. P et. al., where it was demonstrated that exercise regardless of intensity, did significantly increase EV concentrations in serum (133).

In the present study the EV yield was poor in terms of volumes and concentrations which had a consequence of proceeding with the analysis with exosomes only. The low yield might have been as a result of forces applied during the isolation process; centrifugation and ultrafiltration, which can lead to formation of aggregates that disintegrate and can interfere with the EVs concentrations measured on NTA (55). The isolated EVs were stored at -80 °C and were thawed before every analysis performance. It has been demonstrated that EV storage at -80 °C might affect the size and structure of EVs, which can result in an increase in size and a disrupted EV structure. This was confirmed by an analysis done by Maroto et. al., where it was showed that isolated exosomes stored at -80 °C became larger, aggregated and formed multi-lamellar membrane layers (135) which resulted in a distorted structure of EVs. This might reduce the number of particles that can be detected using NTA. The interpretation of data obtained after high-speed, and force applied during centrifugation, must be taken into account since this might affect either the concentration, size or biochemical components of EVs through aggregate formation (136). The EV concentrations might also vary, since NTA detects size distribution of particles and is set with certain parameters that might have excluded the smaller EV size detection (137). To avoid a repeated freezing and defrosting, the isolated EVs were aliquoted in small portions into Eppendorf tubes before storage at -80 °C

The isolated EVs were characterized and identified to be EVs by TEM where the morphology was spherical and a cup shaped structure, typical EVs characteristics.

Western blotting was an analysis done for further characterization of EVs. It is a semiquantitative method, and thus used to compare the protein levels of unstimulated and stimulated (EPS) groups. CD9, CD63 and Hsc70/Hsp70 were used in the analysis. CD9 and CD63 are tetraspanins. In this thesis, western blotting identified surface biomarkers CD63 and heat shock proteins Hsc70/Hsp70, characteristic of exosomes. In a previous master thesis on human myotubes, CD63 was detected by flowcytometry (49). This was also demonstrated *in vivo* by Oliveira G. P et. al., but on EVs isolated from serum (133). Exosomes have been demonstrated to be highly enriched with tetraspanins. Tetraspanins are surface biomarkers and are widely spread in the plasma membrane but can be found in other subpopulations of vesicles. CD63 has been described as mainly of an intracellular compartments of endosome/lysosome origin (80). Hsc70/Hsp70 are heat shock proteins expressed in cells when exposed to stress as a result of physical activity. Hsc70/Hsp70 were detected, and this

was also demonstrated by Tupling A. R. et al. where Hsp70 content increased in the muscles within 48 hours following a treadmill exercise and remained elevated 7 days after exercise. In some participants, Hsp70 increased in the muscles within 24 hours after exercise (138). The Hsp70 levels were not measured in this thesis, but it would have maybe been expected to increase since the myotubes were under electrical stimulation for 24 hours. A lysate from the colorectal cancer cell line SW480 was used as a positive control. All the biomarkers were detected in the cell line SW480, while CD9 was not detected in all the muscle cell derived exosomes. CD9 is one of the tetraspanins most often observed in all EVs, but was negative with both western blotting and flowcytometry analysis in accordance with previous work on EVs from human myotubes (49). Calnexin, which was used as a negative control is a protein that is connected to the endoplasmic reticulum in the cytoplasm and not expected to be present in EVs, and thus not detected (139). From this assay, it is not easy to point out whether EPS had any effect on the levels observed, since western blotting offers only a fairly inaccurate concentration measurement.

### 14.3 Quantification of miRNA

As mentioned above, an RT-qPCR was performed using three miRs in 6 donors. This was to confirm the presence of muscle specific miR and control RNAs integrity. RT-qPCR was performed based on sample volume (2  $\mu$ L) and not concentrations.

The Ct values varied between donors, which is not unexpected, but this was connected to the fact that the output quantity was based on even volume rather than concentration. Even though real time RT-qPCR is a quantitative analysis with high a dynamic range, a comparison between the unstimulated and EPS groups could not be performed, since miR levels varied uncontrolled without any tools to normalize for different RNA. After the variances in Ct levels, there were doubts whether the quantification method used was sufficiently sensitive for such a small RNA amount available. At the same time, RT-qPCR is an interesting and important procedure to learn since this was to be used in the validation of the Affymetrix microarray results in the downstream analysis. However, due to delays and lack of time, validation of the Affymetrix results was not performed. The doubts about the RNA quantification method led to a series of trials of various methods for RNA quantitation. Three methods were used, and these included NanoDrop One that had been used in the first place, Agilent 2100 Bioanalyzer and Qubit 2.0 assay. All these quantification methods contributed a

lot to generate a better knowledge of the composition of total RNA from exosomes, since they all offered different information that was necessary for the subsequent performed analysis.

#### 14.3.1 Total RNA extraction from exosomes

To ascertain that the total RNA extracted from exosomes did not have any artifacts that might have affected the RT-qPCR results, quantification of total RNA using other techniques and methods were suggested. This was to find out RNAs quality (integrity) and (concentration), since this was important for succeeding analysis.

The isolated exosomes were lysed using QIAzol cell lysis reagent where a standard Qiagen total RNA extraction protocol was followed. MiRNeasy micro kit was used for total RNA extraction and the process was carried out in a fume chamber since some of the reagents used such as chloroform were toxic. RNA extraction yielded a low amount, and this might be as a result of several reasons: As a result of different EV isolation methods which include centrifugation, ultrafiltration and purification processes, a low yield of EV is likely (55, 140) which might have happened in our case. And a low yield of exosomes might have led to a low yield of the extracted RNA.

Isolation of RNA using Qiagen that contains phenol and guanidine thiocyanate might explain the low yield of RNA. This is as a result of exosomes having a rigid membrane that entails lipid compilation enriched in sphingomyelin and cholesterol which might lead to insufficient exosomes lysis (141).

According to the protocol, only 14  $\mu$ L of RNase-free water was used to the elution of RNA which is not enough to recover all the RNA amount attached on the column filter. This might have led to the low yield of RNA.

#### 14.3.2 Agilent 2100 Bioanalyzer

EV extraction did not yield enough volume meant for subsequent analysis and thus every drop used counted and had to be utilized where appropriate. Low EV yield might affect the quantity of total RNA extracted from exosomes. This is because a low yield in EV results in a low yield in RNA concentration too which might not be enough for necessary analysis to be performed, a factor that happened in our case. This was illustrated by Tang Y. et al. where various methods were demonstrated to affect the EVs yield and thus RNA yields (140) .

Contradicting observations were made after RNA extraction, where there was no correlation between concentrations of isolated exosomes by NTA and concentration of RNA extracted from the same aliquot. Agilent 2100 Bioanalyzer was used to control RNA integrity and concentrations.

The procedure requires as little as 1  $\mu\text{L}$  sample volume for the analysis which was vital since the recovery of total RNA was low. After the analysis, RIN (ribosomal integrity number) values indicated that the extracted total RNAs were not clean, and the concentrations were very low, an indicate of poor integrity. Another reason for poor integrity might be that there was inconsistency in the methods used to measure such low RNA concentrations, hence no relationship between the amount of EVs isolated and RNA concentration extracted to be detected. This would affect the downstream analyses. For better results, enough and equal RNA concentration with good quality (RIN~10) is warranted (141). From the results only two donors had somewhat better concentrations in terms of particles/mL and pg/ $\mu\text{L}$  and RIN. As a result, a long search for a solution commenced.

#### 14.3.3 Challenges and strategies for finding ways to solutions

Other available RNA samples, several techniques and methods were tried out to find a solution. This was to help find out how to recover the expected good quality total RNA results after Bioanalyzer picokit analysis. In addition, to find out what can be done to obtain better RIN values and concentrations from the RNA already isolated from the exosomes derived RNA. New RNA quantification kits (Qubit microRNA) were bought and ath-miR-159a a spike-in control, miR-39 f2 a HPLC cleaned miR, a pool of other previously extracted EV-total RNA from the same donors and OHS total cellular RNA were prepared for dilution analysis. These different materials were used to provide information on what is expected from exosomes derived total RNA results after NanoDrop measurement and Bioanalyzer picokit analysis. The results after Bioanalyzer analysis were satisfactory. To ascertain the above determined results, same RNA samples were analyzed on Qubit 2.0, and the results were comparable and satisfactory (data not shown).

The extra analysis done on other RNA samples were not only done because of the poor quality and quantity of RNA that was recovered, but also for the need to discover more information about how to work with exosomes derived total RNA samples in general. The

RNA profiles obtained from EVs showed different profiles from cellular RNA.

Having had an idea of what was expected, new isolation of total RNA was performed on the remaining small volumes of isolated exosome samples from unstimulated and stimulated (EPS) myotubes. New measurements by NanoDrop One technique together with Qubit 2.0 assay were performed on the newly extracted RNA to determine the RNA concentrations.

Qubit 2.0 assay is a sensitive method that requires a volume of 1  $\mu$ L sample size and has the capacity to measure very low RNA concentrations, which was a method required for the analysis since our samples had low RNA concentrations. Qubit 2.0 is relatively cheap, easy to use and allows better estimates compared to NanoDrop One as illustrated by Giovanni P. et al. (118, 142).

NanoDrop One is considered to be the fastest and cheapest, since it requires few seconds for sample measurements (142, 143). Some of the constructive values of NanoDrop One are that it doesn't require special training to be able to operate. No sample dilutions are required or addition of reagents. Cleaning after use is done simply by wiping both the top and lower optical surfaces using a laboratory wipe and RNase free water (144). The disadvantage of NanoDrop One is that phenol, a component of the reagent used in RNA extraction is detected as a contamination (143), and it is not sensitive enough to detect slightly degraded RNA (145).

Agilent 2100 Bioanalyzer was used for integrity control. It is a unique and vital quantification method, but the disadvantage is that the chip used for samples can only take 11 samples at a time. In addition, the results are not easy to understand and thus require expert knowledge to interpret (116).

Even though all methods were used in various phases in RNA analysis, Qubit was used as the main RNA analysis, where the results were used as the appropriate input in the Affymetrix microarray analysis. The other methods contributed a lot towards the totality of quality and quantity analysis as well.

## 15 Evaluation of methods

### 15.1 Cell Cultures

The cells used in culturing were human satellite cells that are usually quiescent. They require activation into proliferating myocytes and must differentiate into multinuclear/myotubes in culture to act as a model of human skeletal muscle (25). As observed through studies, the expression of key proteins in myotubes during proliferation phase and increase of metabolism during differentiation of myoblasts into myotubes, exhibited similarities with human skeletal muscle *in vivo* (25). In a study done by Henry R. et al., it was shown that skeletal muscle cells from non-insulin-dependent diabetes mellitus patients, retained the glycogen synthase impaired activity defect. An indicate that muscle cultures reflect the *in vivo* conditions and can provide a model for study (105, 146). As a result, satellite cells were identified as best suitable for this study.

Even though considered as a suitable model of the study, the cells had challenges. Specimens used in the study were from extremely obese donors with type 2 diabetes mellitus (T2DM). The cells growth and proliferation rate varied widely. In some donors, the cells growth was optimal as expected and covered the wells, while in some cases, the cell culturing had to be restarted all over again (circa 14 days after seeding) before acquiring the required (80 – 90) % confluency for EV harvesting.

Another reason for variation might be as a result of altered cellular functions, as proliferative potential of myoblasts reduces as the number of passages increases. The glucose uptake and glycogen synthesis increase in the beginning, but reduces as the proliferative potential become exhausted with time as observed by Nehlin et al. (28). This indicates that the normal cellular functions in muscle cells *in vivo* might not be expected in muscle cells *in vitro*. In addition, as a result of numerous passages, the cell's quality declined as observed by Nehlin et al., (28). During cells passages, the cells are pipetted in cell ampules before storing at -80°C for half an hour and later transferring into a nitrogen tank. As a result of these passages, one might not know the number of cells obtained from each donor with time, which might affect the variation in cells growth. In this thesis the passages used were from 3 – 5, only one donor had a passage 3, the rest had from passages 4 – 5. As a consequence, this might have affected the quality and quantity of the cells obtained which might again affect the succeeding

analysis. An example of donors who might have been affected are 4 and 5 who had a slow development and needed more time to reach the appropriate confluence.

In the course of cell culturing, the media were changed based on different phases in which the cells were. There was the seeding, proliferation and differentiation media that were changed after a 2–3-day period of time. The myotubes had a differing and fluctuating environment that had variations which might have interfered and caused alterations in cells' growth hence not optimal cells growth. After muscle stimulation (EPS), M3-differentiation medium was collected ready for interleukin-6 measurement. The medium used for 24 hours incubation after EPS was serum free, which means that the myotubes didn't have normal differentiations media conditions. Even though the cells had already proliferated and differentiated before incubation in serum free media, this might have affected the cells since the media conditions were abruptly changed, something that might have caused damage to the cells during the 24 hours of incubation. This was done because, as demonstrated by Aswad H. et al., foetal calf serum contains EVs that might have important biological properties, and a depletion of this could alter the proliferation and differentiation of skeletal muscle cells (78).

The above-mentioned conditions might have affected the cells quality and quantity. This might have contributed to low EV yield as a result of decreased number of cell growth, hence a reduced number of EV released into the extracellular environment, what might have again affected total RNA yield. A limitation in number of cell plates that could be stimulated (EPS) at the same time also restricted the total volume of EV-containing media.

## 15.2 Isolation of muscle derived extracellular vesicles

After electrical pulse stimulation, the myotubes were washed twice with S-free medium and later incubated in a serum free medium for 24 hours. The serum free medium was used to eliminate any traces of serum that might have been carried over from the media that contained foetal calf serum (differentiation medium M3). The foetal calf serum contains proteins and EVs that might contaminate the conditioned media. Even though the myotubes were washed twice with serum free media and incubated in the same, it's not certain that all the foetal calf serum traces were completely eradicated. This would then affect the results of succeeding analysis for example, the nanoparticle tracking analysis, where the particle detection would be inaccurate since the foetal calf serum traces would be detected as EV particles.



Knowledge about EV isolation is limited since they are a heterogeneous group of nanoparticles with different sizes and shapes. Methods and protocols of EV isolation employed in the research field are different, and this is very challenging in terms of results comparison. This is because it gives a wide population of EVs (poor yield, purity, mixed populations), a reason that has led to a need for optimal standardized EV isolation methods to minimize variations (90). The choice of isolation methods might be based on different reasons, some of them being, the cost of apparatus, aim of the study (downstream applications), and time consumption (90). Even though there are challenges, there are methods that have been in use and are considered fairly good on average. The most conventional methods used are those that utilize the size and buoyant density for isolation of EV. This includes ultracentrifugation, microfiltration, and gel filtration (55). The methods used in this thesis to separate EVs from serum free media were centrifugation and ultrafiltration followed by washing. These are methods that were employed and gave better results in terms of exosomes particle yield, as observed by Lobb R. et al., (147) and were somewhat fairly better compared to others because they require no additional chemicals and reagents (55). The downside of these methods is that they are time consuming, the equipment used is expensive, few samples can be processed in one centrifugation phase and because of the force applied, EVs might be damaged and form aggregates which reduces the quality and quantity of EVs in terms of nanoparticles to be analyzed by NTA. This can then affect the downstream analysis (55). In addition, one needs to have specialized training in everything entailed in the method prior to its application, and this is time consuming.

### 15.3 Characterization of extracellular vesicles

In this study, numerous methods were used to characterize EVs and the cargo content. The characterization was to certify that what was recovered from EV preparations were indeed EVs. The concentration and size distribution of EVs was analyzed using nanoparticle tracking analysis (NTA) where NanoSight NS500 instrument was used.

Nanoparticle tracking analysis is a unique and useful technique originally commercialized in 2006 (148). According to the manufacturer, NanoSight NS500 can analyze the presence and size distribution, in addition concentration of all types of nanoparticles from 10 – 2000 nm. This is the range within which EVs are; exosomes 30 -100 nm and MV 100 – 1000 nm (54).

The technique is a combination of laser light scattering microscopy with a camera that enables the visualizing and recording of nanoparticles in a solution. The individual nanoparticles moving under a Brownian motion are then tracked and identified. Nanoparticle capabilities to visualize and provide the approximation of the particle concentrations and size is a useful feature. The technique doesn't require many chemical additions except artificial vesicles/beads, 100 nm standard polystyrene beads for calibration and phosphate-buffered saline (PBS) for sample dilution.

Even though it is such a useful technique, it has its limitations. One needs to have special training to be able to operate it. The data quality of NTA depends on the settings done prior to analysis, and thus the instrument requires numerous critical adjustments to be able to obtain measurement results that are accurate. The adjustments done on the software settings every time one has to perform the analysis, might have some effect when it comes to comparing the results (54). The technique is unique and useful, but the instrument (NanoSight NS500) used is very expensive. The instrument must be primed before loading samples. This is to get rid of air bubbles, that might affect the particle detection and chamber leakage as a result of pressure in the chamber, and this takes more time. Only one sample can be analyzed at a time, and the instrument has to be flushed clean after every sample which takes time. The samples are loaded into the instrument through a tube that is normally connected to a syringe, which is the sample holder, which then is placed on an injection pump that pumps the samples in the instrument. This needs a lot of training and experience, and it takes time to reach this level. In addition, the instrument is so sensitivity to vibrations, and is often clogged by aggregates which leads to time consuming clean-up process. NTA determines the particle distribution, and according to ISEV the technique can result in an overestimation of EVs since it is not specific to EVs, but registers co-isolated particles, which include lipoproteins and protein aggregates. In addition, the particle counting may be biased to a particular size range (120).

## 16 Conclusion remarks

Electrical pulse stimulation (EPS) was used to create muscle contractions in half of the cultured skeletal muscle cells (myotubes). This was with the aim of finding out if there was a difference between the skeletal muscle derived EVs from unstimulated and stimulated (EPS) myotubes.

The results obtained showed that skeletal muscle cells do release EVs in the extracellular space. TEM and western blot identified EVs characteristics such as a spherical and cup shaped morphology, and presence of CD63 and heat shock proteins Hsc70/Hsp70. EPS did not have any effects on EV concentration or size. The released EVs were analyzed using Affymetrix microarray and it was confirmed that skeletal muscles do release EVs that contain numerous diverse RNA components. One of the important components was miR.

A download of the Affymetrix microarray data in IPA predicted that 12 miRs were significantly changed by EPS ( $p < 0.05$ ). In addition, top 5 upstream regulators were shown to be involved in miR expression and this included MET which had an inhibiting effect while XPO1, AGO2, TP53 and TGS1 had an activating effect on miR. Several possible targets of the regulated miRs were also identified.

As a conclusion, the data obtained in this study are the first transcriptomic study evidence of analysis performed on electrically stimulated human skeletal muscle cell derived EVs, which suggested that EVs, both exosomes and MV, are released from skeletal muscle cells. The skeletal muscle derived exosomes do contain divergent cargo components, among them microRNA, and that EPS does have a markable effect on these microRNA.

## 17 Reference List

1. Amugsi DA, Dimbuene ZT, Mberu B, Muthuri S, Ezeh AC. Prevalence and time trends in overweight and obesity among urban women: an analysis of demographic and health surveys data from 24 African countries, 1991–2014. *BMJ Open*. 2017;7(10):e017344-e.
2. World health organization. Obesity and overweight. World Health Organization.: World Health Organization.; 2020, April 1 [updated 1st April; cited 2020 13th ]. Available from: <https://www.who.int/news-room/fact-sheets/detail/obesity-and-overweight>.
3. Division of Nutrition PA, and Obesity, National Center for Chronic Disease Prevention and Health Promotion,. Defining adult overweight and obesity 2020, September 17 [updated 2020,September 17. Available from: <https://www.cdc.gov/obesity/adult/defining.html>.
4. Afshin A, Forouzanfar MH, Reitsma MB, Sur P, Estep K, Lee A, et al. Health Effects of Overweight and Obesity in 195 Countries over 25 Years. *N Engl J Med*. 2017;377(1):13-27.
5. Haakon Eduard Meyer and Margarete Erika Maria Torgersen Vollrath. Overweight and obesity in norway. Norwegian Institute of Public Health.: Public Health Report Editorial Group. ; 2017, November [cited 2020 13th ]. Available from: <https://www.fhi.no/en/op/hin/health-disease/overweight-and-obesity-in-norway---/>.
6. Al-Goblan AS, Al-Alfi MA, Khan MZ. Mechanism linking diabetes mellitus and obesity. *Diabetes Metab Syndr Obes*. 2014;7:587-91.
7. World Health Organization. GLOBAL REPORT ON DIABETES. WHO Library Cataloguing-in-Publication Data: World Health Organization; 2016. p. 88.
8. Javeed N. Shedding Perspective on Extracellular Vesicle Biology in Diabetes and Associated Metabolic Syndromes. *Endocrinology*. 2019;160(2):399-408.
9. Kim JH, Cho HT, Kim YJ. The role of estrogen in adipose tissue metabolism: insights into glucose homeostasis regulation [Review]. *Endocr J*. 2014;61(11):1055-67.
10. Fernández-Sánchez A, Madrigal-Santillán E, Bautista M, Esquivel-Soto J, Morales-González A, Esquivel-Chirino C, et al. Inflammation, oxidative stress, and obesity. *Int J Mol Sci*. 2011;12(5):3117-32.
11. Verboven K, Wouters K, Gaens K, Hansen D, Bijnen M, Wetzels S, et al. Abdominal subcutaneous and visceral adipocyte size, lipolysis and inflammation relate to insulin resistance in male obese humans. *Sci Rep*. 2018;8(1):4677-8.
12. Lumeng CN, Saltiel AR. Inflammatory links between obesity and metabolic disease. *J Clin Invest*. 2011;121(6):2111-7.
13. Gesmundo I, Pardini B, Gargantini E, Gamba G, Birolo G, Fanciulli A, et al. Adipocyte-derived extracellular vesicles regulate survival and function of pancreatic  $\beta$  cells. *JCI Insight*. 2021;6(5).
14. Kita S, Maeda N, Shimomura I. Interorgan communication by exosomes, adipose tissue, and adiponectin in metabolic syndrome. *J Clin Invest*. 2019;129(10):4041-9.
15. Pedersen BK, Febbraio MA. Muscles, exercise and obesity: skeletal muscle as a secretory organ. *Nature Reviews Endocrinology*. 2012;8(8):457-65.
16. Florin A, Lambert C, Sanchez C, Zappia J, Durieux N, Tieppo AM, et al. The secretome of skeletal muscle cells: A systematic review. *Osteoarthritis and Cartilage Open*. 2020;2(1):100019.
17. Frontera WR, Ochala J. Skeletal muscle: a brief review of structure and function. *Calcif Tissue Int*. 2015;96(3):183-95.
18. Rome S, Forterre A, Mizgier ML, Bouzakri K. Skeletal Muscle-Released Extracellular Vesicles: State of the Art. *Frontiers in Physiology*. 2019;10(929).

19. Westerblad H, Bruton JD, Katz A. Skeletal muscle: Energy metabolism, fiber types, fatigue and adaptability. *Exp Cell Res.* 2010;316(18):3093-9.
20. Tatsuya H, Jørgen FPW, Laurie JG. Exercise regulation of glucose transport in skeletal muscle. *American Journal of Physiology - Endocrinology And Metabolism.* 1997;273(6):1039-51.
21. Bente Klarlund P, Thorbjörn CAÅ, Anders RN, Christian PF. Role of myokines in exercise and metabolism. *J Appl Physiol (1985).* 2007;103(3):1093-8.
22. Savikj M, Zierath JR. Train like an athlete: applying exercise interventions to manage type 2 diabetes. *Diabetologia.* 2020;63(8):1491-9.
23. Thomas JH, Daniel JG. Myogenic satellite cells: physiology to molecular biology. *J Appl Physiol (1985).* 2001;91(2):534-51.
24. Farup J, Rahbek SK, Riis S, Vendelbo MH, Paoli Fd, Vissing K. Influence of exercise contraction mode and protein supplementation on human skeletal muscle satellite cell content and muscle fiber growth. *J Appl Physiol (1985).* 2014;117(8):898-909.
25. Aas V, Bakke SS, Feng YZ, Kase ET, Jensen J, Bajpeyi S, et al. Are cultured human myotubes far from home? *Cell Tissue Res.* 2013;354(3):671-82.
26. Mauro A. Satellite cell of skeletal muscle fibers. *J Biophys Biochem Cytol.* 1961;9(2):493-5.
27. Frederiksen CM, Højlund K, Hansen L, Oakeley EJ, Hemmings B, Abdallah BM, et al. Transcriptional profiling of myotubes from patients with type 2 diabetes: no evidence for a primary defect in oxidative phosphorylation genes. *Diabetologia.* 2008;51(11):2068-77.
28. Nehlin JO, Just M, Rustan AC, Gaster M. Human myotubes from myoblast cultures undergoing senescence exhibit defects in glucose and lipid metabolism. *Biogerontology.* 2011;12(4):349-65.
29. Beccafico S, Puglielli C, Pietrangelo T, Bellomo R, Fano G, Fulle S. Age-Dependent Effects on Functional Aspects in Human Satellite Cells. *Ann N Y Acad Sci.* 2007;1100(1):345-52.
30. Feng YZ, Nikolić N, Bakke SS, Kase ET, Guderud K, Hjelmæsæth J, et al. Myotubes from lean and severely obese subjects with and without type 2 diabetes respond differently to an in vitro model of exercise. *Am J Physiol Cell Physiol.* 2015;308(7):C548-C56.
31. Nikolić N, Bakke SS, Kase ET, Rudberg I, Flo Halle I, Rustan AC, et al. Electrical pulse stimulation of cultured human skeletal muscle cells as an in vitro model of exercise. *PLoS One.* 2012;7(3):e33203.
32. Nikolić N, Bakke SS, Kase ET, Rudberg I, Flo Halle I, Rustan AC, et al. Electrical pulse stimulation of cultured human skeletal muscle cells as an in vitro model of exercise. *PLoS One.* 2012;7(3):e33203-e.
33. Nikolić N, Görgens SW, Thoresen GH, Aas V, Eckel J, Eckardt K. Electrical pulse stimulation of cultured skeletal muscle cells as a model for in vitro exercise – possibilities and limitations. *Acta Physiol (Oxf).* 2017;220(3):310-31.
34. Pratesi A, Tarantini F, Di Bari M. Skeletal muscle: an endocrine organ. *Clin Cases Miner Bone Metab.* 2013;10(1):11-4.
35. Starkie R, Ostrowski SR, Jauffred S, Febbraio M, Pedersen BK. Exercise and IL-6 infusion inhibit endotoxin-induced TNF- $\alpha$  production in humans. *FASEB J.* 2003;17(8):1-10.
36. Adam S, Christian PF, Charlotte K, Kirsten M, Bente Klarlund P. IL-6 enhances plasma IL-1ra, IL-10, and cortisol in humans. *Am J Physiol Endocrinol Metab.* 2003;285(2):433-7.
37. Vechetti JIJ, Valentino T, Mobley CB, McCarthy JJ. The role of extracellular vesicles in skeletal muscle and systematic adaptation to exercise. *J Physiol.* 2020.

38. Nielsen S, Scheele C, Yfanti C, Åkerström T, Nielsen AR, Pedersen BK, et al. Muscle specific microRNAs are regulated by endurance exercise in human skeletal muscle. *J Physiol.* 2010;588(20):4029-37.
39. Wallberg-Henriksson H, Rincon J, Zierath JR. Exercise in the management of non-insulin-dependent diabetes mellitus. *Sports Med.* 1998;25(1):25-35.
40. Fulle OK, Mathivanan S, Febbraio MA, Whitham M. The Protective Effect of Exercise in Neurodegenerative Diseases: The Potential Role of Extracellular Vesicles. *Cells (Basel, Switzerland).* 2020;9(10):1.
41. Whitham M, Parker BL, Friedrichsen M, Hingst JR, Hjorth M, Hughes WE, et al. Extracellular Vesicles Provide a Means for Tissue Crosstalk during Exercise. *Cell Metab.* 2018;27(1):237-51.e4.
42. Bittel DC, Jaiswal JK. Contribution of Extracellular Vesicles in Rebuilding Injured Muscles. *Front Physiol.* 2019;10:828-.
43. Febbraio MA, Pedersen BK. Muscle-derived interleukin-6: mechanisms for activation and possible biological roles. *FASEB J.* 2002;16(11):1335-47.
44. Pradhan AD, Manson JE, Rifai N, Buring JE, Ridker PM. C-Reactive Protein, Interleukin 6, and Risk of Developing Type 2 Diabetes Mellitus. *JAMA.* 2001;286(3):327-34.
45. Hiscock N, Chan MHS, Bisucci T, Darby IA, Febbraio MA. Skeletal myocytes are a source of interleukin-6 mRNA expression and protein release during contraction: evidence of fiber type specificity. *FASEB J.* 2004;18(9):992-4.
46. Christopher M, Jørgen FPW, Bente Klarlund P, Bente K, Erik AR. Interleukin-6 release from human skeletal muscle during exercise: relation to AMPK activity. *J Appl Physiol (1985).* 2003;95(6):2273-7.
47. Kemp BE, Mitchelhill KI, Stapleton D, Michell BJ, Chen Z-P, Witters LA. Dealing with energy demand: the AMP-activated protein kinase. *Trends Biochem Sci.* 1999;24(1):22-5.
48. Ostrowski K, Schjerling P, Pedersen BK. Physical activity and plasma interleukin-6 in humans – effect of intensity of exercise. *Eur J Appl Physiol.* 2000;83(6):512-5.
49. Qureshi S. Karakterisering av ekstracelulære vesikler fra humane skjelettmuskelceller- effekt av elektrisk pulsstimulering [Master]. None: OsloMet-storbyuniversitet; 2019.
50. Kalra H, Drummen G, Mathivanan S. Focus on Extracellular Vesicles: Introducing the Next Small Big Thing. *Int J Mol Sci.* 2016;17(2):170-.
51. Yáñez-Mó M, Siljander PRM, Andreu Z, Bedina Zavec A, Borràs FE, Buzas EI, et al. Biological properties of extracellular vesicles and their physiological functions. *J Extracell Vesicles.* 2015;4(1):27066-60.
52. O'Brien K, Breyne K, Ughetto S, Laurent LC, Breakefield XO. RNA delivery by extracellular vesicles in mammalian cells and its applications. 2020.
53. Théry C, Witwer KW, Aikawa E, Andriantsitohaina R, Baharvand H, Bauer NN, et al. Minimal information for studies of extracellular vesicles 2018 (MISEV2018): a position statement of the International Society for Extracellular Vesicles and update of the MISEV2014 guidelines. *J Extracell Vesicles.* 2018;7(1):1535750-n/a.
54. Vestad B, Llorente A, Neurauter A, Phuyal S, Kierulf B, Kierulf P, et al. Size and concentration analyses of extracellular vesicles by nanoparticle tracking analysis: a variation study. *J Extracell Vesicles.* 2017;6(1):1344087-.
55. Konoshenko MY, Lekchnov EA, Vlassov AV, Laktionov PP. Isolation of Extracellular Vesicles: General Methodologies and Latest Trends. *Biomed Res Int.* 2018;2018:1-27.

56. Kamińska A, Platt M, Kasprzyk J, Kuśnierz-Cabala B, Gala-Błądzińska A, Woźnicka O, et al. Urinary Extracellular Vesicles: Potential Biomarkers of Renal Function in Diabetic Patients. *J Diabetes Res.* 2016;2016:5741518-12.
57. Yang J, Li C, Zhang L, Wang X. Extracellular Vesicles as Carriers of Non-coding RNAs in Liver Diseases. *Front Pharmacol.* 2018;9:415-.
58. György B, Szabó TG, Pásztói M, Pál Z, Misják P, Aradi B, et al. Membrane vesicles, current state-of-the-art: emerging role of extracellular vesicles. *Cell Mol Life Sci.* 2011;68(16):2667-88.
59. Carnino JM, Ni K, Jin Y. Post-translational Modification Regulates Formation and Cargo-Loading of Extracellular Vesicles. *Frontiers in immunology.* 2020;11:948-.
60. Colombo M, Raposo G, Théry C. Biogenesis, secretion, and intercellular interactions of exosomes and other extracellular vesicles. *Annu Rev Cell Dev Biol.* 2014;30:255-89.
61. Mathivanan S, Ji H, Simpson RJ. Exosomes: Extracellular organelles important in intercellular communication. *Journal of proteomics.* 2010;73(10):1907-20.
62. Dinh Ha Ningning Yang Venkatareddy N. Exosomes as therapeutic drug carriers and delivery vehicles across biological membranes:current perspectives and future challenges. *Acta Pharmaceutica Sinica B.* 2016;6(4):287-96.
63. Babst M, Katzmann DJ, Estepa-Sabal EJ, Meerloo T, Emr SD. Escrt-III: An endosome-associated heterooligomeric protein complex required for mvb sorting. *Dev Cell.* 2002;3(2):271-82.
64. Hessvik NP, Hessvik NP, Llorente A, Llorente A. Current knowledge on exosome biogenesis and release. *Cell Mol Life Sci.* 2018;75(2):193-208.
65. Kalani A, Kalani A, Tyagi A, Tyagi A, Tyagi N, Tyagi N. Exosomes: Mediators of Neurodegeneration, Neuroprotection and Therapeutics. *Mol Neurobiol.* 2014;49(1):590-600.
66. Cocucci E, Racchetti G, Meldolesi J. Shedding microvesicles: artefacts no more. *Trends Cell Biol.* 2008;19(2):43-51.
67. Bevers EM, Comfurius P, Dekkers DWC, Zwaal RFA. Lipid translocation across the plasma membrane of mammalian cells. *BBA - Molecular and Cell Biology of Lipids.* 1999;1439(3):317-30.
68. Muralidharan-Chari V, Clancy J, Plou C, Romao M, Chavier P, Raposo G, et al. ARF6-Regulated Shedding of Tumor Cell-Derived Plasma Membrane Microvesicles. *Curr Biol.* 2009;19(22):1875-85.
69. Akers JC, Gonda D, Kim R, Carter BS, Chen CC. Biogenesis of extracellular vesicles (EV): exosomes, microvesicles, retrovirus-like vesicles, and apoptotic bodies. *J Neurooncol.* 2013;113(1):1-11.
70. Théry C, Segura E, Ostrowski M. Membrane vesicles as conveyors of immune responses. *Nat Rev Immunol.* 2009;9(8):581-93.
71. Muralidharan-Chari V, Clancy JW, Sedgwick A, D'Souza-Schorey C. Microvesicles: mediators of extracellular communication during cancer progression. *J Cell Sci.* 2010;123(Pt 10):1603-11.
72. Skog J, Wurdinger T, van Rijn S, Meijer D, Gainche L, Sena-Esteves M, et al. Glioblastoma microvesicles transport RNA and protein that promote tumor growth and provide diagnostic biomarkers. *Nature cell biology.* 2008;10(12):1470-6.
73. Kerr JF, Wyllie AH, Currie AR. Apoptosis: a basic biological phenomenon with wide-ranging implications in tissue kinetics. *Br J Cancer.* 1972;26(4):239-57.
74. Seow Y, Betts C, Wood MJA, Lakhai S, Yin H, Alvarez-Erviti L. Delivery of siRNA to the mouse brain by systemic injection of targeted exosomes. *Nat Biotechnol.* 2011;29(4):341-5.

75. Mulcahy LA, Pink RC, Carter DRF. Routes and mechanisms of extracellular vesicle uptake. *J Extracell Vesicles*. 2014;3(1):24641-n/a.
76. Sjöstrand M, Ekström K, Lee JJ, Valadi H, Bossios A, Lötvald JO. Exosome-mediated transfer of mRNAs and microRNAs is a novel mechanism of genetic exchange between cells. *Nat Cell Biol*. 2007;9(6):654-9.
77. Bettini E, Locci M. SARS-CoV-2 mRNA Vaccines: Immunological Mechanism and Beyond. Basel, Switzerland :2021. p. 147.
78. Durak-Kozica M, Baster Z, Kubat K, Stępień E. 3D visualization of extracellular vesicle uptake by endothelial cells. *Cell Mol Biol Lett*. 2018;23(1):57-.
79. Morelli AE, Larregina AT, Falo LD, Thomson AW, Shufesky WJ, Sullivan MLG, et al. Endocytosis, intracellular sorting, and processing of exosomes by dendritic cells. *Blood*. 2004;104(10):3257-66.
80. Andreu Z, Yáñez-Mó M. Tetraspanins in extracellular vesicle formation and function. *Front Immunol*. 2014;5:442-.
81. Guo-Zhang Z, Brent JM, Claude B, Eric R, Christopher CL, Richard OH, et al. Residues SFQ (173-175) in the large extracellular loop of CD9 are required for gamete fusion. *Development*. 2002;129(8):1995-2002.
82. Hu W, Song X, Yu H, Sun J, Zhao Y. Therapeutic Potentials of Extracellular Vesicles for the Treatment of Diabetes and Diabetic Complications. *International journal of molecular sciences*. 2020;21(14):5163.
83. Kim A, Shah AS, Nakamura T. Extracellular Vesicles: A Potential Novel Regulator of Obesity and Its Associated Complications. *Children (Basel)*. 2018;5(11):152.
84. Pardo F, Villalobos-Labra R, Sobrevia B, Toledo F, Sobrevia L. Extracellular vesicles in obesity and diabetes mellitus. *Mol Aspects Med*. 2018;60:81-91.
85. Ferrante SC, Nadler EP, Pillai DK, Hubal MJ, Wang Z, Wang JM, et al. Adipocyte-derived exosomal miRNAs: a novel mechanism for obesity-related disease. *Pediatr Res*. 2015;77(3):447-54.
86. Zhong-bin D, Anton P, Robert WH, Ronald C, Cunren L, Yuelong L, et al. Adipose Tissue Exosome-Like Vesicles Mediate Activation of Macrophage-Induced Insulin Resistance. *Diabetes*. 2009;58(11):2498-505.
87. Zhao H, Shang Q, Pan Z, Bai Y, Li Z, Zhang H, et al. Exosomes From Adipose-Derived Stem Cells Attenuate Adipose Inflammation and Obesity Through Polarizing M2 Macrophages and Beiging in White Adipose Tissue. *Diabetes*. 2018;67(2):235-47.
88. Abdille Abdullahi Hussein. Characterization of extracellular vesicles from human skeletal muscle cells from morbidly obese subjects with and without type 2 diabetes mellitus [Biomedicine]: Oslo Metropolitan University; 2020.
89. Guescini M, Canonico B, Lucertini F, Maggio S, Annibalini G, Barbieri E, et al. Muscle Releases Alpha-Sarcoglycan Positive Extracellular Vesicles Carrying miRNAs in the Bloodstream. *PLoS One*. 2015;10(5):e0125094-e.
90. Lötvald J, Hill AF, Hochberg F, Buzás EI, Di Vizio D, Gardiner C, et al. Minimal experimental requirements for definition of extracellular vesicles and their functions: a position statement from the International Society for Extracellular Vesicles. *J Extracell Vesicles*. 2014;3(1):26913-n/a.
91. Hill AF, Pegtel DM, Lambert U, Leonardi T, O'Driscoll L, Pluchino S, et al. ISEV position paper: extracellular vesicle RNA analysis and bioinformatics. *J Extracell Vesicles*. 2013;2.



92. Lener T, Gimona M, Aigner L, Börger V, Buzas E, Camussi G, et al. Applying extracellular vesicles based therapeutics in clinical trials - an ISEV position paper. *J Extracell Vesicles*. 2015;4(1):30087-n/a.
93. Gardiner C, Vizio DD, Sahoo S, Théry C, Witwer KW, Wauben M, et al. Techniques used for the isolation and characterization of extracellular vesicles: results of a worldwide survey. *J Extracell Vesicles*. 2016;5(1):32945-n/a.
94. Ratajczak J, Miekus K, Kucia M, Zhang J, Reca R, Dvorak P, et al. Embryonic stem cell-derived microvesicles reprogram hematopoietic progenitors: evidence for horizontal transfer of mRNA and protein delivery. *Leukemia*. 2006;20(5):847-56.
95. Feinberg MW, Moore KJ. MicroRNA Regulation of Atherosclerosis. *Circ Res*. 2016;118(4):703-20.
96. Lee RC, Feinbaum RL, Ambros V. The *C. elegans* heterochronic gene *lin-4* encodes small RNAs with antisense complementarity to *lin-14*. *Cell*. 1993;75(5):843-54.
97. Meister G. Argonaute proteins: functional insights and emerging roles. *Nat Rev Genet*. 2013;14(7):447-59.
98. Sayed D, Abdellatif M. MicroRNAs in Development and Disease. *Physiol Rev*. 2011;91(3):827-87.
99. O'Brien J, Hayder H, Zayed Y, Peng C. Overview of MicroRNA Biogenesis, Mechanisms of Actions, and Circulation. *Frontiers in endocrinology (Lausanne)*. 2018;9:402-.
100. Williams AH, Liu N, van Rooij E, Olson EN. MicroRNA control of muscle development and disease. *Curr Opin Cell Biol*. 2009;21(3):461-9.
101. Ingolia NT, Guo H, Bartel DP, Weissman JS. Mammalian microRNAs predominantly act to decrease target mRNA levels. *Nature*. 2010;466(7308):835-40.
102. Wang Q, Wang Y, Minto AW, Wang J, Shi Q, Li X, et al. MicroRNA-377 is up-regulated and can lead to increased fibronectin production in diabetic nephropathy. *FASEB J*. 2008;22(12):4126-35.
103. Bin Yi, Piazza GA, Xiulan SU, Yaguang XI. MicroRNA and Cancer Chemoprevention. *Cancer Prev Res (Phila)*. 2013;6(5):401-9.
104. Lötvall J, Hill AF, Hochberg F, Buzás EI, Di Vizio D, Gardiner C, et al. Minimal experimental requirements for definition of extracellular vesicles and their functions: a position statement from the International Society for Extracellular Vesicles. *J Extracell Vesicles*. 2014;3(1):26913-.
105. Gaster M, Kristensen SR, Beck-Nielsen H, Schroder HD. A cellular model system of differentiated human myotubes. *APMIS*. 2001;109(11):735-44.
106. Nikolic N, Aas V. Electrical pulse stimulation of primary human skeletal muscle cells. 2018.
107. Bradford MM. A rapid and sensitive method for the quantitation of microgram quantities of protein utilizing the principle of protein-dye binding. *Anal Biochem*. 1976;72:248-54.
108. Millipore. Certificate of Analysis / Protocol Merck: Millipore; 2021 [updated 2021; cited 2021 January 2021]. Available from: <https://www.sigmaaldrich.com/catalog/CertOfAnalysisPage.do?symbol=RAB0306&LotNo=0915H0140&brandTest=SIGMA>.
109. LLC. S-AC. TECHNICAL BULLETIN; ELISA Kit Information Sigma-Aldrich: Sigma-Aldrich; 2018 [updated 2018; cited 2021 January 29]. Available from: <https://www.sigmaaldrich.com/catalog/CertOfAnalysisPage.do?symbol=RAB0306&LotNo=0915H0140&brandTest=SIGMA>.

110. Spindel S, Sapsford KE. Evaluation of optical detection platforms for multiplexed detection of proteins and the need for point-of-care biosensors for clinical use. *Sensors (Basel)*. 2014;14(12):22313-41.
111. Zewail AH. Four-Dimensional Electron Microscopy. 2010:187.
112. Thermo Fisher Scientific Inc. Nanodrop one, user guide 2017, May [updated 2017, May; cited 2020 26]. p. 55.]. Available from: [www.thermoscientific.com/nanodrop](http://www.thermoscientific.com/nanodrop)
113. Fattorini P, Bonin S, Marrubini G, Bertoglio B, Grignani P, Recchia E, et al. Highly degraded RNA can still provide molecular information: An in vitro approach. *Electrophoresis*. 2020;41(5-6):386-93.
114. QIAGEN. Quick-Start Protocol miRNeasy Micro Kit. RNeasy® (QIAGEN Group) <https://www.qiagen.com/us/products/discovery-and-translational-research/dna-rna-purification/rna-purification/mirna/mirneasy-kits/?clear=true2016>. p. 1-2.
115. QIAGEN. Qiagen sample and assay technologies [Protocol Handbook]. 2012, July [updated 01/2020; cited 2020 21st November 2020]. P. 9]. Available from: <https://www.qiagen.com/us/resources/resourcedetail?id=682963a5-737a-46d2-bc9f-fa137b379ab5&lang=en>.
116. Schroeder A, Mueller O, Stocker S, Salowsky R, Leiber M, Gassmann M, et al. The RIN: an RNA integrity number for assigning integrity values to RNA measurements. *BMC Mol Biol*. 2006;7(1):3-.
117. Life Technologies Corporation. Agilent RNA 6000 Pico Kit Quick Start Guide. © Agilent Technologies [www.agilent.com/genomics/bioanalyzer](http://www.agilent.com/genomics/bioanalyzer) [https://www.agilent.com/cs/library/usermanuals/public/RNA-6000-Pico\\_QSGpdf2017](https://www.agilent.com/cs/library/usermanuals/public/RNA-6000-Pico_QSGpdf2017).
118. Life Technologies. Qubit® microRNA Assay Kits; . [https://www.mbledu/jbpc/files/2014/05/Qubit2\\_Fluorometer\\_UserManualpdf](https://www.mbledu/jbpc/files/2014/05/Qubit2_Fluorometer_UserManualpdf) Thermo Fisher Scientific,: Molecular Probes Life Technologies; ; 2015 p. 12.
119. Scientific TF. TaqMan® Advanced miRNA Assays User Guide. ThermoFisher Scientific Inc.: ThermoFisher Scientific Inc; 2016.
120. Théry C, Witwer KW, Aikawa E, Andriantsitohaina R, Baharvand H, Bauer NN, et al. Minimal information for studies of extracellular vesicles 2018 (MISEV2018): a position statement of the International Society for Extracellular Vesicles and update of the MISEV2014 guidelines. *J Extracell Vesicles*. Sweden: Sweden: Taylor & Francis; 2018. p. 1535750-n/a.
121. Le Bihan M-C, Bigot A, Jensen SS, Dennis JL, Rogowska-Wrzesinska A, Lainé J, et al. In-depth analysis of the secretome identifies three major independent secretory pathways in differentiating human myoblasts. *Journal of proteomics*. 2012;77:344-56.
122. Ultimo S, Zauli G, Martelli AM, Vitale M, McCubrey JA, Capitani S, et al. Influence of physical exercise on microRNAs in skeletal muscle regeneration, aging and diseases. *Oncotarget*. 2018;9(24):17220-37.
123. Townley-Tilson WHD, Callis TE, Wang D. MicroRNAs 1, 133, and 206: Critical factors of skeletal and cardiac muscle development, function, and disease. *Int J Biochem Cell Biol*. 2010;42(8):1252-5.
124. Nielsen S, Åkerström T, Rinnov A, Yfanti C, Scheele C, Pedersen BK, et al. The miRNA plasma signature in response to acute aerobic exercise and endurance training. *PLoS One*. 2014;9(2):e87308-e.

125. Tsiloulis T, Pike J, Powell D, Rossello FJ, Canny BJ, Meex RCR, et al. Impact of endurance exercise training on adipocyte microRNA expression in overweight men. *FASEB J*. 2017;31(1):161-71.
126. Taurino C, Miller William H, McBride Martin W, McClure John D, Khanin R, Moreno María U, et al. Gene expression profiling in whole blood of patients with coronary artery disease. *Clinical Science*. 2010;119(8):335-43.
127. Handschin C, Spiegelman BM. The role of exercise and PGC1alpha in inflammation and chronic disease. *Nature*. 2008;454(7203):463-9.
128. Sell H, Dietze-Schroeder D, Kaiser U, Eckel J. Monocyte Chemotactic Protein-1 Is a Potential Player in the Negative Cross-Talk between Adipose Tissue and Skeletal Muscle. *Endocrinology*. 2006;147(5):2458-67.
129. Thelen MHM, Simonides WS, van Hardeveld C. Electrical stimulation of C2C12 myotubes induces contractions and represses thyroid-hormone-dependent transcription of the fast-type sarcoplasmic reticulum Ca<sup>2+</sup>-ATPase gene. *Biochem J*. 1997;321(3):845-8.
130. Taku H, Edward BA, Gregory DC. Increased submaximal insulin-stimulated glucose uptake in mouse skeletal muscle after treadmill exercise. *J Appl Physiol* (1985). 2006;101(5):1368-76.
131. Lambernd S, Taube A, Schober A, Platzbecker B, Görgens SW, Schlich R, et al. Contractile activity of human skeletal muscle cells prevents insulin resistance by inhibiting pro-inflammatory signalling pathways. *Diabetologia*. 2012;55(4):1128-39.
132. Tsigos C, Papanicolaou DA, Kyrou I, Defensor R, Mitsiadis CS, Chrousos GP. Dose-Dependent Effects of Recombinant Human Interleukin-6 on Glucose Regulation. *The journal of clinical endocrinology and metabolism*. 1997;82(12):4167-70.
133. Oliveira GP, Porto WF, Palu CC, Pereira LM, Petriz B, Almeida JA, et al. Effects of Acute Aerobic Exercise on Rats Serum Extracellular Vesicles Diameter, Concentration and Small RNAs Content. *Frontiers in physiology*. 2018;9:532-.
134. Dragovic RAM, Gardiner CP, Brooks ASMD, Tannetta DSP, Ferguson DJPP, Hole PP, et al. Sizing and phenotyping of cellular vesicles using Nanoparticle Tracking Analysis. *Nanomedicine*. 2011;7(6):780-8.
135. Maroto R, Zhao Y, Jamaluddin M, Popov VL, Wang H, Kalubowilage M, et al. Effects of storage temperature on airway exosome integrity for diagnostic and functional analyses. *J Extracell Vesicles*. 2017;6(1):1359478-n/a.
136. Linares R, Tan S, Gounou C, Arraud N, Brisson AR. High-speed centrifugation induces aggregation of extracellular vesicles. *J Extracell Vesicles*. 2015;4(1):29509-n/a.
137. Bachurski D, Schuldner M, Nguyen P-H, Malz A, Reiners KS, Grenzi PC, et al. Extracellular vesicle measurements with nanoparticle tracking analysis - An accuracy and repeatability comparison between NanoSight NS300 and ZetaView. *J Extracell Vesicles*. 2019;8(1):1596016-n/a.
138. Tupling AR, Bombardier E, Stewart RD, Vigna C, Aquí AE. Muscle fiber type-specific response of Hsp70 expression in human quadriceps following acute isometric exercise. *J Appl Physiol* (1985). 2007;103(6):2105-11.
139. Williams DB. Beyond lectins: The calnexin/calreticulin chaperone system of the endoplasmic reticulum. *J Cell Sci*. 2006;119(4):615-23.
140. Tang Y-T, Huang Y-Y, Zheng L, Qin S-H, Xu X-P, An T-X, et al. Comparison of isolation methods of exosomes and exosomal RNA from cell culture medium and serum. *International Journal of Molecular Medicine*. 2017;40(3):834-44.

141. Eldh M, Lötvall J, Malmhäll C, Ekström K. Importance of RNA isolation methods for analysis of exosomal RNA: Evaluation of different methods. *Mol Immunol.* 2012;50(4):278-86.
142. Ponti G, Maccaferri M, Manfredini M, Kaleci S, Mandrioli M, Pellacani G, et al. The value of fluorimetry (Qubit) and spectrophotometry (NanoDrop) in the quantification of cell-free DNA (cfDNA) in malignant melanoma and prostate cancer patients. *Clin Chim Acta.* 2018;479:14-9.
143. Giron Koetsier PDaEC, Ph.D., New England Biolabs. A Practical Guide to Analyzing Nucleic Acid Concentration and Purity with Microvolume Spectrophotometers. 2019:8.
144. Desjardins P, Hansen JB, Allen M. Microvolume protein concentration determination using the NanoDrop 2000c spectrophotometer. *J Vis Exp.* 2009(33).
145. Imbeaud S, Graudens E, Boulanger V, Barlet X, Zaborski P, Eveno E, et al. Towards standardization of RNA quality assessment using user-independent classifiers of microcapillary electrophoresis traces. *Nucleic Acids Res.* 2005;33(6):e56-e.
146. Henry RR, Ciaraldi TP, Abrams-Carter L, Mudaliar S, Park KS, Nikoulina SE. Glycogen synthase activity is reduced in cultured skeletal muscle cells of non-insulin-dependent diabetes mellitus subjects. Biochemical and molecular mechanisms. *J Clin Invest.* 1996;98(5):1231-6.
147. Lobb RJ, Becker M, Wen Wen S, Wong CSF, Wiegmanns AP, Leimgruber A, et al. Optimized exosome isolation protocol for cell culture supernatant and human plasma. *J Extracell Vesicles.* 2015;4(1):27031-n/a.
148. Filipe V, Hawe A, Jiskoot W. Critical Evaluation of Nanoparticle Tracking Analysis (NTA) by NanoSight for the Measurement of Nanoparticles and Protein Aggregates. *Pharm Res.* 2010;27(5):796-810.

# 18 Appendixes

## Appendix 1

First approval letter from REK for the onset of the project



### UNIVERSITETET I OSLO DET MEDISINSKE FAKULTET

Førsteamanuensis Vigdis Aas  
Høgskolen i Oslo  
Postboks 4 St. Olavs Plass  
0130 Oslo

Regional komité for medisinsk og helsefaglig  
forskningsetikk Sør-Øst D (REK Sør-Øst D)  
Postboks 1130 Blindern  
NO-0318 Oslo

Telefon: 22 85 05 93

Telefaks: 22 85 05 90

E-post: [i.m.middelthun@medisin.uio.no](mailto:i.m.middelthun@medisin.uio.no)

Nettadresse: [www.etikkom.no](http://www.etikkom.no)

**Dato:** 14.04.09

**Deres ref.:**

**Vår ref.:** S-09078d, 2009/166

**Vedr. svar på merknader for studien "Sammenheng mellom sykkelig overvekt og insulinresistens i skjelettmuskulatur"**

Vi viser til svar på merknader av 01.04.09 med følgende vedlegg: Revidert informasjonsskriv

Komiteen behandlet svar på merknader 14.04.09. Prosjektet er vurdert etter lov om behandling av etikk og redelighet i forskning av 30. juni 2006, jfr. Kunnskapsdepartementets forskrift av 8. juni 2007 og retningslinjer av 27. juni 2007 for de regionale komiteer for medisinsk og helsefaglig forskningsetikk.


Komiteen konstaterer at våre merknader er tilfredsstillende besvart.

**Vedtak:**

**Prosjektet godkjennes slik det nå foreligger.**

Med vennlig hilsen

Stein A. Evensen (sign.)  
Professor dr.med.  
leder

  
Ingrid Middelthun  
komitésekretær

Kopi:

- Farmasøytisk institutt, v/Arild Chr. Rustan, Pb 1068 Blindern, 0316 Oslo,

## Appendix 2

### Second approval letter for the extension of the project



<b>Region:</b> REK sør-øst A	<b>Saksbehandler:</b> Tove Irene Klokk	<b>Telefon:</b> 22845522	<b>Vår dato:</b> 19.12.2019	<b>Vår referanse:</b> 39115
<b>Deres referanse:</b>				

Vigdis Aas

#### **39115 Sammenheng mellom sykkelig overvekt og insulinresistens i skjelettmuskulatur**

**Forskningsansvarlig:** OsloMet - storbyuniversitetet

**Søker:** Vigdis Aas

#### **REKs vurdering**

Vi viser til søknad om prosjektendring datert 12.12.2019 for ovennevnte forskningsprosjekt (tidligere REK S-09078). Søknaden er behandlet av leder REK sør-øst A på fullmakt, med hjemmel i helseforskningsloven § 11.

Det søkes om å forlenge studien med tilhørende biobank til 31.12.2024. Dette begrunnes med at prosjektet fortsatt er pågående, og det er ønske om å fullføre påbegynte studier og ha mulighet til å benytte det innsamlede biologiske materialet videre. Det er utarbeidet et informasjonsskriv som skal sendes til forskningsdeltakerne, hvor de blir opplyst om videre bruk av materialet og hvor de gis mulighet til å trekke seg fra studien.

Komiteens leder har vurdert endringene og har ingen forskningsetiske innvendinger mot at disse gjennomføres slik som beskrevet.

#### **Vedtak**

Godkjent

Komiteen godkjenner med hjemmel i helseforskningsloven § 11 annet ledd at prosjektet videreføres i samsvar med det som fremgår av søknaden om prosjektendring og i samsvar

Alle skriftlige henvendelser om saken må sendes via REK-portalene  
Du finner informasjon om REK på våre hjemmesider [rekportalen.no](http://rekportalen.no)

## Media

All mediums used in different phases were prepared in the laboratory under sterile conditions in a Laminar flow cabinet bench (LAF).

### Appendix 3

#### M1-Seeding medium

Ingredients
500 mL DMEM-Glutamax low glucose 1g/L
50 mL FCS (Foetal Calf Serum)
0,5 mL Gentamicin 50mg/mL
2,5 mL Amphotericin 250 µg/mL

### Appendix 4

#### M2-Proliferation medium

Ingredients
500 mL DMEM-Glutamax low glucose 1g/L
10 mL FCS (Foetal Calf Serum)
10 mL Ultrosor G
0,5 mL Gentamicin 50mg/mL
2,5 mL Amphotericin B 250 µg/mL

### Appendix 5

#### M3-Differentiation medium

Ingredients
500 mL DMEM-Glutamax low glucose 1g/L
10 mL FCS (Foetal Calf Serum)
0,5 mL Gentamicin 50mg/mL
2,5 mL Amphotericin B 250 µg/mL
25 pmol insulin 100IE/mL

## Appendix 6

### Serum free Differentiation Medium (S-free)

Ingredients
500 mL DMEM-Glutamax low glucose 1g/L
0,5 mL Gentamicin 50mg/mL
2,5 mL Amphotericin B 250 µg/mL
25 pmoL insulin 100IE/mL

## Appendix 7

### Reagents/Chemicals and equipment used for cell culture

Reagents/Chemicals	Manufacturer
DMEM (Dulbeccó's Modified Eagle medium) (IX) + GlutaMAX™-1 1 g/L D-glucose, Pyruvate (Ref:21885-108)	Gibco® by life technologies™, Paisley, Scotland, Britain
FCS (Foetal Calf Serum) (Ref: 10108-165)	Sigma Aldrich™, Non-USA Origin
Amphotericin B 250 µg/mL (Ref: A2942)	Sigma-Aldrich™, St. Louis, MO, USA
Gentamicin 50 mg/mL (Ref: G1397)	
ECM (Extracellular Matrix) gel (Ref: E1270)	
PBS (Phosphate Buffered Saline)	
NovoRapid Penfill 100IE/mL	Novo Nordisk A/S Bagsværd, Denmark
Ultrosert™G (Ref: 15950-017)	PALL Life Sciences, Cergy-Saint-Christophe, France
NaOH (Sodium hydroxide)	Merck KgaA, Darmstadt, Germany

Equipment	Manufacturer
LAF-bench	Ivfttech, Stainless, Denmark
CO <sub>2</sub> incubator, Model: MCO-18AIC	Sanyo Electric Biomedical Co., Ltd., Japan
Hettich ROTOFIX 32 centrifuge	Hettich LAB technology North America, Massachusetts, USA
Sab Aqua Pro Water bath	Grant Instruments Ltd, Cambridge, Britain
Motic AE31 Microscope	Motic®, Kowloon, Hong Kong
6-well C-Dish™ Culture Dish Electrode system	IonOptix LLC, MA, USA
Costar® 6 well plates with a lock	Corning Incorporated, NY, USA



Corning 15 mL/50 mL Centrifuging Tubes	Corning Sciences, Mexico S. A. de C.V, Tamaulipas, Mexico
Nunc™ EasYFlask™ 75 cm <sup>2</sup> Nunclon™ Delta Surface	Thermo Fisher Scientific, Made in Denmark
Electrical Pulse Stimulator	Electronic Laboratory, Chemical Institute, University of Oslo

## Appendix 8

### Reagents/Chemicals and equipment used for Protein concentration measurement using Bradford's method

#### Protein concentration measurement

Reagents/Chemicals	Manufacturer
Bovine Serum Albumin (BSA)	Sigma-Aldrich™, St. Louis, MO, USA
Sodium Hydroxide (NaOH)	Merck KgaA, Darmstadt, Germany
Bio-Rad Protein Assay Color reagent concentrate.	BioRad Laboratories Inc, CA, USA

Equipment	Manufacturer
Costar® 96 well plates with flat bottom	Corning Incorporated, NY, USA
Perkin Elmer 1420 Multilabel Counter Victor <sup>3</sup> ™	PerkinElmer, Inc., Waltham, MA 02451 USA
Sterile Syringe Filter 0.2 µm Cellulose Acetate membrane. Lot No. 12926566	VWR™ INTERNATIONAL, North America, USA

## Appendix 9

### Interleukin-6 Measurement

Reagents/Chemicals	Manufacturer
Human IL-6 ELISA kit Lot: 1102H140 Contents: <ul style="list-style-type: none"> <li>- Human IL-6 antibody coated ELISA plate</li> <li>- 20X Wash Buffer</li> <li>- ELISA 5X Diluent Buffer B</li> <li>- HRP-Streptavidin</li> </ul>	Sigma-Aldrich Co. Spruce Street. St. Louise, USA

<ul style="list-style-type: none"> <li>- Biotinylated Human IL-6 Detection Antibody</li> <li>- Lyophilized Human IL-6 Protein Standard</li> <li>- ELISA Stop Solution</li> <li>- ELISA Colorimetric TMB Reagent (HRP Substrate)</li> </ul>	
--	--

<b>Equipment</b>	<b>Manufacturers</b>
Perkin Elmer 1420 Multilabel Counter Victor™3	PerkinElmer, Inc., Waltham, MA 02451 USA
IKA-VIBRAX-VXR Shake plate	Janke & Kunkel GmbH & -Co., Germany

## Appendix 10

### Reagents/Chemicals and Equipment for Isolation of EVs

<b>Reagents/Chemicals</b>	<b>Manufacturer</b>
PBS (Phosphate Buffered Saline) Ref:10010-015	Gibco® by life technologies Limited, Fountain Drive, Paisley, UK

<b>Equipment</b>	<b>Manufactures</b>
Sorvall tube	Beckman Coulter Inc., CA, USA
Sorvall RC 5C Plus Centrifuge	Kendro Laboratory Products, Newtown, USA.
15 ml/50 mL Falcon Tube	Corning Sciences, Mexico S. A. de C.V, Tamaulipas, Mexico
Amicon® Ultra 4, filter, Ultracel® 100K: Lot No. R7NA70079	Merc Millipore Ltd., Tullagreen, Carrigtwohill, Co Cork, Ireland
Centricon® Plus-70, Ultracel® PL-100: Lot No. R9PA39808	
Millex®GV Filter Unit 0,22 µm: Lot No. R8NA18936	
Sterile Syring 10/20 mL	B. Braun Melsungen AG, Melsungen, Germany
Biosphere® Safeseal Tube; Lot No. 8081511	SARSTEDT AG & Co. KG Nümbrecht, Germany
Inorganic Membrane Filter Anotop™ 25, 0.02µm: Lot No. A10602265	GE Healthcare Life Sciences, Bukinghamshire, UK
Hettich® ROTINA 420R Centrifuge	Merck KgaA, Darmstadt, Germany

## Appendix 11

### Reagents/Chemicals and Equipment for EVs size analysis and Yield using NanoSight NanoSight

Reagents/Chemicals	Manufacturer
PBS (Phosphate Buffered Saline) Ref: 10010-015	Gibco® by life technologies™, Paisley, Scotland, Britain
Polystyrene Latex Microspheres 100 nm beads	Life technologies™ Thermo Fisher Scientific, USA

Equipment	Manufacturer
NanoSight NS500	Malvern Instruments, Amesbury, Britain
Inorganic Membrane Filter Anotop™ 25, 0,02 µm: Lot No. A10602265	GE Healthcare UK Limited, Buckinghamshire, Britain
Biosphere® SafeSeal tube 1.5 mL: Lot No. 8081511	SARSTEDT AG & Co., Numbrecht, Germany
B Braun Syringe 1 mL: Lot No: 20G20C8	B. Braun Melsungen AG, Germany
MS2 Minishaker IKA® (Vortex mixer)	IKA® Works, Inc., Wilmington, NC, USA

## Appendix 12

### Isolation of Total RNA

Reagents/Chemicals	Manufacturer
miRNeasy Micro Kit Contents: <ul style="list-style-type: none"><li>- Buffer RWT: Lot No. 166023253</li><li>- Buffer PRE: Lot No. 166023255</li><li>- Collection tube 1.5 mL and 2 mL</li><li>- RNeasy® MinElute® Spin Column (packed with 2 mL collection tube): Lot No. 166033609</li><li>- RNase-Free Water: Lot No. 166018375</li></ul>	QIAGEN GmbH, QIAGEN Strasse 1, Germany
- QIAzol K Lysating reagent: Lot No. 44503618	
Nuclease-Free Water: Lot No. 1705246	Ambion Nuclease Free Water-Thermo Fisher® Products and Kits
100 % ethanol: Batch Nr: SE10067822	Antibac AS, Sankt Hallvards, Lierstranda
Chloroform: K1203445	E. Merck, D-6100 Darmstadt, F. R. Germany

<b>Equipment</b>	<b>Manufacturer</b>
Eppendorf centrifuge 5115 R	Eppendorf AG, Hamburg, Germany
RNeasy MinElute Spin Column: Lot No. 166033609	
Collection tubes (2 mL): Lot No. 166033505	QIAGEN GmbH, QIAGEN Strasse 1, Germany
Sample Tubes RB (2 mL): Lot No. 0030118	
Thermo Scientific™ Nanodrop™ One	Life Technologies Thermo Fisher Scientific
CELLTORK (Laboratory Wipe)	Mölnlycke Health Care AB, Göteborg Sweden

### Appendix 13

#### Agilent 2100 bioanalyzer

<b>Reagents/Chemicals</b>	<b>Manufacturer</b>
The Kit contained: RNA 6000 Pico Dye Concentrate (blue) RNA 6000 Pico Marker (green) RNA 6000 Pico Gel Matrix (red) RNA 6000 Pico Conditioning solution No: 5067.1513	Agilent Technologies Manufacturing GmbH & Co. KG, Germany

<b>Equipment</b>	<b>Manufacturer</b>
MS2 S8 Minishaker – IKA vortexer	IKA® Works Inc. Wilmington, NC, USA
Thermomixer comfort	
Agilent 2100 Bioanalyzer Serial No. DE24802301	Agilent Technologies, Lithuania
Eppendorf AG centrifuge 5415 R No. 542605769	Hamburg, Germany
RNA Pico Chips. Lot No. XK23BK30	Agilent Technologies, USA

### Appendix 14

#### Qubit microRNA Assay

<b>Reagent/Chemicals</b>	<b>Manufacturer</b>
Qubit™ microRNA Assay Kit contained all the reagents required. LOT: 2256781	Invitrogen by Thermo Fisher Scientific. Life Technologies Corporation, Oregon USA

<ul style="list-style-type: none"> <li>- Qubit™ microRNA Reagent</li> <li>- Qubit™ microRNA Buffer</li> <li>- Qubit™ microRNA Standard #1</li> <li>- Qubit™ microRNA Standard #2</li> </ul>	
---	--

<b>Equipment</b>	<b>Manufacturer</b>
PCR Eppendorf tubes - DNA LoBind Tube 0.5 mL LOT: G175099P	Eppendorf AG 22331 Hamburg. Germany.
Qubit® 2.0 Fluorometer	Invitrogen by Life technologies Corporation 5791 Van Allen Way Carlsbad CA USA
MS2 Minishaker IKA – Vortex mixer	IKA® Wrks do Brasil Ltd a Taquara.

## Appendix 15

### Reagents/Chemicals and Equipment for RT-qPCR and cDNA synthesis

#### cDNA synthesis

<b>Reagents/Chemicals</b>	<b>Manufacturer</b>
Taq® Advanced miRNA cDNA Synthesis Kit: Lot: 2137409 (Contained all cDNA Synthesis Reagents. Details in Appendix .....??)	Thermo Fisher Scientific, Applied Biosystems by Life Technologies™. CA, USA
RNase-free water	
TE Buffer (0.1X TE) Lot: 2076883	Invitrogen, Life Technologies Corp. Thermo Fisher Scientific. Van Allen Way, Carlsbad, CA USA

#### Poly(A) Reaction Mix

<b>Component</b>	<b>Volume per reaction tube &amp; sample solution</b>
10X Poly(A) Buffer	0.5µL
ATP	0.5 µL
Poly(A) Enzyme	0.3 µL
RNase-free water	1.7 µL
<b>Total Poly(A) Reaction Mix Volume</b>	<b>3.0 µL</b>

### Adaptor Ligation Reaction Mix

<b>Component</b>	<b>Volume per reaction tube &amp; sample solution</b>
5X DNA Ligase Buffer	3 $\mu$ L
50 % PEG 8000 <sup>[2]</sup>	4.5 $\mu$ L
25X Ligation Adaptor	0.6 $\mu$ L
RNA Ligase	1.5 $\mu$ L
RNase-free water	0.4 $\mu$ L
<b>Total Ligation Reaction Mix Volume</b>	<b>10 <math>\mu</math>L</b>

### Reverse Transcription (RT) Reaction Mix

<b>Component</b>	<b>Volume per reaction tube &amp; sample solution</b>
5X RT Buffer	6 $\mu$ L
dNTP Mix (25 mM each)	1.2 $\mu$ L
20X Universal RT Primer	1.5 $\mu$ L
10X RT Enzyme Mix	3 $\mu$ L
RNase-free water	3.3 $\mu$ L
<b>Total RT Reaction Mix Volume</b>	<b>15 <math>\mu</math>L</b>

### miR-Amp reaction Mix

<b>Component</b>	<b>Volume per reaction tube &amp; sample solution</b>
2X miR-Amp Master Mix	25 $\mu$ L
20X miR-Amp Primer Mix	2.5 $\mu$ L
RNase-free Water	17.5 $\mu$ L
<b>Total miR-Amp Reaction Mix Volume</b>	<b>45 <math>\mu</math>L</b>

### PCR Reaction Plate Mix

<b>Component</b>	<b>Volume per reaction tube &amp; sample solution</b>
TaqMan Fast Advanced Master Mix (2X)	10 $\mu$ L
TaqMan Advanced miRNA Assay (20X)* <ul style="list-style-type: none"> <li>- miR-1-3p</li> <li>- miR-133a</li> <li>- miR-206</li> <li>- miR-223</li> </ul>	1 $\mu$ L
RNase-free Water	4 $\mu$ L
<b>Total PCR Reaction Mix Volume</b>	<b>15 <math>\mu</math>L</b>

\*Each miR was prepared for a PCR reaction mix.

<b>Equipment</b>	<b>Manufacturer</b>
VWR™ Galaxy MiniStar – Centrifuge	VWR International, Korea
MS2 Minishaker IKA – Vortex mixer	IKA® Wrks do Brasil Ltd a Taquara.
Veriti® 96 Thermal Cycler Model no: 9902	Life Technologies Holdings Pte Ltd. Singapore
ViiA7™ Real-Time PCR System	Thermo Fisher Scientific, Applied Biosystems by Life Technologies™. CA, USA
Eppendorf Centrifuge 5430 R Serial No. 5428YR406994	Hamburg, Germany
96 PCR Plate half-skirted standard profile Batch No. 581453	VWR® International, Researchpark Haasrode, Germany
0.2 mL PCR tube strips Batch No. 626620	
Adhesive PCR Plate foils	Thermo Fisher Scientific

## Appendix 16

### Affymetrix microarray guide

appliedbiosystems

# FlashTag™ Biotin HSR RNA Labeling Kit

For GeneChip™ miRNA Arrays

For Research Use Only. Not for use in diagnostic procedures.

**ThermoFisher**  
SCIENTIFIC



Information in this document is subject to change without notice.

**DISCLAIMER**

TO THE EXTENT ALLOWED BY LAW, THERMO FISHER SCIENTIFIC AND/OR ITS AFFILIATE(S) WILL NOT BE LIABLE FOR SPECIAL, INCIDENTAL, INDIRECT, PUNITIVE, MULTIPLE OR CONSEQUENTIAL DAMAGES IN CONNECTION WITH OR ARISING FROM THIS DOCUMENT, INCLUDING YOUR USE OF IT.

**Important Licensing Information**

These products may be covered by one or more Limited Use Label Licenses. By use of these products, you accept the terms and conditions of all applicable Limited Use Label Licenses.

**Corporate entity**

Life Technologies | Carlsbad, CA 92008 USA | Toll free in USA 1.800.955.6288

**Trademarks**

All trademarks are the property of Thermo Fisher Scientific and its subsidiaries unless otherwise specified. All other trademarks are the property of their respective owners.

© 2017 Thermo Fisher Scientific Inc. All rights reserved.

P/N 703095

## Contents

<b>Chapter 1 Introduction</b> .....	<b>4</b>
Background Information.....	4
Procedure Overview.....	5
Materials Required.....	6
FlashTag™ Biotin HSR RNA Labeling Kit.....	6
Other Required Materials.....	7
RNA Sample and Quantitation.....	8
RNA Isolation.....	8
Quantitation.....	8
RNA Input for FlashTag™ Biotin HSR.....	8
<b>Chapter 2 FlashTag™ Biotin HSR RNA Labeling Procedure</b> .....	<b>9</b>
Poly (A) Tailing.....	9
FlashTag™ Biotin HSR Ligation.....	10
<b>Chapter 3 GeneChip™ miRNA Array Procedure</b> .....	<b>11</b>
Preparation of Ovens, Arrays, and Sample Registration Files.....	11
Hybridization.....	12
Washing and Staining.....	14
Scanning.....	15
Analysis.....	16
<b>Chapter 4 miRNA Array Plates Procedure</b> .....	<b>17</b>
Reagents and Materials Required.....	17
Prepare the Hybridization Cocktail Mix.....	17
<b>Appendix A ELOSA QC Assay</b> .....	<b>19</b>
Additional Required Materials.....	19
Procedural Notes.....	20
Experimental Design Recommendations.....	20
Coating Wells with ELOSA Spotting Oligos.....	21
Washing and Blocking.....	21
Sample Hybridization.....	21
SA-HRP Binding.....	22
Signal Development.....	22
<b>Appendix B Array Rehybridization Procedure</b> .....	<b>23</b>

## Chapter 1 Introduction

### Background Information

The FlashTag™ Biotin HSR Labeling Kit will label any RNA sample, including total RNA, severely degraded RNA, plant RNA, and low molecular weight RNA. This protocol describes labeling total RNA or low molecular weight (LMW) RNA for analysis by GeneChip™ miRNA Arrays and includes an in-process ELOSA QC Assay.

LMW RNA molecules (snRNA, hnRNA, piRNA, miRNA, etc.) have recently been shown to be involved in important biological processes such as mRNA degradation, transcriptional gene silencing (TGS) and translational repression.<sup>1,2,3,4,5,6,7,8</sup> As a result, these newly discovered biomolecules are gaining the interest of the scientific community as possible new drug targets and for use in diagnostics. FlashTag Biotin HSR provides the necessary tools to identify such targets.

FlashTag Biotin HSR labeling is fast, simple, accurate, highly sensitive and reproducible. Starting with total RNA (see Table 1.2 for recommended input amounts), the process begins with a brief tailing reaction followed by ligation of the biotinylated signal molecule to the target RNA sample (see Figure 1.1). The labeling process is complete in less than one hour.

The high sensitivity of FlashTag Biotin HSR is due to proprietary 3DNA™ dendrimer signal amplification technology. The 3DNA dendrimer is a branched structure of single and double stranded DNA conjugated with numerous labels.<sup>9,10</sup> The 3DNA molecule in the FlashTag Biotin HSR Labeling Kit provides ultrasensitive biotin labeling.

Please review this manual before beginning experiments. Materials needed for GeneChip miRNA Arrays are listed. Materials needed for the ELOSA QC Assay are listed in Appendix A. Note that ELOSA wells must be coated with DNA Spotting Oligos and incubated overnight before the ELOSA assay may be run.

<sup>1</sup> Schembri et al. *MicroRNAs as modulators of smoking-induced gene expression changes in human airway epithelium. PNAS* 2009 vol. 106 no. 7, 2319-2324.

<sup>2</sup> Taylor and Gant. *Emerging fundamental roles for non-coding RNA species in toxicology. Toxicology* 2008 vol. 246 Issue 1, 34- 39.

<sup>3</sup> Ronemus, M. et al. *MicroRNA-Targeted and Small Interfering RNA-Mediated mRNA Degradation Is Regulated by Argonaute, Dicer, and RNA-Dependent RNA Polymerase in Arabidopsis. The Plant Cell.* 2006, 18(7):1559-1574.

<sup>4</sup> Morel, JB. et al. *Hypomorphic ARGONAUTE (ago1) Mutants Impaired in Post-Transcriptional Gene Silencing and Virus Resistance. The Plant Cell.* 2002, Vol. 14(3), 629-639.

<sup>5</sup> Krichevsky, AM. et al. *A microRNA array reveals extensive regulation of microRNAs during brain development. RNA.* 2003, 9(10):1274-1281.

<sup>6</sup> Schmittgen, TD. et al. *A high-throughput method to monitor the expression of microRNA precursors. Nucleic Acids Res.* 2004, 32(4):e43.

<sup>7</sup> Thomson, JM. et al. *A Custom Microarray Platform for Analysis of MicroRNA Gene Expression. Nature Methods.* 2004, 1(1) 47-53.

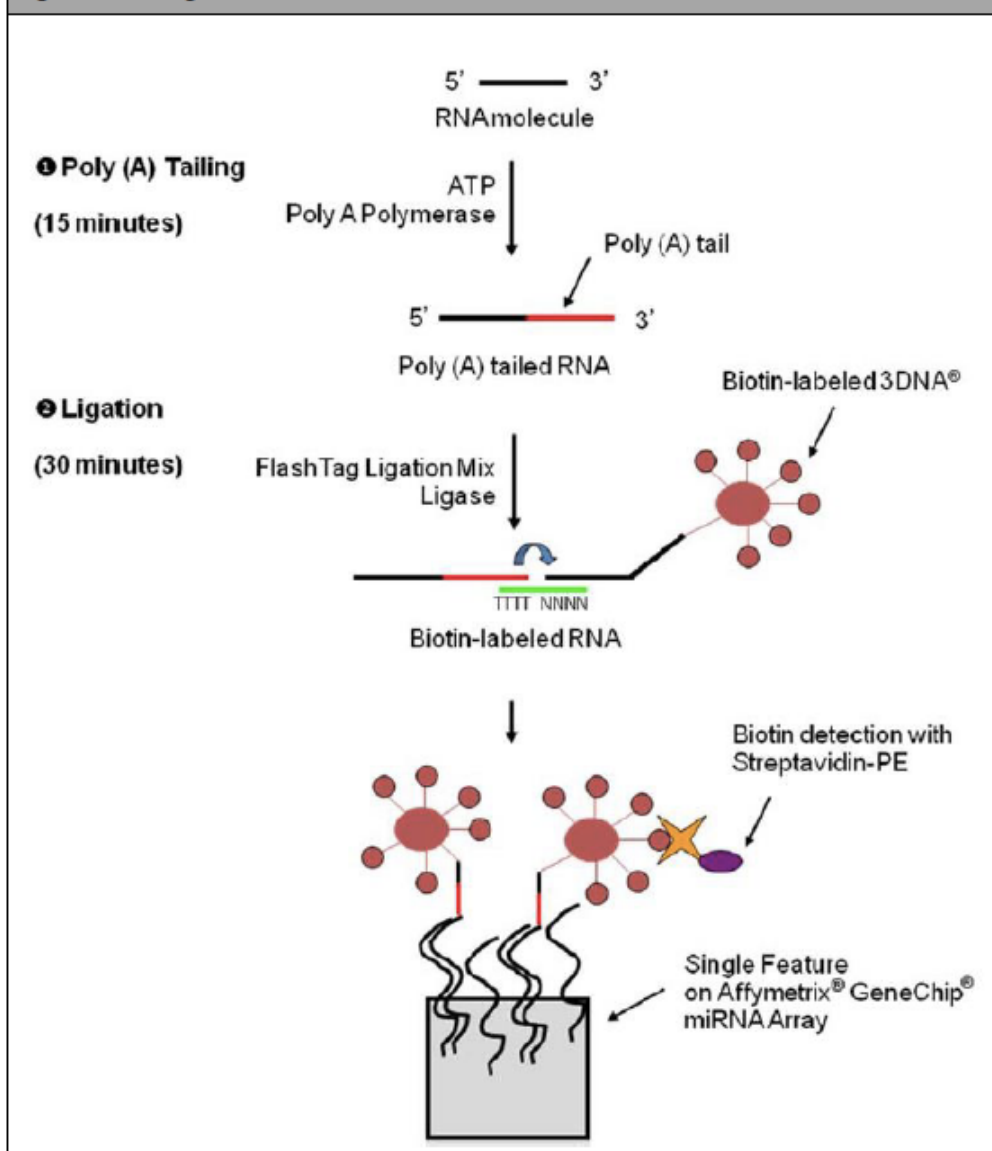
<sup>8</sup> Ambros, V. *The functions of animal microRNAs. Nature.* 2004, 431:350.

<sup>9</sup> Nilsen, TW. et al. *Dendritic Nucleic Acid Structures. J. Theor. Biol.* 1997, 187:273-284.

<sup>10</sup> Stears, RL. et al. *A novel, sensitive detection system for high-density microarrays using dendrimer technology. Physiol. Genomics.* 2000, 3:93-99.

## Procedure Overview

Figure 1.1 FlashTag™ HSR: Procedure Overview



## Materials Required

### FlashTag™ Biotin HSR RNA Labeling Kit

FlashTag Biotin HSR RNA Labeling Kit, 10 rxn (P/N 901910) or 30 rxn (P/N 901911).

**Table 1.1** FlashTag™ Biotin HSR RNA Labeling Kit Reagents and Storage Conditions

Vial	Component	Storage	Handling
1	10X Reaction Buffer	-20°C	Thaw at room temperature, vortex, and briefly microfuge.
2	25mM MnCl <sub>2</sub>	-20°C	Thaw at room temperature, vortex, and briefly microfuge.
3	ATP Mix	-20°C	Thaw on ice, microfuge if necessary, and keep on ice at all times.
4	PAP Enzyme	-20°C	Remove from freezer just prior to use, and briefly microfuge. Keep on ice at all times. Do not vortex.
5	5X FlashTag Biotin HSR Ligation Mix	-20°C	Thaw at room temperature, vortex, and briefly microfuge.
6	T4 DNA Ligase	-20°C	Remove from freezer just prior to use, and briefly microfuge. Keep on ice at all times. Do not vortex.
7	HSR Stop Solution	-20°C	Thaw at room temperature, vortex, and briefly microfuge.
8	RNA Spike Control Oligos	-20°C	Thaw on ice, microfuge if necessary, and keep on ice at all times.
9	ELOSA Spotting Oligos	-20°C	Thaw at room temperature, vortex, and briefly microfuge.
10	ELOSA Positive Control	-20°C	Thaw on ice, microfuge if necessary, and keep on ice at all times.
11	Nuclease-Free Water	-20°C	Thaw at room temperature, vortex, and briefly microfuge.
12	27.5% Formamide	-20°C	Thaw at room temperature, vortex, and briefly microfuge.



**NOTE:** The FlashTag Biotin HSR RNA Labeling Kit is recommended for no more than three freeze-thaw cycles.

## Other Required Materials

Refer to Appendix C for example reagent preparation and storage.

**I** **IMPORTANT: All materials should be nuclease-free, and all reagents should be prepared with nuclease-free components.**

- RNA sample containing low molecular weight (LMW) RNA (see *RNA Sample and Quantitation*)
- Nuclease-free water (Applied Biosystems P/N AM9932 or equivalent)
- 1mM Tris (Appendix C)
- Reagents and materials for analysis by GeneChip miRNA Array:
  - miRNA Array
  - Reagents for ELOSA QC Assay: Refer to Appendix A, *ELOSA QC Assay* and Appendix C, *Example Reagent Preparation and Storage*.
  - GeneChip™ Eukaryotic Hybridization Control Kit (P/N 900454)
  - GeneChip™ Hybridization, Wash and Stain Kit (P/N 900720)
  - Laser Tough-Spots™ 3/8" diameter (Diversified Biotech P/N SPOT-1000)
  - Laser Tough-Spots™ 1/2" diameter (Diversified Biotech P/N SPOT-2000)
  - GeneChip™ Command Console™ Software (AGCC)
  - Expression Console™ Software (EC) v1.2 or higher
  - GeneChip™ Fluidics Station 450 (P/N 00-0079)
  - GeneChip™ Hybridization Oven 645
  - GeneChip™ Scanner 3000 7G
- Reagents and materials for analysis by miRNA Plates:
  - miRNA Plate
  - Reagents for ELOSA QC Assay: Refer to Refer to Appendix A, *ELOSA QC Assay* and Appendix C, *Example Reagent Preparation and Storage*.
  - GeneChip™ Eukaryotic Hybridization Control Kit (P/N 900457)
  - GeneTitan™ Hybridization, Wash and Stain Kit for miRNA Array Plates (P/N 902276)
  - GeneChip™ Command Console™ Software (AGCC)
  - Expression Console™ Software (EC) v1.2 or higher
  - GeneTitan™ SC or MC Instrument

## RNA Sample and Quantitation

Either Total RNA or LMW (Low Molecular Weight) RNA can be labeled with FlashTag Biotin HSR. Using total RNA can save time and money, and prevent sample loss.<sup>1,2</sup>

<sup>1</sup> <http://www.genetics.pitt.edu/forms/flyers/miRNAextractionevaluation.pdf>

<sup>2</sup> Masotti et al. *Quantification of Small Non-Coding RNAs Allows an Accurate Comparison of miRNA Expression Profiles. Journal of Biomedicine and Biotechnology 2009, Article ID 659028*

### RNA Isolation

Any kit for purification of total RNA or LMW RNA will be compatible with FlashTag Biotin HSR. Elute or resuspend the RNA in nuclease-free water. Ensure that the purification method retains low molecular weight species. Some commercial products that have been tested successfully with FlashTag Biotin HSR include:

- Applied Biosystems: mirVana™ miRNA Isolation Kit
- Applied Biosystems: RecoverAll™ Total Nucleic Acid Isolation Kit for FFPE
- QIAGEN: miRNeasy Mini Kit
- Invitrogen: PureLink™ miRNA Isolation Kit
- Invitrogen: TRIzol™ reagent (total RNA only) with additional overnight -20°C precipitation step during isopropanol precipitation<sup>1</sup>

### Quantitation

To accurately determine the concentration of the RNA sample, we recommend the use of the Quant-iT™ RiboGreen RNA Assay Kit (Invitrogen P/N R11490) or the NanoDrop™ ND-1000 Spectrophotometer (NanoDrop Technologies).

### RNA Input for FlashTag™ Biotin HSR

Table 1.2 describes general recommendations for RNA input for FlashTag Biotin HSR labeling. To maintain comparability to previous generation arrays, a minimum of 130 ng input is recommended for 100 format arrays.

Table 1.2

RNA Sample	Input for FlashTag Biotin HSR Labeling for miRNA 400/169 Format Arrays (miRNA 1.0 and 2.0 Arrays)	Input for FlashTag Biotin HSR Labeling for miRNA 100 Format Arrays (miRNA 3.0 and later designs)
Total RNA containing LMW RNAT	100 - 1000 ng total RNA	130 - 1000 ng total RNA
Enriched LMW RNA, quantitated	100 - 400 ng LMW RNA	130 - 400 ng LMW RNA
Enriched LMW RNA, not quantitated	Enriched from 100 - 1000 ng total RNA	Enriched from 130 - 1000 ng total RNA

<sup>1</sup> Wang et al. *The Expression of MicroRNA miR-107 Decreases Early in Alzheimer's Disease and May Accelerate Disease Progression through Regulation of ?-Site Amyloid Precursor Protein-Cleaving Enzyme. The Journal of Neuroscience, January 30, 2008, 28(5):1213-1223*

## Chapter 2

### FlashTag™ Biotin HSR RNA Labeling Procedure

To confirm target labeling, we suggest running an ELOSA QC Assay prior to array hybridization. Refer to Appendix A, *ELOSA QC Assay*. Note that ELOSA wells must be coated with DNA Spotting Oligos and incubated overnight before the ELOSA assay may be run, and that Plate Washing and Blocking steps may be completed prior to or during the FlashTag Biotin HSR labeling procedure.

#### Poly (A) Tailing

- Adjust the volume of RNA to 8  $\mu\text{L}$  with Nuclease-Free Water (Vial 11).
- Transfer the 8  $\mu\text{L}$  RNA to ice. Add 2  $\mu\text{L}$  RNA Spike Control Oligos (Vial 8) and return to ice.
- Dilute the ATP mix (Vial 3) in 1 mM Tris as follows:
  - For total RNA samples, dilute the ATP Mix 1:500.
  - For enriched, quantitated samples, calculate the dilution factor according to the following formula:  

$$5000 \div \text{ng input LMW RNA}$$
 Example: If using 100 ng of enriched LMW RNA, the dilution factor is  $5000 \div 100 = 50$ .  
 Dilute the ATP Mix 1:50.
  - For enriched samples that are not quantitated, calculate the dilution factor according to the following formula:  

$$1000 \div \mu\text{g input total RNA}$$
 Example: If the sample was enriched from 500 ng total RNA, the dilution factor is  $1000 \div 0.5 = 2000$ .  
 Dilute the ATP Mix 1:2000.
- Assemble a Poly A Tailing Master Mix in a nuclease-free tube in the order listed in Table 2.1. Include 10% overage to cover pipetting errors.

Table 2.1 Poly A Tailing Master Mix

Component	Volume per miRNA Array	16-Array Plate*	24-Array Plate*	96-Array Plate*
10X Reaction Buffer (Vial 1)	1.5 $\mu\text{L}$	26.4 $\mu\text{L}$	39.6 $\mu\text{L}$	158.4 $\mu\text{L}$
25mM MnCl <sub>2</sub> (Vial 2)	1.5 $\mu\text{L}$	26.4 $\mu\text{L}$	39.6 $\mu\text{L}$	158.4 $\mu\text{L}$
Diluted ATP Mix (Vial 3 dilution from Step 3)	1.0 $\mu\text{L}$	17.6 $\mu\text{L}$	26.4 $\mu\text{L}$	105.6 $\mu\text{L}$
PAP Enzyme (Vial 4)	1.0 $\mu\text{L}$	17.6 $\mu\text{L}$	26.4 $\mu\text{L}$	105.6 $\mu\text{L}$

\* Includes ~10% overage to cover pipetting error.



5. Add 5  $\mu\text{L}$  of Master Mix to the 10  $\mu\text{L}$  RNA/Spike Control Oligos (Step 2 above), for a volume of 15  $\mu\text{L}$ .
6. Mix gently (do not vortex) and microfuge.
7. Incubate in a 37°C heat block for 15 minutes. Discard any unused, diluted ATP mix from Step 3.

## FlashTag™ Biotin HSR Ligation

1. Briefly microfuge the 15  $\mu\text{L}$  of tailed RNA and place on ice.
2. Add 4  $\mu\text{L}$  5X FlashTag Biotin HSR Ligation Mix (Vial 5) to each sample.
3. After the Ligation Mix has been added, add 2  $\mu\text{L}$  of T4 DNA Ligase (Vial 6) to each sample. Do not make a master mix at this step, as auto-ligation can occur.
4. Mix gently (do not vortex) and microfuge.
5. Incubate at 25°C (room temperature) for 30 minutes.
6. Stop the reaction by adding 2.5  $\mu\text{L}$  HSR Stop Solution (Vial 7). Mix and microfuge the 23.5  $\mu\text{L}$  of ligated sample.
7. Remove 2  $\mu\text{L}$  of the biotin-labeled sample for use with the ELOSA QC Assay (Appendix A). It is acceptable to store the 2  $\mu\text{L}$  of biotin-labeled sample on ice for up to 6 hours or at -20°C for up to 2 weeks, and run the ELOSA QC Assay at a convenient time. If the ELOSA QC Assay is not performed, it is recommended that 2  $\mu\text{L}$  of biotin-labeled sample be saved until the array QC is complete. Retaining this sample will enable one the ability to troubleshoot possible target preparation issues, if needed.
8. The remaining 21.5  $\mu\text{L}$  biotin-labeled sample may be stored on ice for up to 6 hours, or at -20°C for up to 2 weeks, prior to hybridization on GeneChip™ miRNA Arrays or miRNA Array Plates.

## Chapter 3

# GeneChip™ miRNA Array Procedure

### Preparation of Ovens, Arrays, and Sample Registration Files

1. Download and install the miRNA Array library file package (if not performed previously) into GeneChip™ Command Console™ (AGCC) software using the Command Console Library File Importer tool. The files can be found on our web site.
2. Turn the Hybridization Oven 645 on and set the temperature to 48°C. Set the RPM to 60.

Turn the rotation on and allow the oven to preheat for at least one hour.

3. Upload the sample and array information (sample names, barcode IDs, etc.) into AGCC.
4. Unwrap the arrays and place on the bench top. Allow the arrays to warm to room temperature (10- 15 minutes). Mark each array with a meaningful designation.
5. Insert a 20 µL or 200 µL pipet tip (unfiltered type recommended) into the upper right septum to allow for proper venting when hybridization cocktail is injected.

For more information, refer to the *Command Console™ User Guide* (P/N 702569).

## Hybridization

1. Bring the reagents listed in Step 3, below, to room temperature.
2. Completely thaw and then heat the 20X Eukaryotic Hybridization Controls (*bioB*, *bioC*, *bioD*, *cre* from GeneChip™ Eukaryotic Hybridization Control Kit) for 5 minutes at 65°C.
3. Add the following components in Table 3.1 to the 21.5 µL biotin-labeled sample in the order listed, to prepare the array hybridization cocktail:

Table 3.1 Hybridization Cocktail (for a single reaction)

Component	Volume for a 400/169 Format Array (miRNA 1.0 and 2.0 Arrays)	Volume for a 100 Format Array (miRNA 3.0 and later designs)	Final Concentration
2X Hybridization Mix	50 µL	66 µL	1X
27.5% Formamide (Vial 12)	15 µL	19.2 µL	4%
DMSO	10 µL	12.8 µL	9.7%
20X Hybridization Controls	5 µL	6.6 µL	1X
Control Oligo B2, 3nM	1.7 µL	2.2 µL	50 pM
Nuclease-free Water	N/A	3.7 µL	
<b>Total Volume</b>	<b>81.7 µL</b>	<b>110.5 µL</b>	



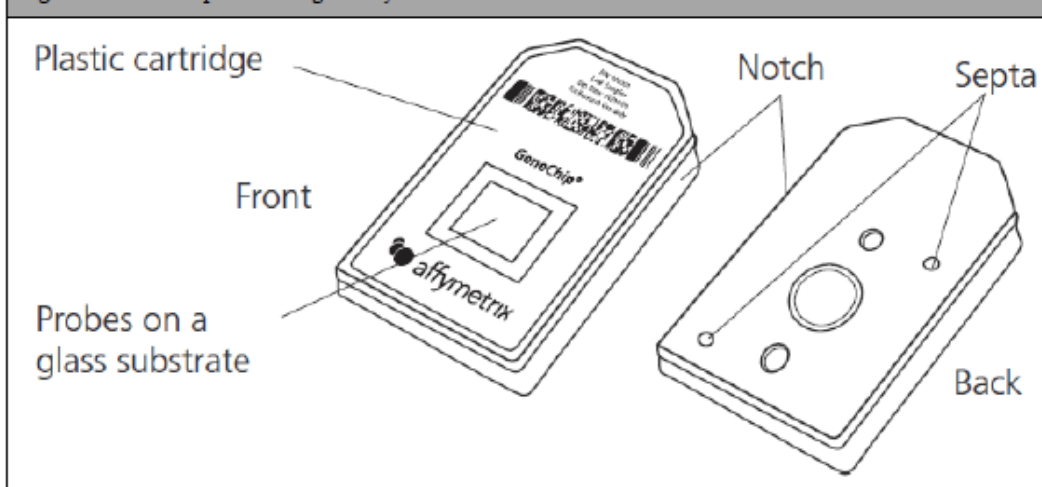
**NOTE:** If preparing multiple samples, a master mix of the hybridization cocktail components in Table 3.1 may be prepared by multiplying the volumes by the number of arrays plus 10% overage to cover pipetting error. Refer to Table 3.2 for appropriate Hybridization Master Mix volumes to add to the biotin-labeled sample

**Table 3.2 Hybridization Cocktail Using a Hybridization Master Mix**

Component	400/169 Format Array (miRNA 1.0 and 2.0 Arrays)	100 Format Array (miRNA 3.0 and later designs)
Biotin-labeled Sample	21.5 $\mu\text{L}$	21.5 $\mu\text{L}$
Hybridization Master Mix	81.7 $\mu\text{L}$	110.5 $\mu\text{L}$

4. Incubate at 99°C for 5 minutes, then 45°C for 5 minutes.
5. Aspirate 100  $\mu\text{L}$  (400/169 format array) or 130  $\mu\text{L}$  (100 format array) and inject into an array.

**Figure 3.1 GeneChip™ Cartridge Array**



6. Remove the pipet tip from the upper right septum of the array.
7. Cover both septa with 1/2" Tough-Spots™ to minimize evaporation and/or prevent leaks.
8. Place the arrays into hybridization oven trays.
9. Load the trays into the hybridization oven.
10. Incubate the arrays at 48°C and 60 rpm for 16 to 18 hours.

## Washing and Staining

For additional information about washing, staining, and scanning, refer to the *Genechip™ Expression Wash, Stain, and Scan User Guide for Cartridge Arrays* (PN 702731) and the *Command Console™ User Guide* (P/N 702569).

1. After 16 to 18 hours of hybridization, remove the arrays from the oven. Remove the Tough-Spots from the arrays.
2. Extract the hybridization cocktail from each array and transfer it to a new tube or well of a 96-well plate in order to save the hybridization cocktail. Store on ice during the procedure, or at  $-80^{\circ}\text{C}$  for long-term storage. Refer to Appendix B, *Array Rehybridization Procedure*, if necessary.
3. Fill each array completely with Array Holding Buffer.
4. Allow the arrays to equilibrate to room temperature before washing and staining.



---

**NOTE:** Arrays can be stored in the Array Holding Buffer at  $4^{\circ}\text{C}$  for up to 3 hours before proceeding with washing and staining. Equilibrate arrays to room temperature before washing and staining.

---

5. Place vials into sample holders on the fluidics station:
  1. Place one (amber) vial containing 600  $\mu\text{L}$  Stain Cocktail 1 in sample holder 1.
  2. Place one (clear) vial containing 600  $\mu\text{L}$  Stain Cocktail 2 in sample holder 2.
  3. Place one (clear) vial containing 800  $\mu\text{L}$  Array Holding Buffer in sample holder 3.
6. Wash and stain with Fluidics Station 450 using the appropriate fluidics script for the array format.

**Table 3.3 Fluidics Protocols**

	<b>Fluidics Station 450 Protocol FS450_0002 (100 format array)</b>	<b>Fluidics Station 450 Protocol FS450_0003 (400/169 format array)</b>
<b>Post Hyb Wash #1</b>	10 cycles of 2 mixes/cycle with Wash Buffer A at 30°C	10 cycles of 2 mixes/cycle with Wash Buffer A at 25°C
<b>Post Hyb Wash #2</b>	6 cycles of 15 mixes/cycle with Wash Buffer B at 50°C	8 cycles of 15 mixes/cycle with Wash Buffer B at 50°C
<b>1st Stain</b>	Stain the probe array for 5 minutes with Stain Cocktail 1 (Vial Position 1) at 35°C	Stain the probe array for 10 minutes with Stain Cocktail 1 (Vial Position 1) at 25°C
<b>Post Stain Wash</b>	Wash 10 cycles of 4 mixes/cycle with Wash Buffer A at 30°C	Wash 10 cycles of 4 mixes/cycle with Wash Buffer A at 30°C
<b>2nd Stain</b>	Stain the probe array for 5 minutes with Stain Cocktail 2 (Vial Position 2) at 35°C	Stain the probe array for 10 minutes with Stain Cocktail 2 (Vial Position 2) at 25°C
<b>3rd Stain</b>	Stain the probe array for 5 minutes with Stain Cocktail 1 (Vial Position 1) at 35°C	Stain the probe array for 10 minutes with Stain Cocktail 1 (Vial Position 1) at 25°C
<b>Final Wash</b>	15 cycles of 4 mixes/cycle with Wash Buffer A at 35°C	15 cycles of 4 mixes/cycle with Wash Buffer A at 35°C
<b>Array Holding Buffer</b>	Fill the probe array with Array Holding Buffer (Vial Position 3)	Fill the probe array with Array Holding Buffer (Vial Position 3)

7. Check for air bubbles. If there are air bubbles, manually fill the array with Array Holding Buffer. If there are no air bubbles, cover both septa with 3/8" Tough-Spots. Inspect the array glass surface for dust and/or other particulates and, if necessary, carefully wipe the surface with a clean lab wipe before scanning.

## Scanning

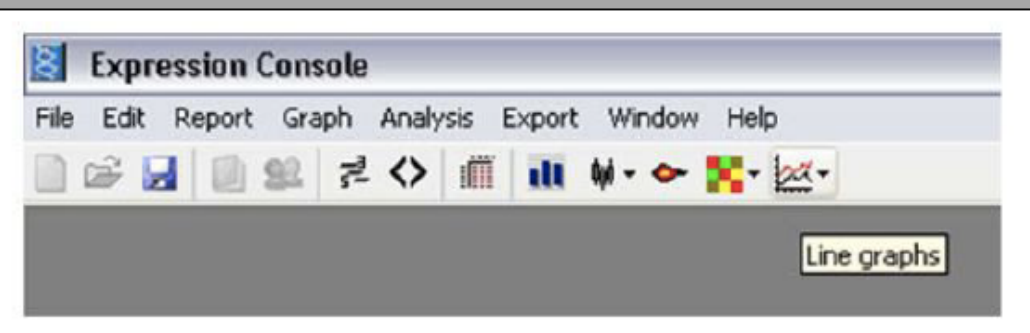
The instructions for using the scanner and scanning arrays can be found in the *Command Console™ User Guide* (P/N 702569).

## Analysis

Use Expression Console software for data summarization, normalization, and quality control (v. 1.2 and higher). Please refer to the website for Expression Console for instructions on miRNA Array analysis. We recommend using RMA + DABG for analysis.

To evaluate the success of the labeling protocol and array processing, open line graphs for the spike-in labeling control probe sets in Expression Console. Once the RMA+DABG analysis is complete, click on the icon for line graphs or select Graph → Line Graph · Report Metrics and select the check boxes for desired probe sets.

Figure 3.2



If the labeling protocol was successful, the following spike-in control probe sets (representing synthetic miRNAs present in vial 8) should have signal greater than or equal to 1000 (or 9.96 for log<sub>2</sub> signal):

- spike\_in-control-2\_st
- spike\_in-control-23\_st
- spike\_in-control-29\_st
- spike\_in-control-31\_st
- spike\_in-control-36\_st.

Oligos 2, 23 and 29 are RNA, and confirm the poly(A) tailing and ligation. Oligo 31 is poly(A) RNA and confirms ligation. Oligo 36 is poly(dA) DNA and confirms ligation and the lack of RNases in the RNA sample.

If the array hybridization, wash, stain and scan procedure was successful, the arrays should be gridded successfully and cel and chp files should be generated. The hybridization control probe sets should have signal commensurate with concentration:

AFFX-r2-Ec-c1-BioB-3\_at < AFFX-r2-Ec-c1-BioC-3\_at < AFFX-r2-Ec-c1-BioD-3\_at < AFFX-r2-Ec-c1-cre-3\_at

Export the data into third party software for further analysis.

## Chapter 4 miRNA Array Plates Procedure

This chapter includes hybridization cocktail preparation instructions for processing miRNA Array Plates using the GeneTitan™ Instrument and the FlashTag Biotin HSR RNA Labeling Assay. The hybridization mix described below was specifically formulated for use with the FlashTag Biotin HSR RNA Labeling Kit P/N 901910 (10 rxn) and P/N 901911 (30 rxn). For instructions on setting up hybridizations on cartridge arrays, please go to Chapter 3, GeneChip™ miRNA Array Procedure.

### Reagents and Materials Required

- GeneTitan™ Hybridization, Wash and Stain Kit for miRNA Array Plates (P/N 902276, 96 Rxn) consists of:
  - GeneTitan™ Hybridization Module for miRNA Array Plates (P/N 902275)
  - GeneTitan™ Wash Buffers A & B Module (P/N 901583)
- GeneChip™ Hybridization Control Kit (P/N 900457, 150 rxns)

### Prepare the Hybridization Cocktail Mix

1. Bring the reagents listed in Step 3, below, to room temperature.
2. Completely thaw and then heat the 20X Eukaryotic Hybridization Controls (*bioB*, *bioC*, *bioD*, *cre* from GeneChip™ Eukaryotic Hybridization Control Kit) for 5 minutes at 65°C.
3. Prepare a Hybridization Cocktail Master mix according to Table 4.1 below:

Table 4.1 Hybridization Cocktail (for a single reaction and for multiple reactions)

Component	Volume per miRNA 16-Array Plate*	24-Array Plate*	96-Array Plate*	Final Concentration
2X Hybridization Mix	62.5 µL	1100 µL	1650 µL	1X
27.5% Formamide (Vial 12)	18.2 µL	320.3 µL	480.5 µL	4%
DMSO	12.1 µL	213 µL	319.4 µL	9.7%
20X Hybridization Controls	6.3 µL	110.9 µL	166.3 µL	1X
Control Oligo B2, 3nM	2.1 µL	37 µL	55.4 µL	50pM
Nuclease-free Water	2.3 µL	40.5 µL	60.7 µL	
<b>Total Volume</b>	<b>103.5 µL</b>	<b>1821.7 µL</b>	<b>2732.3 µL</b>	<b>10929.7 µL</b>

\* Includes ~10% overage to cover pipetting error.

4. Add 103.5 µL cocktail mix to 21.5 µL of labeled sample for each array.



5. Denature the hybridization cocktail with target at 99°C for 5 minutes, followed by 45°C for 5 minutes.
6. After denaturation, centrifuge hybridization cocktail with target to remove any insoluble material from the hybridization mixture.
7. Carefully transfer 120 µL of the denatured and centrifuged supernatant hybridization target into the appropriate well of the HT Hybridization Tray.
8. Please follow the instructions provided in the *GeneTitan™ Instrument User Guide for Expression Array Plates* (P/N 702933 rev. 1 or higher) to process miRNA array plates on the GeneTitan™ Instrument.

## Appendix A

### ELOSA QC Assay

The Enzyme Linked Oligosorbent Assay (ELOSA) is designed to provide confirmation that the FlashTag Biotin HSR Labeling Kit has performed appropriately as a biotin labeling process. Specifically, the ELOSA is designed to detect the RNA Spike Control Oligos (Vial 8) included in all FlashTag Biotin HSR labeling reactions. Only 2  $\mu\text{L}$  of the labeling reaction is required for the ELOSA assay. Successful biotin labeling is verified via a simple colorimetric ELOSA assay through the hybridization of the biotin-labeled RNA Spike Control Oligos (Vial 8) to complementary ELOSA Spotting Oligos (Vial 9) immobilized onto microtiter plate wells. The ELOSA Positive Control (Vial 10) confirms the ELOSA assay is working properly.

We suggest that this assay be run prior to the use of any labeling reaction on microarrays to ensure the FlashTag Biotin HSR labeling process worked appropriately with known controls. As an alternative, the 2  $\mu\text{L}$  aliquot from the labeling reaction may be stored at  $-20^{\circ}\text{C}$  for up to two weeks and used for troubleshooting, if needed. Please note that this procedure does not assure the performance of any RNA sample on a microarray.

### Additional Required Materials

Refer to Appendix C for example preparation and storage.

- Flat bottom Immobilizer™ Amino – 8 well strips  
Nunc P/N 436013 (30 plates)  
Do not use strips or plates from other manufacturers.
- Adhesive plate sealers (VWR P/N 62402-921) or equivalent
- Wash bottle (or washing instrument) for vigorous washing
- 1X PBS
- 1X PBS, 0.02% Tween-20
- 5X SSC, 0.05% SDS, 0.005% BSA (If a precipitate forms in this buffer, warm at  $42^{\circ}\text{C}$  to dissolve. Use at room temperature.)
- 5% BSA in 1X PBS
- 25% dextran sulfate – see Appendix C
- Streptavidin-HRP (Thermo Scientific / Pierce P/N N100) or equivalent
- TMB Substrate Solution (Thermo Scientific / Pierce P/N N301) or equivalent
- Optional: TMB Stop Reagent (Thermo Scientific / Pierce P/N N600) or equivalent
- Optional: Plate reader or instrument capable of reading absorbance at 450 nm

## Procedural Notes

- All materials should be nuclease-free, and all reagents should be prepared with nuclease-free components.
- 2  $\mu$ L of each biotin labeling reaction (Step 6 on page TBD), will be used in the ELOSA. It is acceptable to store the 2  $\mu$ L of biotin-labeled sample on ice (up to 6 hours) or at  $-20^{\circ}\text{C}$  (up to 2 weeks) and run the ELOSA at a convenient time.
- The ELOSA Positive Control (Vial 10) is already labeled with biotin and should be added to its own well each time the ELOSA assay is run.
- Bring all solutions to room temperature before using them in the ELOSA.
- During all incubation steps, cover the plate with an adhesive plate sealer.
- To blot dry, expel the liquid into a sink, and repeatedly tap the inverted plate on a stack of paper towels. Do not insert laboratory wipes into the ELOSA wells.
- A multichannel pipette (8 or 12 tip) is recommended, but not required.
- Do not touch pipette tips to the bottom of the ELOSA wells at any step of the procedure.
- Vigorous washing is required to minimize non-specific background signals in negative control wells. Vigorous manual washing of the ELOSA wells with a squirt bottle filled with washing buffer is a simple and inexpensive method that works well when performed over a sink; alternatively, an automated washing instrument capable of vigorous washing may be used.

## Experimental Design Recommendations

To understand the validity of this ELOSA method, appropriate controls should be included in all ELOSA assays.

- Negative controls should include a FlashTag Biotin HSR labeling reaction that does not contain any RNA Spike Control Oligos (Vial 8). It is optional to include Total RNA in the negative control. This type of control should result in a negative reaction in the ELOSA assay and will define any baseline non-specific background signals. If a Negative control FlashTag Biotin HSR reaction is not run, another acceptable negative control is 50  $\mu$ L 5X SSC, 0.05% SDS, 0.005% BSA + 2.5  $\mu$ L 25% Dextran sulfate.
- Spike controls should include a FlashTag Biotin HSR labeling reaction containing both total RNA and the RNA Spike Control Oligos (Vial 8). Labeled samples that have previously demonstrated appropriate reactivity for the ELOSA assay should be used. Labeled samples that have shown appropriate performance on microarrays may also be of value.
- Positive controls should include the ELOSA Positive Control (Vial 10), an oligo which is already biotinylated and confirms the ELOSA is working properly.

## Coating Wells with ELOSA Spotting Oligos

1. Dilute the ELOSA Spotting Oligos (Vial 9) 1:50 in 1X PBS according to the table below:

**Table A.1**

Number of Wells	Total Volume Required	ELOSA Spotting Oligos	1X PBS
3	225 $\mu$ L	4.5 $\mu$ L	220.5 $\mu$ L
12	900 $\mu$ L	18 $\mu$ L	882 $\mu$ L
24	1800 $\mu$ L	36 $\mu$ L	1764 $\mu$ L

2. Add 75  $\mu$ L of the diluted ELOSA Spotting Oligos to each well of the plate or strip. Avoid touching the bottom of the ELOSA wells with the pipette tip.
3. Cover with an adhesive plate sealer and incubate overnight at 2-8°C. The plates (or wells) may be stored at 2-8°C for up to 2 weeks if covered tightly with an adhesive plate sealer and no evaporation occurs, but for best results, incubate overnight.

## Washing and Blocking

These steps may be completed prior to or during the FlashTag Biotin HSR labeling procedure.

1. Remove the ELOSA Spotting Oligos by expelling the liquid into a sink.
2. Wash 2 times with 1X PBS, 0.02% Tween-20, blot dry.
3. Add 150  $\mu$ L of 5% BSA in 1X PBS to each well.
4. Cover the wells and incubate for 1 hour at room temperature.

## Sample Hybridization

1. Make up a Hybridization Master Mix, by adding the following components to a tube and gently vortexing until the dextran sulfate is in solution. It is recommended that a larger master mix volume be made than is needed, as the dextran sulfate is difficult to pipette. Briefly microfuge.

**Table A.2 Hybridization Master Mix**

Component	Volume
5X SSC, 0.05% SDS, 0.005% BSA (Appendix C)	48.0 $\mu$ L
25% Dextran sulfate (Appendix C)	2.5 $\mu$ L

2. For the positive control, add 2  $\mu$ L of vial 10 to 50.5  $\mu$ L of Master Mix for a total volume of 52.5  $\mu$ L.
3. For the negative control, add 2  $\mu$ L of water to 50.5  $\mu$ L of Master Mix for a total volume of 52.5  $\mu$ L.
4. For each sample, add 2.0  $\mu$ L of biotin labeling reaction (Step 6 on page 10) to 50.5  $\mu$ L of Master Mix for a total volume of 52.5  $\mu$ L.
5. Remove the BSA blocking solution by expelling the liquid into a sink. Blot dry.
6. Add all 52.5  $\mu$ L of hybridization solution to a designated well.
7. Cover the wells and incubate for 1 hour at room temperature.

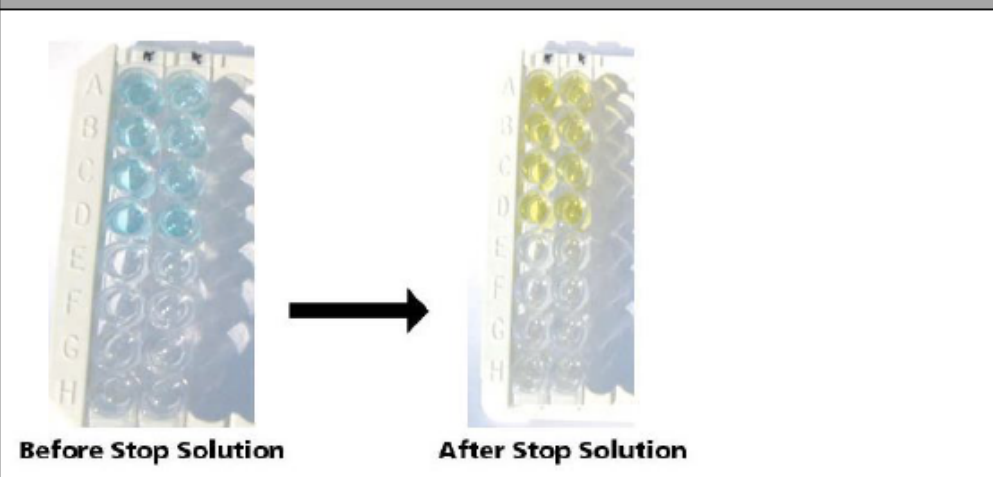
## SA-HRP Binding

1. Dilute SA-HRP in 5% BSA in 1X PBS. If using Thermo Scientific SA-HRP, a dilution of 1:4000 to 1:8000 is recommended.
2. Remove the hybridization solution by expelling the liquid into a sink.
3. Wash 3-4 times with 1X PBS, 0.02% Tween 20, blot dry.
4. Add 75  $\mu$ L of the diluted SA-HRP from Step 1 to each well.
5. Cover the wells and incubate for 30 minutes (up to 2 hours) at room temperature.

## Signal Development

1. Remove the SA-HRP by expelling the liquid into a sink.
2. Wash 3 times with 1X PBS, 0.02% Tween-20, blot dry.
3. Add 100  $\mu$ L of TMB Substrate to each well.
4. Cover the wells and incubate at room temperature for 5-30 minutes in the dark (or covered with aluminum foil).
5. The blue substrate color indicates a positive result and may be used as qualitative results (see Figure A.1).
6. Optional: For instrument quantitation, remove the adhesive plate sealer and add 100  $\mu$ L Stop Reagent (or equivalent acidic TMB stop reagent) to each well. This will convert the blue substrate to a yellow color (see Figure A.1). Read the absorbance at 450 nm on a plate reader. Readings of greater than 0.10 OD (450 nm) over a negative control should be considered positive. Typically, this assay generates positive results of at least 0.15 -1.00 OD when working appropriately.

Figure A.1



7. After a successful ELOSA QC Assay, proceed to Chapter 3, *GeneChip™ miRNA Array Procedure*.

## Appendix B

### Array Rehybridization Procedure

Follow the procedure below if it is necessary to rehybridize another GeneChip™ miRNA Array.

1. Record the volume of recovered hybridization cocktail from page TBD, *Washing and Staining*, Step 2.
2. Prepare a 1X Hyb Mix:

**Table B.1**

Component	Volume for 400/169 Format Array (miRNA 1.0 and 2.0 Arrays):	Volume for 100 Format Array (miRNA 3.0 and later designs):
Nuclease-Free Water (Vial 11)	21.5 µL	25.2 µL
2X Hybridization Mix (from GeneChip™ Hyb, Wash and Stain Kit, P/N 900720)	50 µL	66 µL
27.5% Formamide (Vial 12)	15 µL	19.2 µL
DMSO (from GeneChip™ Hyb, Wash and Stain Kit, P/N 900720)	10 µL	12.8 µL
20X Eukaryotic Hybridization Controls <i>bioB</i> , <i>bioC</i> , <i>bioD</i> , <i>cre</i> (from GeneChip™ Eukaryotic Hybridization Control Kit, P/N 900454)	5 µL	6.6 µL
Control Oligonucleotide B2, 3nM (P/N 900301)	1.7 µL	2.2 µL

3. Adjust the volume of recovered hybridization cocktail (Step 1) to 103.2 µL (169 format array) or 132 µL (100 format array) with 1X Hyb Mix (Step 2, above).
4. Follow the hybridization instructions to complete the hybridization process.
5. Continue with *Washing and Staining*.

## Appendix C

### Example Reagent Preparation and Storage

For all of the reagents below, it is important to remove the amount that is needed for the day (or step of the protocol) by carefully pouring off or using a long pipette to avoid contamination of the stock buffer. All components should be nuclease-free and stored in nuclease-free tubes or bottles. Recommended suppliers and part numbers are listed. Equivalent suppliers may be used for reagents other than BSA. We strongly recommend BSA from Sigma (Sigma P/N A3294).

#### 1mM Tris (50 mL)

- Transfer 50 mL nuclease-free water (Applied Biosystems P/N AM9932) to a 50 mL conical tube.
- Remove and discard 50  $\mu$ L water.
- Add 50  $\mu$ L of 1M Tris-HCl, pH 8 (USB P/N 22638).
- After this dilution is made, do not take a pH reading.
- Store at room temperature up to 3 months.

#### 25% Dextran Sulfate (10 mL)

- Slowly pour 5 mL 50% dextran sulfate (Millipore P/N S4030) into a 15 mL conical tube.
- Add 5 mL nuclease-free water (Applied Biosystems P/N AM9932) and vortex thoroughly.
- Store at room temperature up to 3 months.

#### 1X PBS (1L)

- 100 mL 10X PBS pH 7.4 (Applied Biosystems P/N AM9625)
- 900 mL nuclease-free water (Applied Biosystems P/N AM9932)
- Store at room temperature up to 3 months.

#### 1X PBS, 0.02% Tween-20 (1L)

- 100 mL 10X PBS pH 7.4 (Applied Biosystems P/N AM9625)
- 0.2 mL Tween-20 (200  $\mu$ L) (Sigma P/N P-9416)
- Add water to a final volume of 1L.
- Store at room temperature up to 3 months.

### **5% BSA in 1X PBS (40 mL)**

- Transfer 2g of powdered BSA (Sigma P/N A3294) to a 50 mL conical tube.
- Slowly add 1XPBS to a final volume of 40 mL.
- Shake or vortex to mix.
- Make 8 aliquots of 5 mL.
- Store each aliquot at  $-20^{\circ}\text{C}$ , up to 6 months. Do not freeze/thaw each 5 mL aliquot more than 4 times.
- Once thawed, store one aliquot at  $4^{\circ}\text{C}$  for 1 week.

### **5X SSC, 0.05% SDS, 0.005% BSA (10mL)**

- 2.5 mL 20X SSC (Applied Biosystems P/N AM9763)
- 0.05 mL 10% SDS (50  $\mu\text{L}$ ) (Applied Biosystems P/N AM9823)
- 0.01 mL 5% BSA in 1XPBS (10  $\mu\text{L}$ )
- Add water to a final volume of 10 mL.
- Make 10 aliquots of 1 mL.
- Store each aliquot at  $-20^{\circ}\text{C}$ , up to 6 months. Do not freeze/thaw each 1 mL aliquot more than 4 times.
- Once thawed, store one aliquot at  $4^{\circ}\text{C}$  for 1 week.
- If a precipitate forms in this buffer, warm at  $42^{\circ}\text{C}$  to dissolve. Use at room temperature.



## Documentation and support

---

### Obtaining support

Technical support	<p>For the latest services and support information for all locations, visit <a href="http://www.thermofisher.com">www.thermofisher.com</a>.</p> <p>At the website, you can:</p> <ul style="list-style-type: none"><li>• Access worldwide telephone and fax numbers to contact Technical Support and Sales facilities</li><li>• Search through frequently asked questions (FAQs)</li><li>• Submit a question directly to Technical Support (<a href="http://thermofisher.com/support">thermofisher.com/support</a>)</li><li>• Search for user documents, SDSs, vector maps and sequences, application notes, formulations, handbooks, certificates of analysis, citations, and other product support documents</li><li>• Obtain information about customer training</li><li>• Download software updates and patches</li></ul>
Safety Data Sheets (SDS)	<p>Safety Data Sheets (SDSs) are available at <a href="http://thermofisher.com/support">thermofisher.com/support</a>.</p>
Limited product warranty	<p>Life Technologies Corporation and/or its affiliate(s) warrant their products as set forth in the Life Technologies' General Terms and Conditions of Sale found on Life Technologies' website at <a href="http://www.thermofisher.com/us/en/home/global/terms-and-conditions.html">www.thermofisher.com/us/en/home/global/terms-and-conditions.html</a>. If you have any questions, please contact Life Technologies at <a href="http://www.thermofisher.com/support">www.thermofisher.com/support</a>.</p>

---

For support visit [thermofisher.com/support](http://thermofisher.com/support) or email [techsupport@lifetech.com](mailto:techsupport@lifetech.com)

[thermofisher.com](http://thermofisher.com)

23 January 2017

**ThermoFisher**  
S C I E N T I F I C

## Appendix 17

### Top 10 ranked targets for miR

#### miR-1233-5p

Gene symbol	Gene description
<b>ZFHX3</b>	Zinc finger homeobox 3
<b>RELN</b>	Reelin
<b>TP53INP2</b>	Tumor protein p53 inducible nuclear protein 2
<b>USB1</b>	U6 snRNA biogenesis phosphodiesterase 1
<b>TNS1</b>	Tensin 1
<b>UCP3</b>	Uncoupling protein 3
<b>TCAF2</b>	TRPM8 channel associated factor 2
<b>GSTM2</b>	Glutathione S-transferase mu 2
<b>BRPF3</b>	Bromodomain and PHD finger containing 3
<b>AP1G1</b>	Adaptor related protein complex 1 subunit gamma 1
<b>PKLR</b>	Pyruvate kinase L/R

#### miR-320b

Gene symbol	Gene description
<b>YOD1</b>	YOD1 deubiquitinase
<b>CDKL5</b>	Cylin dependent kinase like 5
<b>ONECUT2</b>	One cut homeobox 2
<b>SPOPL</b>	Speckle type BTB/POZ protein like
<b>SH2B3</b>	SH2B adaptor protein 3
<b>PLPPR1</b>	Phospholipid phosphatase related 1
<b>KITLG</b>	KIT ligand
<b>GPBP1</b>	GC-rich promotor binding protein 1
<b>GCG</b>	Glucagon
<b>CNKSR2</b>	Connector enhancer of kinase suppressor of Ras 2

**miR-92b-5p**

<b>Gene symbol</b>	<b>Gene description</b>
<b>FN3K</b>	Fructosamine 3 kinase
<b>AGO2</b>	Argonaute RISC catalytic component 2
<b>PPP2R2D</b>	Protein phosphatase 2 regulatory subunit Bdelta
<b>ID1</b>	Inhibitor of DNA binding 1, HLH protein
<b>RABGEF1</b>	RAB guanine nucleotide exchange factor 1
<b>KNOP1</b>	Lysine rich nucleolar protein 1
<b>CRTC1</b>	CREB regulated transcription coactivator 1
<b>SLC7A5</b>	Solute carrier family 7 member 5
<b>ATP6V1C2</b>	ATPase H <sup>+</sup> transporting V1 subunit C2
<b>CPNE5</b>	Copine 5

**miR-3141**

<b>Gene symbol</b>	<b>Gene description</b>
<b>BHLHE22</b>	Basic helix-loop-helix family member e22
<b>NXN</b>	Nucleoredoxin
<b>NAAA</b>	N-acylethanolamine acid amidase
<b>MCM3</b>	Minichromosome maintenance complex component 3
<b>GPX1</b>	Glutathione peroxidase 1
<b>ZC3H12A</b>	Zinc finger CCCH-type containing 12A
<b>PRR23C</b>	Proline rich 23C
<b>PCBP3</b>	Poly(rC) binding protein 3
<b>ITGA10</b>	Integrin subunit alpha 10
<b>CTXN1</b>	Cortexin 1

**miR-4634**

<b>Gene symbol</b>	<b>Gene description</b>
<b>TLR8</b>	Toll like receptor 8
<b>BRPF1</b>	Bromodomain and PHD finger containing 1
<b>AGAP3</b>	ArfGAP with GTPase domain, ankyrin repeat and PH domain 3
<b>KLK9</b>	Kallikrein related peptidase 9
<b>GAS8</b>	Growth arrest specific 8

**miR-4649-5p**

<b>Gene symbol</b>	<b>Gene description</b>
<b>MEX3C</b>	Mex-3 RNA binding family member C
<b>SH3GL1</b>	SH3 domain containing GRB2 like 1, endophilin A2
<b>GART</b>	Phosphoribosylglycinamide formyltransferase, phosphoribosylglycinamide synthetase, phosphoribosylaminoimidazole synthetase
<b>RSPO4</b>	R-spondin 4
<b>DCLK1</b>	Doublecortin like kinase 1
<b>GALNS</b>	Galactosamine (N-acetyl)-6-sulfatase
<b>PPP2R5B</b>	Protein phosphatase 2 regulatory subunit B'beta
<b>PDSS1</b>	Decaprenyl diphosphate synthase subunit 1
<b>AFDN</b>	Afadin, adherens junction formation factor
<b>CCDC12</b>	Coiled-coil domain containing 12

**miR-4467**

<b>Gene symbol</b>	<b>Gene description</b>
<b>POU3F3</b>	POU class 3 homeobox 3
<b>FAM104A</b>	Family with sequence similarity 104 member A
<b>NKX2-5</b>	NK2 homeobox 5
<b>IQSEC2</b>	IQ motif and Sec7 domain 2
<b>FBXL16</b>	F-box and leucine rich repeat protein 16
<b>CAMK2N2</b>	Calcium/calmodulin dependent protein kinase II inhibitor 2
<b>PIAS4</b>	Protein inhibitor of activated STAT 4
<b>CELF4</b>	CUGBP Elav-like family member 4
<b>SLC9A3</b>	Solute carrier family 9 member A3
<b>H2AFX</b>	H2A histone family member X

**miR-4433b-3p**

<b>Gene symbol</b>	<b>Gene description</b>
<b>EFHC1</b>	EF-hand domain containing 1
<b>JPH1</b>	Junctophilin 1
<b>FAM83H</b>	Family with sequence similarity 83 member H
<b>CCDC43</b>	Coiled-coil domain containing 43
<b>SUCLA2</b>	Succinate-CoA ligase ADP-forming beta subunit
<b>ARL17A</b>	ADP ribosylation factor like GTPase 17A
<b>TMIGD1</b>	Transmembrane and immunoglobulin domain containing 1
<b>SPRY2</b>	Sprouty RTK signaling antagonist 2
<b>MTRR</b>	5-methyltetrahydrofolate-homocysteine methyltransferase reductase
<b>LPCAT3</b>	Lysophosphatidylcholine acyltransferase 3

**miR-1909-3p**

<b>Gene symbol</b>	<b>Gene description</b>
<b>ZFP41</b>	ZFP41 zinc finger protein
<b>ORMDL3</b>	ORMDL sphingolipid biosynthesis regulator 3
<b>ATG9A</b>	Autophagy related 9A
<b>NPTX1</b>	Neuronal pentraxin 1
<b>INO80</b>	INO80 complex subunit
<b>FBXL18</b>	F-box and leucine rich repeat protein 18
<b>PSD3</b>	Pleckstrin and Sec7 domain containing 3
<b>PRRT2</b>	Proline rich transmembrane protein 2
<b>SOGA1</b>	Suppressor of glucose, autophagy associated 1
<b>DPPA4</b>	Developmental pluripotency associated 4